# Integrating Laser Scanning with Discrete Element Modeling for Improving Safety in Underground Stone Mines

Juan José Monsalve Valencia

*Thesis submitted to the faculty of the Virginia Polytechnic Institute and State University in partial fulfillment of the requirements for the degree of*

**Master in Sciences**
**In**
**Mining Engineering**

Nino S. Ripepi, Chair

Mario G. Karfakis
Cheng Chen
Jim Hazzard

May 10, 2019
Blacksburg, VA

Keywords: Terrestrial Laser Scanning, Discrete Element Method, 3DEC, Discrete Fracture Network, Ground control, Underground Limestone Mine

# Integrating Laser Scanning with Discrete Element Modeling for Improving Safety in Underground Stone Mines

Juan José Monsalve Valencia

## ACADEMIC ABSTRACT

According to the Mine Health and Safety Administration (MSHA), between 2006 and 2016, the underground stone mining industry had the highest fatality rate in 4 out of 10 years, compared to any other type of mining in the United States. Additionally, the National Institute for Occupational Safety and Health (NIOSH) stated that structurally controlled instability is a predominant failure mechanism in underground limestone mines. This type of instability occurs when the different discontinuity sets intercept with each other forming rock blocks that displace inwards the tunnel as the excavation takes place, posing a great hazard for miners and overall mine planning. In recent years, Terrestrial laser scanning (TLS) has been used for mapping and characterizing fractures present in a rock mass. TLS is a technology that allows to generate a three-dimensional multimillion point cloud of a scanned area. In addition to this, the advances in computing power throughout the past years, have allowed numerical modeling codes to represent more realistically the behavior of a fractured rock masses. This work presents and implements a methodology that integrates laser scanning technology along with Discrete Element Modeling as tools for characterizing, preventing, and managing structurally controlled instability that may affect large-opening underground mines. The stability of an underground limestone mine that extracts a dipping ore body with a room and pillar (and eventual stoping) mining method is analyzed with this approach. While this methodology is proposed based on a specific case study that does not meet the requirements to be designed with current NIOSH published guidelines, this process proposes a general methodology that can be applied in any mine experiencing similar failure mechanisms, considering site-specific conditions. The aim of this study is to ensure the safety of mine workers and to reduce accidents that arise from ground control issues. The results obtained from this methodology allowed us to generate Probability Density Functions to estimate the probability of rock fall in the excavations. These models were also validated by comparing the numerical model results with those obtained from the laser scans.

# Integrating Laser Scanning with Discrete Element Modeling for Improving Safety in Underground Stone Mines

Juan José Monsalve Valencia

## GENERAL AUDIENCE ABSTRACT

According to the Mine Health and Safety Administration (MSHA), between 2006 and 2016, the underground stone mining industry had the highest fatality rate in 4 out of 10 years, compared to any other type of mining in the United States. Additionally, the National Institute for Occupational Safety and Health (NIOSH) stated that structurally controlled instability is one of the main causes of rock falls in underground limestone mines. This type of instability occurs when the fractures present in the rock mass intercept each other forming rock blocks that displace into the tunnel as the excavation takes place and poses a great hazard for miners. In recent years, Terrestrial laser scanning (TLS) has been used for mapping and characterizing fractures present in a rock mass. TLS is a technology that allows to generate a three-dimensional multimillion point cloud of a scanned area. In addition to this, the advances in computing power throughout the past years, have allowed simulation softwares such as the Discrete Element Model (DEM) to represent more realistically the behavior of a fractured rock mass under excavation. The aim of this work was to develop and evaluate a methodology that could complement already exisiting design guidelines that may not apply to all kind of underground mines. The presented methodology evaluates rock failure due to presence of discontinuites, through the integration of TLS with DEM and considers site specific conditions. An area of a case study mine was assessed with this methodology, where several laser scans were performed. Information extracted from this laser scans was used to simulate the response of the rock mass under excavation by running Discrete Element Numerical Models. Results from these models allowed us to estimate the probability of rock failure in the analized areas. These, rock block failure probability estimations provide engineers a tool for characterizing, preventing, and managing structurally controlled instability, and ultimately improving workers safety.

# DEDICATION

In memory of Bernardo Monsalve Castaño, my grandfather. He became a miner when he was thirteen years old and devoted his whole life to Colombian Mining Industry. He was mentor of many mining engineers that worked in different companies such as Peldar, Geominas S.A. and Frontino Gold Mines. All his stories and teachings remain in my memory.

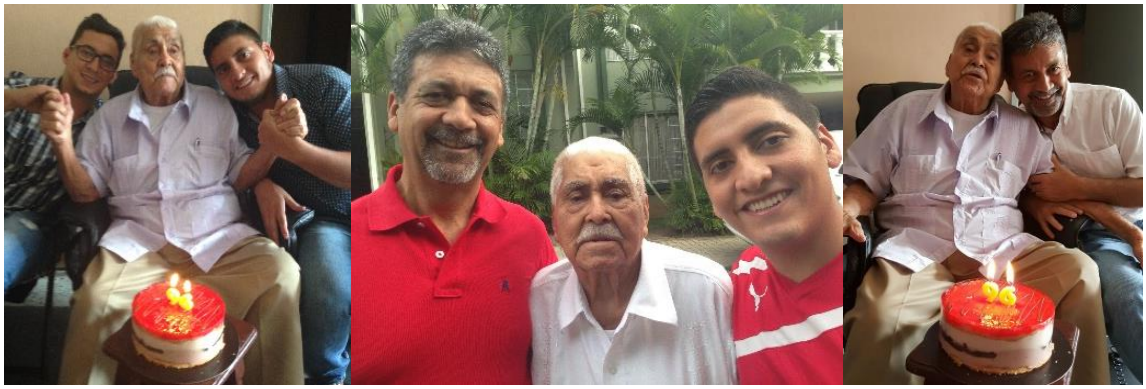

This work is also dedicated to my parents Juan Eugenio Monsalve and Francia Elena Valencia, and my sister Maria Alejandra Monsalve. They have been a fundamental pillar in both my personal and professional development. For their unconditional love and constant support.

Professor Oscar Jaime Restrepo from Universidad Nacional de Colombia whom showed me early on my career how to open doors and windows to find a way to make my dreams and the ones of those around me come true.

# ACKNOWLEDGMENTS

First of all, I would like to acknowledge Dr. Nino Ripepi for his unconditional support and all the trust he has placed on me since we met for the first time. I hope I have given back all that trust during these two years of joint work.

I would like to thank the members of my committee Dr. Cheng Chen and Dr. Mario G. Karfakis for their constant support and their will to discuss and offer ideas that allowed me to accomplish this work.

In addition to Dr. Ripepi and my committee, I would also like to acknowledge each faculty, employee, graduate student and undergraduate student, that make the Mining and Minerals Engineering Department of Virginia Tech an amazing place for studying, researching, working and networking. After two years of being here, I can call this place home. Thank you all!

This work was funded by the National Institute for Occupational Safety and Health's Mining Program under Contract No. 200-2016-91300. I acknowledge as well NIOSH for the great work they do supporting education and research in order to improve health and safety in the Mining Industry not only in the U.S. but also all over the world. Particularly, I would like to acknowledge and thank Dr. Michael Murphy and Dr. Brent Slaker for all their support and guidance during these two years.

During this project we received support from many industrial partners. One of them was MAPTEK. I would like to acknowledge them for their constant support regarding laser scanning, point cloud processing and virtual discontinuity mapping. Thank you very much for providing us with a free license of their software I-Site Studio, which was very helpful in the development of this research. I would like to thank Engineer Mark Nelson from MAPTEK for his unconditional support since this project started.

Other of our industrial partner that has been since the beginning of this project is ITASCA Consulting Group Inc. I would like to thank ITASCA for their will and interest to work with us. During this process, I was awarded with the ITASCA Educational Partnership Program (IEP). I also want to thank them for that opportunity. Particularly, I want to acknowledge and thank Dr. Jim Hazzard, whom has been my mentor throughout this year. He has been of great help not only with questions that have arisen working with 3DEC, but also to clear and structure better my ideas.

I would like acknowledge L'hoist mining engineers for their constant support and recommendations during field work, data collection and results interpretation.

Last but not least, I want to acknowledge my research buddies Jon Baggett, Richard Bishop and Aman Soni, without their support and ideas this work would not have been materialized.

# TABLE OF CONTENTS

# TABLE OF FIGURES

# LIST OF TABLES

# PREFACE

This thesis is composed of three main chapters, which describe progression of work to develop and test a methodology that combines Terrestrial Laser Scanning (TLS) and Discrete Element Modeling (DEM) for the design of underground stone mines aimed at ensuring safety of the workers and reducing accidents due to ground control issues. Even though, this work is based off of a case study mine, the methodology here described can be applied to any mine posing a similar failure mechanism.

Chapter 1 presents the case study mine and describes the failure mechanisms that pose risks for workers and the overall operation. This paper explains and compares current engineering methods to design excavations under structurally controlled failure mechanism. Finally, A methodology that integrates TLS and DEM is proposed. This methodology included the following stages: Preliminary evaluation and site selection, site scanning and rock mass characterization, structural data processing, sample collection, rock mechanics laboratory testing, numerical modeling and design considerations and monitoring.

Chapter 2 provides further details on how to plan and perform a laser scanning survey for rock mass characterization, virtual discontinuity mapping and Discrete Fracture Network (DFN) generation. In addition to this, nine laser scans were performed. The resulting point cloud was processed and virtual discontinuity mapping was carried out. A total of 874 fractures were mapped. These were later used in order to identify the main structural sets and generating DFNs for subsequent numerical modeling.

Chapter 3 focusses in the Discrete Element Modeling and proposes a stochastic approach to analyze block failure in the case study mine. These work describes the assumptions made to generate the model. Thirty iterations were run to generate probability density functions for total volume and number of failed blocks in a 20 m long tunnel, considering the four discontinuity sets defined in previous work and the geometries of the excavation. In addition, information about failed block such as geometries, sizes and kinematics were obtained. The results obtained from the models were validated by comparing blocks sizes and geometries with gaps left after rock fall in the laser scanned tunnels.

Finally, Chapter 4 summarizes the overall work and highlights the accomplishments of it. A series of conclusions derived from this work are presented, as well as a series of recommendations aimed at implementing this methodology in underground limestone industry for improving safety and reducing ground control related accidents.

# Chapter 1 A Preliminary Investigation for Characterization and Modeling of Structurally Controlled Underground Limestone Mines by Integrating Laser Scanning with Discrete Element Modeling.[1]

**Authors:** Juan J. Monsalve[a], Jon Baggett[a], Richard Bishop[a], Nino Ripepi[a]
[a] Mining and Minerals Department, Virginia Polytechnic Institute &State University

**Abstract.**

Stability of large opening underground excavations in jointed rock masses primarily depends on the distribution and properties of the geological discontinuities. Conventional methods for structural mapping may not be optimal for rock mass characterization. Laser scanning is a technology that rapidly sends out laser pulses in order to measure the position of certain objects by generating a massive point cloud with millimeter precision. This paper reviews the application of laser scanning along with discrete element method (DEM) modeling, to produce a more realistic response of the rock mass behavior during excavation compared to analytical approaches. Additionally, a methodology to evaluate the stability in a structurally controlled underground limestone mine with these two technologies is proposed.

**Key words.** Limestone Mines, Terrestrial Laser Scanning, 3DEC, Structurally Controlled Instability.

## 1. INTRODUCTION

Over the past ten years, 40% of underground mining fatalities were caused by ground control issues related to roof, rib collapses, and pillar bursts (MSHA, 2016). Over the same time period, the underground stone mining industry had the highest fatality rate in four of those ten years (MSHA, 2016), more than any other sector. Underground limestone mines in the eastern U.S. have become more common over the past decade and typically there is less underground experience compared to underground mines in the western part of the country, resulting in a need for more engineering, education and training. In addition, the large openings and great spans between pillars can create instability conditions, leading to a large collapse of the roof or pillar if the mining system is not designed properly or if pillars deteriorate over time.

In 2011, the National Institute for Occupational Safety and Health (NIOSH) developed empirical guidelines for designing underground stone mines. This was limited to room and pillar mines in flat-lying bedded formations located in the eastern and Midwestern United States (NIOSH, 2011). However, these guidelines are not necessarily applicable to mines that do not share the same conditions as the mines in which the study was performed.

[1] Conference paper published in the **North American Tunneling Conference: 2018 Proceedings**, Washington D.C.

A case study mine (CSM) in which NIOSH guidelines does not apply will be evaluated. The CSM is a dipping (approximately 30°), underground room and pillar limestone mine. This rock has UCS of 159.2 MPa ± 21.25 MPa, a tensile strength of 6.3 MPa ± 1.99 MPa and a Young's modulus of 64.11 GPa ± 2.37 MPa. The deepest point in the mine is approximately 700 m below ground surface. This mine leaves 24 m by 24 m pillars and the dimensions of the drifts and crosscuts are generally 12.8 m wide and 7.6 m high. The mine's main failure mechanism is structurally controlled failure, evidenced by the jointing pattern and spacing observed in the tunnels, the amount of fallen blocks observed on the floor, and other geological structures such as faults and contacts that may generate a rock fall in the absence of ground support. In this case, further analysis may be performed in order to ensure the stability of the excavation and safety during operation. Even though general guidelines may not apply for this case, analysis methodologies may be proposed in order to analyze mines that present similar modes of failure.

In recent years, the development of digital mapping techniques through Terrestrial Laser Scanning (TLS) and photogrammetry have allowed the development of three-dimensional digital terrain models as tools for characterizing, modeling, and designing underground structures, not only in tunneling projects but also in mining environments (Cacciari & Futai,2017; Rogers, Bewick, Brzovic, & Gaudreau, 2017; Fekete & Diedrichs, 2013; Slaker, Westman, Fahrman, & Luxbacher, 2013; Grenon, Landry, Hadjigeorgiou, & Lajoie, 2017). In addition, it has been proven that this technology is useful, faster, and cheaper than conventional mapping methods, and also that with the right analyses and data interpretation the results may offer a better representation of the rock mass structure than conventional methods.

Not only have great advances been made in digital mapping techniques during the past decade, but the advances in computing power allow numerical models to more realistically represent the behavior of rock masses (Lorig & Varona, 2013). Due to these current advances, the use of distinct element codes such as 3DEC, is proposed over conventional analysis methods to evaluate the stability of the mine workings in order to better understand the rock mass behavior and ultimately improve safety performance in the operation.

The following paper reviews both technologies: Laser Scanning for rock mass characterization and discrete element model software for analyzing the instability of a structurally controlled limestone mine. Additionally, a methodology that integrates these technologies is proposed for analyzing the stability in the case study mine.

## 2. STRUCTURALLY CONTROLLED INSTABILITY

Structurally controlled instability has been widely described by many authors (Goodman, 1989; Brady & Brown, 1985; Hudson & Harrison, 2000; Hoek, 2000). This mode of failure has been defined as the sliding or natural falling of rock blocks either from the roof or the

walls due to gravity action (Brady & Brown, 1985). This type of instability occurs in rock masses that present two or more structural features that intersect, generating wedges; once the tunnel is excavated, these wedges generate blocks that tend to displace or rotate towards the opening. Additionally, researchers such as Martin, Kaiser, & Christiansson (2003) have proposed risk assessment charts in order to identify whether the conditions of the rock mass allow for either streess controlled instability or structurally controlled instability based on the stress condition, strength of the intact rock ($\sigma_{ci}$) and the Geological Strength Index (GSI); they state that when the rock mass has a GSI less than 30 and the $\sigma_{ci}$ is greater than 2 times the vertical stress ($\sigma_v$), or when the GSI is greater than 40 and the principal stress ($\sigma_1$) is less than 0.15 $\sigma_{ci}$, the rock mass is under structurally controlled instability.


**Figure 1.1. Geotechnical conditions observed in the CSM.**

Figure 1.1 presents the geotechnical condition observed in the CSM, where the structurally controlled instability was defined as main failure mechanism. This was evidenced by the jointing pattern and joint spacing observed in the tunnels, the amount of fallen blocks observed on the floor, and other geological structures such as faults and contacts that may generate a rock fall in the absence of the required support. This failure mechanism was enhanced by the multiple karst formations present in the mine, which during excavation have generated rock blocks up to 4 $m^3$ (144 $ft^3$) that pose high risk for workers, equipment, and the overall mining plan. Table 1.1 presents intact rock properties obtained form previous studies in CSM. During recent visits, GSIs greater than 75 have been identified throughout the mine. Considering the minimum strength conditions (137.95 MPa) and the greatest stress condition (20 MPa) the stress/strength relationship ($\sigma_{1/}$ $\sigma_{ci}$) is lower than 0.15, therefore, according to Martin, Kaiser, & Christiansson (2003) this mine is also defined as a structurally controlled mine.

**Table 1.1. Intact rock property test results from CSM.**

| Lithology | Density (ton/m3) | | UCS (MPa) | | Brazilian Tensile Strength (MPa) | | Young's Modulus (GPa) | |
|---|---|---|---|---|---|---|---|---|
| | Mean | SD | Mean | SD | Mean | SD | Mean | SD |
| Hanging Wall | 2.69 | 0.01 | 163.74 | 37.84 | 11.96 | 3.14 | 61.02 | 6.79 |
| Ore Body | 2.69 | 0.01 | 159.20 | 21.25 | 6.30 | 1.99 | 64.11 | 2.37 |
| Footwall | 2.72 | 0.01 | 217.29 | 36.12 | 13.72 | 2.62 | 61.43 | 3.15 |

## 3. ANALYSIS METHODS FOR STRUCTURALLY CONTROLLED INSTABILITY

As described by Lorig & Varona (2013), two main analysis methods exist for the failure mechanism present in the CSM (structurally controlled instability); the limit equilibrium theory, also known as key block theory, described by Goodman & Shi (1985), Brady & Brown (1985) and Hudson & Harrison (2000); and the two and three dimensional discontinuous modeling methods, initially developed by Cundall (1971).

### 3.1. Limit Equilibrium Method

The limit equilibrium method is an analytical analysis method that consists of determining the geometry of the wedge formed by the intersection of 3 joint planes and the excavation using the block theory described by Goodman & Shi (1985). The forces acting on the wedge are then determined and its respective vectors calculated; The sliding direction is determined and so are the normal forces acting on each wedge plan; finally resisting forces due to joint shear strength and tensile strength are calculated, allowing for the calculation of a safety factor. These calculations may be performed by hand or using specialized software such as Unwedge (Rocscience, 2017).

Table 1.2 presents some capabilities and limitations of using a limit equilibrium software for stability analysis in jointed rock masses. Although, it is clear that this analysis method is not able to represent the real structural setting of the rock mass, it allows a general interpretation of the sizes, volumes and kinematics of the possible blocks to be performed.

**Table 1.2. Advantages and Disadvantages of Using Limit Equilibrium Method for Analyzing Structurally Controlled Instability (Rocscience, 2017)**

| Limit Equilibrium Method (UNWEDGE) | |
|---|---|
| **Capabilities** | **Limitations** |
| - User friendly<br>- Reproduce multiple models in short time.<br>- Ability to consider support such as rock bolts and shotcrete.<br>- Allows to perform statistical analysis based on the mechanical properties of the discontinuities. | - can only use three discontinuity sets at a time for the analysis.<br>- discontinuity surfaces are assumed to be persistent and to extend through the volume of interest.<br>- complex geometries may not be analyzed. |

| | |
|---|---|
| | - discontinuities can occur at any location in the rock mass.<br>- only considered one joint of the actual joint set. |

### 3.2. Two and three dimensional discontinuous methods

A discrete or distinct element method (DEM) according to Cundall & Hart (1985) refers to a computer program that allows finite displacements and rotations of discrete bodies, including complete detachment; and recognizes new contacts automatically as the calculation progresses.

3DEC is a numerical code that simulates the response of discontinuous media (such as a rock mass) subjected to either static or dynamic loading. In order to perform the analysis, it applies the discrete element model (DEM) proposed by Cundall (1971), which uses a time-stepping explicit algorithm to solve the equations of motion of the blocks. This software divides the rock mass into a mesh where each block is free to break or maintain its connection with the blocks that surround it. Additionally, it recognizes the new contacts between the displaced blocks as the calculation takes place. The input to this software consist on a series of parameters including physical and mechanical properties of both intact rock and discontinuities (ITASCA, 2016). Figure 1.2 presents an example of a 3DEC model in a road tunnel in Norway evidencing the effects of input parameters such as persistence on displaced blocks after the excavation, modified after (Fekete & Diedrichs, 2013).

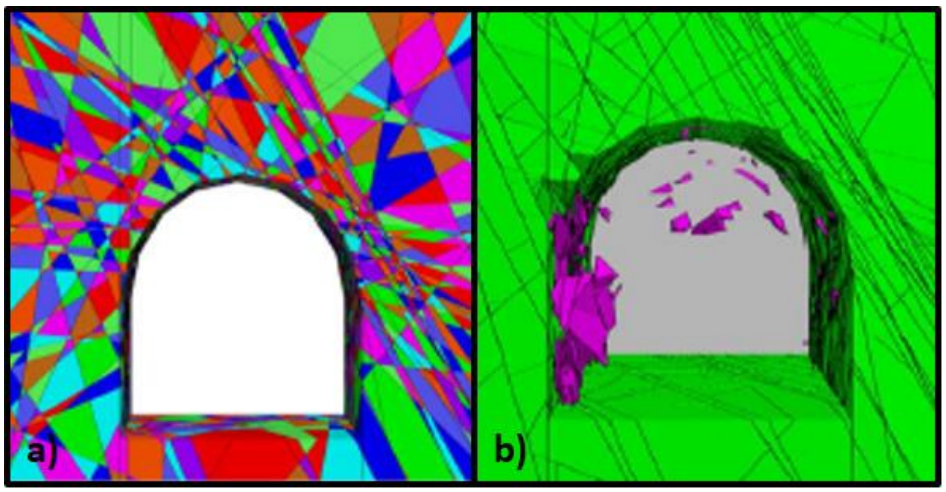


**Figure 1.2. a) Construction of a deterministic model in a tunnel b) Deterministic model showing the block displacement in a tunnel, modified after (Fekete S. , 2010)**

This numerical tool permits working with different constitutive models for both intact rock and discontinuities, generating models based on laboratory and field test data. Staged models can be performed using 3DEC due to its workflow methodology that allows running models stage by stage reproducing mining or excavation sequences. Complex geometries can be represented, thanks to its compatibility with CAD based software and other meshing plug-

ins such as Griddle to facilitate modeling. However, one of the most important characteristics of 3DEC is that it has its own programming language allowing the user to program their own functions, in order to create automated models.

3DEC is able to reproduce more reliable models that provide a better representation of the rock mass. This is possible due to its capability of elaborating discrete fracture networks (DFN) which simulate the structural setting in the rock mass. A DFN is a three-dimensional geometric representation of a geological structure based on statistical information of its characteristics measured on the field (Pierce, 2017). The parameters required to reproduce a DFN are joint orientation, density of the fractures (number of fractures per unit volume) and joint size generally quantified by the joint trace length (Grenon, Landry, Hadjigeorgiou, & Lajoie, 2017). All of these parameters can be collected by manual rock mass characterization; however, in order to generate reliable DFN's, great amounts of statistical data may be required, which may be difficult to obtain through manual mapping alone.

Some of the drawbacks of the 3DEC software are that when the model is very complex, it may take several iterations to process and significant time (days to weeks), compared to other modeling software it is expensive, and the reliability on the results strongly depends on the quality of the input data from the rock mass characterization.

Table 1.3 presents a summary of the capabilities and limitations described for discontinuous analysis methods such as 3DEC (ITASCA, 2016) for stability analysis in jointed rock masses. The application of this analysis tool will help to obtain a better understanding of the failure mechanism present in the CSM under present geotechnical conditions and propose alternative engineering designs, support measures and excavation methods to reduce structurally controlled instability and enhance safety conditions in the operation.

**Table 1.3. Advantages and Disadvantages of Using Discontinuous Analysis Method for Analyzing Structurally Controlled Instability (ITASCA, 2016)**

| **Discontinuous Analysis Methods (UDEC & 3DEC)** | |
|---|---|
| **Advantages (Capabilities)** | **Disadvantages (Limitations)** |
| - Works with different constitutive models, both for discontinuities and intact rocks.<br>- Ability to input statistical parameters of discontinuities properties.<br>- Can represent complex geometries and sequential excavations.<br>- Ability to consider multiple discontinuity sets by generating Discrete Fracture Networks (DFN). | - Complex models are time consuming.<br>- Representation of the behavior of the rock mass depends on the reliability on the geotechnical data. |

## 4. ROCK MASS CHARACTERIZATION

In order to have sufficient information to perform any kind of analysis in a structurally controlled rock mass, a detailed survey of the geological structure must be done. Figure 1.3 presents a schematic representation modified after (Hudson & Harrison, 2000) of the properties to be measured in discontinuities present in a rock mass during a detailed rock mass characterization, according to (ISRM, 1978). These properties include spacing and frequency, orientation, persistence, roughness, aperture, seepage, filling, and wall strength. These properties are used in order to evaluate both geometrical and strength parameters of each discontinuity set along the rock mass.

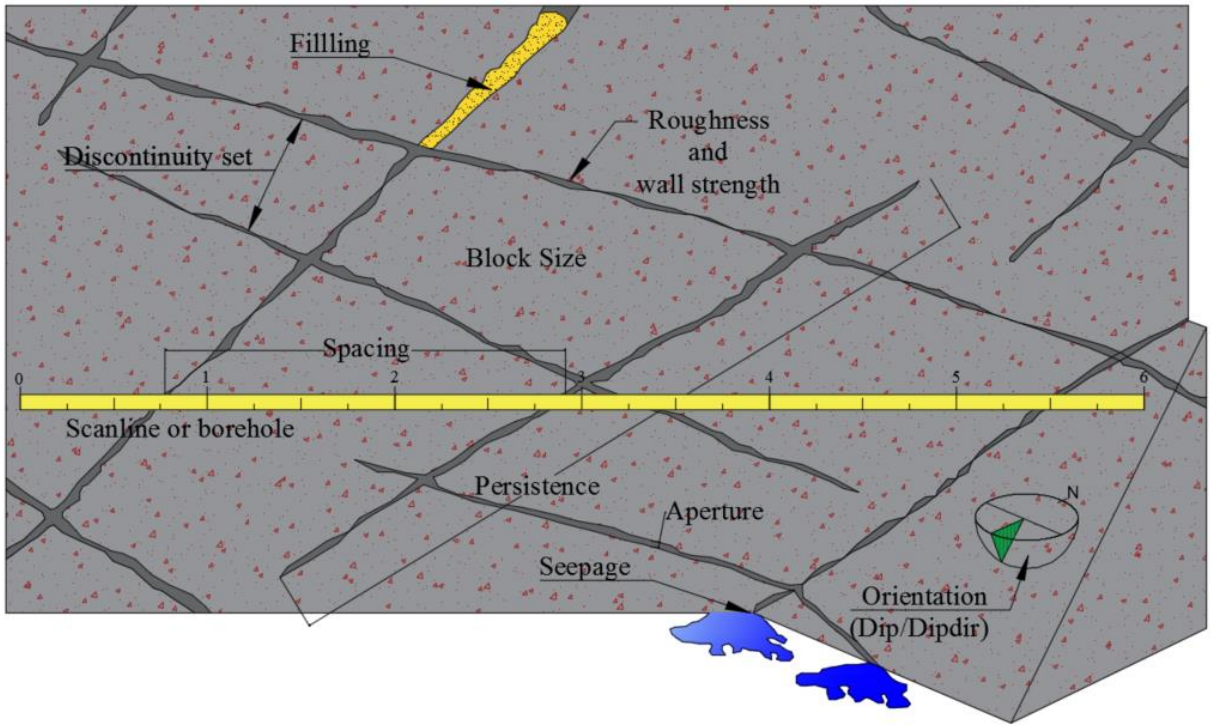


**Figure 1.3. Schematic of the primary geometrical properties of discontinuities in rock, modified after (Hudson & Harrison, 2000)**

According to Voyay, Roncella, Forlani, & Ferrero (2006), in many cases a traditional survey performed manually may be dangerous or difficult, provide a small sample size, and take a considerable amount of time. Alternatively, digital mapping techniques such as laser scanning and photogrammetry have been proposed by different authors. Although these technologies were initially proposed for slope stability analysis, today their applications have been extended to underground environments. In this study, laser scanning was selected over photogrammetry due to its time savings while acquiring and processing the data. Photogrammetry requires illumination in order to obtain the images, which may present a logistic complication during field work. It is worth remarking that photogrammetry can also offer an alternative to laser scanning and present great results as shown by Grenon, Landry,

Hadjigeorgiou, & Lajoie (2017) and Rogers, Bewick, Brzovic, & Gaudreau (2017) who have used photogrammetry to generate DFN to analyze wedge stability in mining drifts.

### 4.1. Laser Scanning

Laser scanning is a technology that rapidly sends out laser pulses in order to calculate the position of certain objects by generating a massive point cloud with millimeter precision (Kemeny, Turner, & Norton, 2006). Laser scans provide a three dimensional detailed image of the rock mass that allows one to quickly map, with more precision and less bias, the structural features present in the rock mass. Additionally, it has also been proven that laser scanning obtains qualitatively sound data in a short time without affecting the mining plan in an active tunnel environment; it provides detailed quality control information on the precision excavation and installed support (Fekete & Diedrichs, 2013). Other authors such as Slaker, Westman, Fahrman, & Luxbacher (2013) have used laser scanning for deformation measurements in pillars in underground mines.

Even though laser scanning has proved to be a useful tool for analyzing instability in structurally controlled rock masses, its greatest challenges are related to structural data analysis. As mentioned before the main properties of interest for each joint set are joint orientation, density of the fractures and joint size. Many authors have been centering their research in identifying the best way to analyze the structural data in order to generate more reliable numerical models. Fekete & Diedrichs (2013) proposed a workflow for integrating structural data obtained from TLS into DEM analysis. They discuss some of the advantages and challenges of TLS data in underground rock mass evaluation considering some of the bias that can be present during the extraction of discontinuity properties. Additionally, they proposed two approaches (deterministic and stochastic) for modeling the excavation using TLS data, allowing the designer to have a widened view of the rock mass performance. Cacciari, Morikawa, & Futai (2015) generated a 3D block model using 3DEC based on a DFN obtained from discontinuity mapping analysis from laser scans. The results from the stability analysis were not presented. Cacciari & Futai (2015) analyzed different methods for estimating the mean trace length of the discontinuities from laser scans; they defined that the trace length estimation method proposed by Wu, Kulatilake, & Tang (2011) presented better results than other methodologies proposed by other authors. Cacciari & Futai (2017) proposed a practical approach to create single and continuous DFNs considering the variations of the fracture density along the tunnel. Additionally, they performed numerical models based on the methodology obtaining similar behaviors in the model than those presented in the field.

## 5. PROPOSED METHODOLOGY

Figure 1.4 presents the workflow proposed in order to integrate laser scanning with numerical modeling in the CSM. This methodology is divided into seven phases: Preliminary evaluation and site selection, site scanning and rock mass characterization, structural data processing,

sample collection, rock mechanics laboratory testing, numerical modeling and design considerations and monitoring. The stages are explained in detail below.

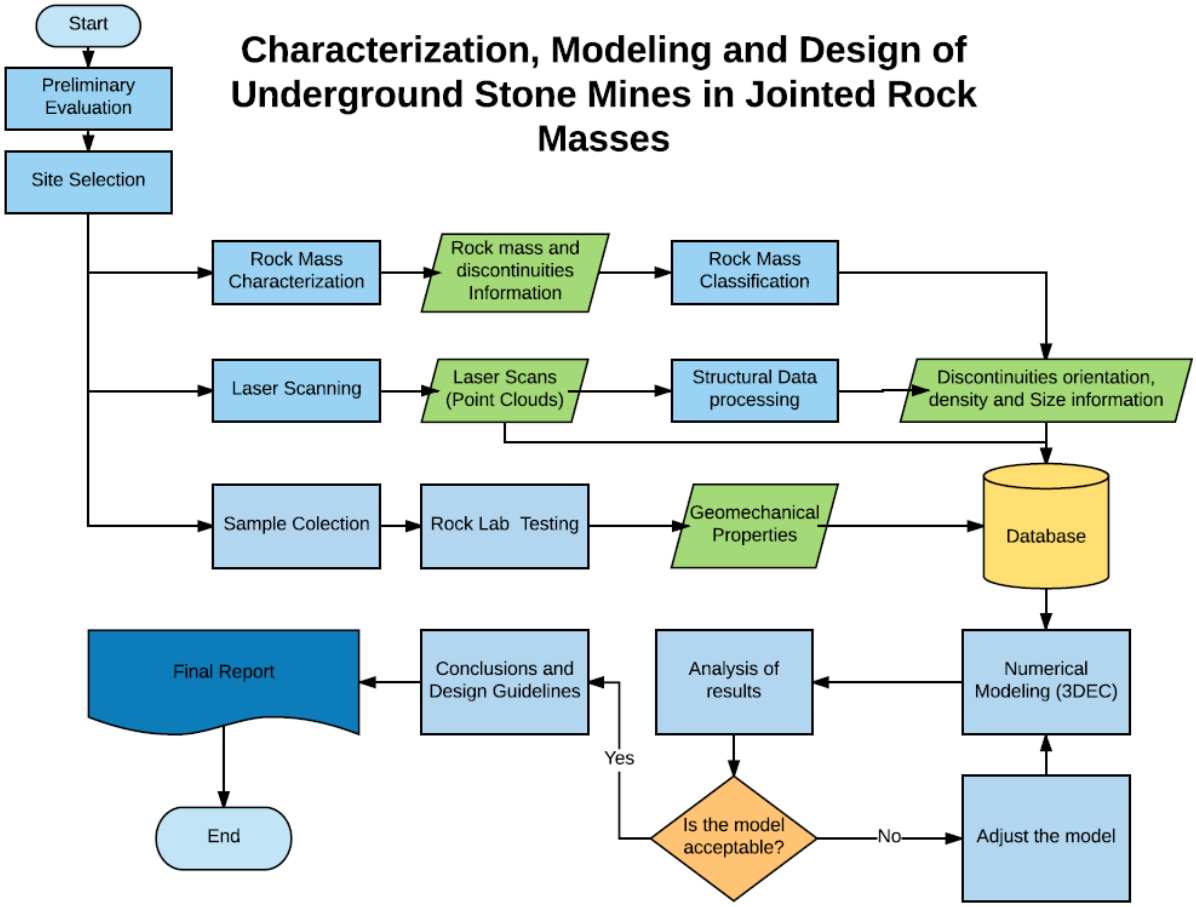


**Figure 1.4. Proposed workflow for the integration of laser scanning and 3DEC modeling in the CSM**

### 5.1. Preliminary evaluation and site selection

Several visits were made to the mine. Initial visits were carried out in order to get familiar with the mining method and geotechnical conditions of the mine. The main areas of concern for this study are working areas and travel ways where miners are at risk of roof falls. The areas in which the research will be performed will not only be those areas presenting greater geotechnical risks for the miners, but also those that present great interest for mine planning. These areas will be selected with mine management.

### 5.2. Site scanning and rock mass characterization

Once the locations for study are defined, the laser scans will be performed. In order to define what are the most appropriate operational conditions, a series of laser scans will be taken. Table 1.4 presents different operational conditions used by different authors, which will be

used as a reference to set the scanning conditions. A Faro Focus$^{3D}$ laser scanner will be used for taking the scans, considering safety precautions defined by the manufacturer.

**Table 1.4. Laser scan conditions used by different authors.**

| Research | Equipment | Measurement Speed (points/s) | Distance Accuracy (mm) | Spacing between scan Stations (m) |
|---|---|---|---|---|
| (Fekete & Diedrichs, 2013) | Leica Geosystems HDS6000 | 500,000 | 0.6 | 1 Diameter |
| (Cacciari & Futai, 2015) | Faro Focus$^{3D}$ | 976,000 | 2 | 10 |
| (Slaker, Westman, Fahrman, & Luxbacher, 2013) | Faro Focus$^{3D}$ | 976,000 | 2 | 10 |

Additionally, conventional rock mass characterization will be performed in order to have control information that allows a comparison of results obtained from the scans and have a better understanding on the rock mass structure. This information also will be used in order to classify the rock mass with the conventional rock mass classifications such as Q, MRMR, GSI and RMi.

### 5.3. Structural data processing

In order to process the scans and extract discontinuities' properties the software I-Site Studio provided by MAPTEK will be used. I-Site is a point cloud processing and modeling software that extracts geotechnical information from laser scans by using a set of geotechnical tools (MAPTEK, 2017). This software will be used in order to identify the orientation, density and size of the discontinuities. Figure 1.5 present a preliminary structural analysis with a scan obtained from CSM.

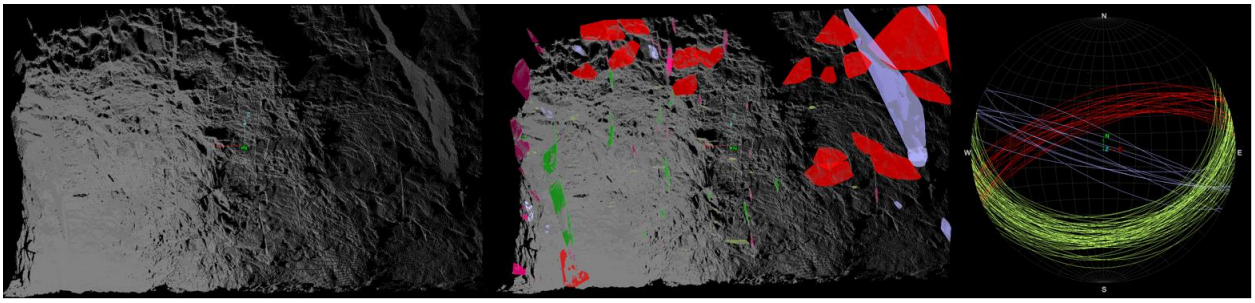

**Figure 1.5. Extraction of joint sets from a laser scans using the software I-SITE.**

### 5.4. Sample collection

Sample collection will take place in the areas previously selected. Due to the fact that the ore body lies between the two different types of limestone on both Hanging Wall and Footwall, samples from these formations will also be considered. The samples will be rock blocks which will be transported to the rock mechanics preparation lab, where NQ diameter cores will be extracted. The goal will be to obtain at least 3 samples for Triaxial test, 3 samples for direct shear, 3 samples for tensile strength, 3 samples for uniaxial compressive strength and

4 samples for point load, for each type of rock at each location. The results from this sampling stage will be the maps showing the different locations where the samples where extracted.

### 5.5. Rock mechanics laboratory testing

Among the properties to be considered for the blocks include mass density, intrinsic deformability properties (bulk & shear modulus or Young modulus or Poisson's ratio), intrinsic strength properties (Constitutive models and strength parameters such as compressive strength and tensile strength) and post-failure properties. On the other hand, joint properties including physical properties for joint friction angle, cohesion, dilation angle, and tensile strength, as well as joint normal and shear stiffness. The joint cohesion and friction angle correspond to the parameters in the Coulomb strength criterion (ITASCA, 2016). Generally, these parameters are obtained from rock laboratory tests. The laboratory tests proposed are presented in Table 1.5. This table also shows the intact rock properties and the discontinuity properties obtained from each test. These properties are the parameters that will feed numerical models.

**Table 1.5. Rock lab testing standards defined by the ASTM description and properties obtained.**

| ASTM Standard | Description | Properties obtained |
|---|---|---|
| **D2664-04** | Standard test methods for Triaxial compressive strength of undrained rock core specimens without pore pressure measurements | -Hoek & Brown failure criteria<br>-Young's modulus at different confinement pressures<br>- Basic friction angle for artificial joints |
| **D7012-14** | Standard test methods for compressive strength and elastic moduli of intact rock core specimens under varying states of stress and temperatures | - Uniaxial compressive Strength<br>- Young modulus<br>- Poisson's ratio |
| **D5607-08** | Standard test method for performing laboratory direct shear strength tests of rock specimens under constant normal force | - Mohr-Coulomb failure criteria for discontinuities (phi, c)<br>- Shear stiffness |
| **D5731-08** | Standard test method for determination of the point load strength index of rock and application to rock strength classifications | - Uniaxial compressive Strength (Indirect) |
| **D3967-16** | Standard test method for splitting tensile strength of intact rock core specimens | - Tensile strength of the rock (indirect) |
| **D2845-08** | Standard test method for laboratory determination of pulse velocities and ultrasonic elastic constants of rock | - Young's modulus (indirect)<br>- density<br>- Poisson's ratio |
| **D57873-14** | Standard test method for determination of rock hardness by rebound hammer method | - Uniaxial compressive Strength (Indirect) |

The expected results from the laboratory plan will be descriptive statistics comparing the results for all the geomechanical parameters (UCS, tensile strength, E, & Poisson's) comparing the properties between different types of rock. Additionally, the spatial variability of this properties will be analyzed. Summary maps will be elaborated in order to present the variability of the geomechanical properties of the mine.

### 5.6. Numerical modeling and design Considerations

A modeling plan has been developed in order to define a route that allows to generate models that provide a better understanding on the usage of 3DEC, but also to obtain models that represent the actual conditions of the CSM. The models include a continuous single pillar, a single pillar with a single oblique discontinuity, a single tunnel considering a discrete fracture network, a single pillar considering a discrete fracture network, the mining sequence of the CSM without considering any discontinuities and the mining sequence of the same mine considering the geotechnical conditions represented using a DFN. The numerical models predict and anticipate the potential wedges before mining into a new area. The aim of these models will be to set guidelines and methodologies that can apply to any underground project and help them to obtain particular answers to each specific problem.

### 5.7. Monitoring

After numerical modeling results are obtained, a site evaluation will be performed in order to verify these results. Once the simulations coincide with the actual behavior observed in the rock mass, design considerations and engineering measures to control the instability mode will be proposed.

## 6. CONCLUSIONS

Different authors have proven that TLS technologies are a powerful suite of tools for rock mass characterization. Not only are they time efficient, but they also provide detailed information, which processed adequately considering actual limitations in both processing and modeling software, allows to generate models that represent accurately jointed rock mass behavior. DEM software is a powerful tool to interpret and analyze structurally controlled instability in underground excavations. This software with detailed structural information may provide not only deterministic but also stochastic analysis allowing the engineer to have a better understanding of rock mass behavior and provide better engineering solutions. The integration of both technologies (TLS and DEM) may be potentially used in order to prevent rock falls in underground excavations to enhance worker's safety. The CSM is an ideal environment to apply both technologies, and to develop risk analysis methodologies based on these technological advances, ultimately reducing accidents related to rock falls in the underground stone mine industry. The proposed methodology will be applied in the CSM and results will be presented in further work.

## 7. ACKNOWLEDGEMENTS

This work is funded by the National Institute for Occupational Safety and Health's Mining Program under Contract No. 200-2016-91300. The author's would like to thank Lhoist mining engineers and management for their support and guidance during this project. MAPTEK is acknowledged for providing a license of the software I-Site. Views expressed here are those of the authors and do not necessarily represent those of any funding source.

## REFERENCES


Brady, B., & Brown, E. (1985). *Rock Mechanics for Underground Mining.* UK: Chapman & Hall.

Cacciari, P., & Futai, M. (2015). Mapping and Characterization of Rock Discontinuities in a tunnel Using 3D Terrestrial Laser Scanning. *Bulletin of Engineering Geology and the Environment*.

Cacciari, P., & Futai, M. (2017). Modeling a Shallow Rock Tunnel Using Terrestrial Laser Scanning and Discrete Fracture Networks. *Rock Mechanics and Rock Engineering*, 1217-1242.

Cacciari, P., Morikawa, D., & Futai, M. (2015). Modelling a Railway Rock Tunnel Using Terrestrial Laser Scanning and The Distinct Element Method. *Integrating Innovations of Rock Mechanics*, 101-108.

Cundall, P. (1971). A computer model for simulating progressive large scale movements in blocky rock systems. *Proc. Symp. Rock Fracture (ISRM)*, II-8.

Cundall, P., & Hart, R. (1985). "Development of Generalized 2-D and 3-D Distinct Element Programs for Modeling Jointed Rock," Itasca Consulting Group. *Misc. Paper SL-85-1*. US Army Corps of Engineers.

Fekete, S. (2010). *Geotechnical Applications of LiDAR for Geomechanical Characterization in Drill and Blast Tunnels and Representative 3-Dimensional Discontinuum Modelling.* Kingston: Queen's University.

Fekete, S., & Diedrichs, M. (2013). Integration of Three-dimensional Laser Scanning with Discontinuum Modelling for Stability Analysis of Tunnels in Blocky Rockmasses. *International Journal of Rock Mechanics & Mining Sciences*, 11-23.

Goodman, R. (1989). *Introduction to Rock Mechanics.* New York: Wiley.

Goodman, R., & Shi, G. (1985). *Block Theory and Its Application to Rock Engineering.* London: Prentice-Hall.

Grenon, M., Landry, A., Hadjigeorgiou, & Lajoie, P. (2017). Discrete Fracture Network Based Drift Stability at the Éléonore Mine. *Mining Technology*, 22-33.

Hoek, E. (2000). *Rock Engineering.* North Vancouver: A.A. Balkema Publishers.

Hudson, J., & Harrison, J. (2000). *Engineering Rock Mechanics.* Oxford: Imperial College of Science, Technology and Medicine, University of London, UK.

ISRM. (1978). Suggested Methods for the Quantitative Description of Discontinuities in Rock Masses. *International Journal on Rock Mechanics, Mining sciences & Geomechanics. Vol 15*, 319-368.

ITASCA. (2016). *3 Dimensional Discrete Element Code User's Guide.* Minneapolis: Itasca Consulting Group.

Kemeny, J., Turner, K., & Norton, B. (2006). LIDAR for Rock Mass Characterization: Hardware, Software, Accuaracy and Best-Practices. *Laser and Photogrammetric Methods for Rock Face Characterization*, 49-61.

Lorig, L., & Varona, P. (2013). Guidelines for numerical modelling of rock support for mines. *Ground Suport 2013*, 81-105.

MAPTEK. (2017, October 05). *MAPTEK I-Site Studio: Geotechnical Module.* Retrieved from http://www.maptek.com/pdf/i-site/Maptek_I-Site_Studio_Geotechnical_Module.pdf

Martin, C., Kaiser, P., & Christiansson, R. (2003). Stress, instability and design of underground excavations. *Rock Mechanics and Mining Sciences*, 1-21.

MSHA. (2016). *Accident Injuries Data Set.* Mine Safety and Health Administration.

MSHA. (2016). *Metal/Nonmetal Daily Fatality Report.* Mine Safety and Health Administration.

NIOSH. (2011). *Pillar and Roof Span Design Guidelines for Underground Stone Mines.* Pittsburg: National Institute for Occupational Safety and Health.

Pierce, M. (2017). An Introduction to Random Disk Discrete Fracture Network (DFN) for Civil and Mining Engineering Applications. *ARMA e-Newslatter 20*, 3-8.

Rocscience. (2017, October 3). *Unwedge Online Help*. Retrieved from Program Assumptions: https://www.rocscience.com/help/unwedge/webhelp4/Unwedge.htm

Rocscience. (2017, September 13). *Unwedge Theory.* Retrieved from rocscience Website: https://www.rocscience.com/help/unwedge/webhelp4/Unwedge.htm

Rogers, S., Bewick, R., Brzovic, A., & Gaudreau, D. (2017). Integrating Photogrametry and Discrete Fracture Network Modelling for Improved Conditional Simulation of Underground Wedge Stability. *8th International Conference in Deep and High Stress Mining*, 599-610.

Slaker, B., Westman, E., Fahrman, B., & Luxbacher, M. (2013). Determination of Volumetric Changes from Laser Scanning at an Underground Limestone Mine. *Mining Engineering, Vol. 65 Issue 11*, 50-54.

Voyay, I., Roncella, R., Forlani, G., & Ferrero, A. (2006). Advanced techniques for geo structural surveys in modelling fractured rock masses: application to two Alpine sites. *Laser and Photogrammetric Methods for Rock Face Characterization*, 102-108.

Wu, Q., Kulatilake, P., & Tang, H. (2011). Comparison of rock discontinuity mean trace length and density estimation methods using discontinuity data from an outcrop in Wenchuan area, China. *Comput Geotech*, 258-268.

# Chapter 2 Application of Laser Scanning for Rock Mass Characterization and Discrete Fracture Network Generation in an Underground Limestone Mine[2]

Juan J. Monsalve, Jon Baggett, Richard Bishop, Nino Ripepi
Mining and Minerals Department, Virginia Polytechnic Institute & State University

**Abstract.**

Terrestrial laser scanning (TLS) is a useful technology for rock mass characterization. A laser scanner produces a massive point cloud of a scanned area, such as an exposed rock surface in an underground tunnel, with millimeter precision. The density of the point cloud depends on several parameters from both the TLS operational conditions and the specifications of the project, such as the resolution and the quality of the laser scan, the section of the tunnel, the distance between scanning stations, and the purpose of the scans. One purpose of the scan can be to characterize the rock mass and statistically analyze the discontinuities that compose it for further discontinuous modeling. In these instances, additional data processing and a detailed analysis should be performed on the point cloud to extract the parameters to define a discrete fracture network (DFN) for each discontinuity set. I-Site Studio is a point cloud processing software that allows users to edit and process laser scans. This software contains a set of geotechnical analysis tools that assist engineers during the structural mapping process, allowing for greater and more representative data regarding the structural information of the rock mass, which may be used for generating DFNs. This paper presents the procedures used during a laser scan for characterizing discontinuities in an underground limestone mine and the results of the scan as applied to the generation of DFNs for further discontinuous modeling.

Keywords: rock mass characterization, laser scanning, discrete fracture network, I-Site Studio

## 1. INTRODUCTION

According to the Mine Health and Safety Administration (MSHA), between 2006 and 2016, the underground stone mining industry had the highest fatality rate in 4 out of 10 years, compared to any other kind of mining (MSHA, 2016). Additionally, during that same time, 40% of the fatalities were due to ground control issues, such as roof and rib collapses and pillar bursts. The National Institute for Occupational Safety and Health (NIOSH) developed

[2] Conference paper published in the proceedings of the **37th International Conference on Ground Control in Mining** in Morgantown , WV. This paper was also selected to be published in the **International Journal of Mining Science and Technology,** Available on line 12 December 2018.

guidelines for designing underground stone mines (Esterhuizen, Dolinar, Ellenberger, and Prosser, 2011). However, these guidelines do not apply to all underground stone mines.

Monsalve, Baggett, Bishop, and Ripepi (2018) present a case study of an underground limestone mine experiencing a structurally controlled mode of failure. The authors analyze different methods to study that type of instability. They conclude that the integration of terrestrial laser scanning (TLS) with discrete element modeling (DEM) can be used to prevent rock falls in underground excavations to enhance worker safety. However, an adequate rock mass characterization and structural mapping must be performed in order to generate reliable models that allow the engineer to have a better understanding of the rock mass behavior.

The final product of a laser scan is a point cloud that represents the surfaces of the objects scanned, in this case the rock surface in an underground environment. The density of the point cloud depends on a series of parameters from both the laser scanner operational conditions and the specifications of the project, such as the resolution and the quality of the laser scan, the section of the tunnel, the distance between scanning stations, and the purpose of the scans. The lead engineer defines these parameters. One purpose of the scan can be to characterize the rock mass and statistically analyze the discontinuities that compose it for further discontinuous modeling. In these instances, additional data processing and a detailed analysis should be performed on the point cloud to extract the parameters that define a discrete fracture network (DFN) for each discontinuity set. A DFN is a geometric representation in three dimensions of a geological structure defined by statistical information of the structure characteristics measured in the field, such as orientation, density, and size (Pierce, 2017).

This paper describes the methodology used in a case study mine to perform a structural mapping on a rock mass in order to obtain the input data needed to create a DFN for DEM. Different software packages were used to perform these analyses:

1) SCENE was used to import the laser scans and generate a project point cloud (Faro, 2018).
2) I-Site Studio was used to perform the structural mapping and to estimate the trace length and spacing of the different fractures (Maptek, 2018).
3) Dips was used to characterize and group the discontinuity sets (Rocscience, 2018).
4) 3DEC™ was used to generate the DFN (Itasca, 2018).

## 2. GEOTECHNICAL CONDITIONS

A specific area was defined in the case study mine to focus the present research. The mine research team and personnel selected this area because of the presence of significant ground control issues, mainly defined as structurally controlled instability failure. This was evidenced by:

1) jointing pattern where at least four joint sets were well defined,

2) observed wide-joint spacing, generally ranging from 0.6 m to 2 m,
3) amount of fallen blocks observed on the floor with cubical and tabular shapes,
4) joint surfaces defined as mostly closed, flat and smooth, with a JRC ranging from 2 to 4, completely dry and fresh,
5) other geological structures, such as faults and contacts, that could generate a rock fall in the absence of the required support

This failure mechanism is enhanced by the multiple karst formations present in the mine, which, during excavation, tends to generate rock blocks up to 4 $m^3$ (144 $ft^3$) that pose a high risk for workers, equipment, and the overall mining plan (Monsalve, Baggett, Bishop, and Ripepi, 2018).

Figure 2.1 shows a plan view of the area of interest. This illustrates a karst structure that crosses both tunnels and has a variable aperture reaching up to 0.5 m. Figure 2.1.A) is a view from the tunnel to the karst void, while Figure 2.1.B) presents a pile of material that fell down from the karst structure. Water and mud have also fallen out of the karst void. For these reasons, laser scans were carried out close to this area in order to map the structural conditions and to perform further numerical modeling to understand and prevent rock falls in this section of the mine.

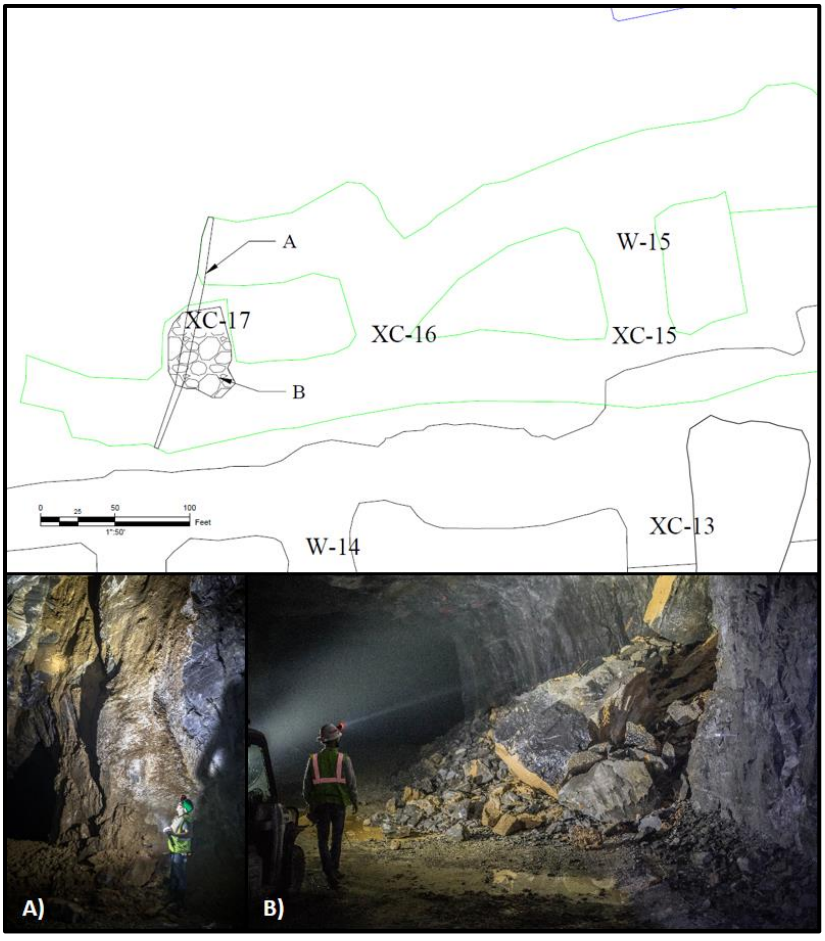


**Figure 2.1. Geotechnical conditions observed in the study area. A) View from the tunnel towards the karst void on the upper half of the drift. B) Pile of fallen material from the karst void on the lower drift.**

# 3. METHODOLOGY

The following methodology describes in detail the procedures used by the authors to perform the laser scans in the study area, to import and process the information obtained from those scans, and to create the respective DFNs resulting from the virtual structural mapping. This methodology was designed based on lessons learned from experiences presented in previous works (Fekete, 2010a; Fekete 2010b; Slaker, 2015) and practices using the laser scan and different software packages for these procedures. Additionally, documents, such as the Laser Scan User Manual (FARO, 2011) and user guides on planning and performing the laser scans provided by the laser scan provider company (DiCarlo, 2013), were used to complement this methodology.

## 3.1. Definition of operational conditions

A laser scanner is a surveying apparatus that produces a massive point cloud (millions of points per scan), indicating the positions of the scanned objects. This equipment sends an infrared laser beam into the center of a rotating mirror, which deflects the laser beam onto a vertical rotation into the environment being scanned (Figure 2.2.A). Scattered light from surrounding objects is then reflected back into the scanner. The equipment is able to identify two waves: the one sent out by the equipment and the one reflected by the object. The phase shift between both waves is used to calculate the distance of the measured object (FARO, 2011). Then, by using angle encoders to measure the mirror rotation and horizontal rotation of the scanner, the x, y, z coordinates of each point are calculated, resulting in a point cloud that is stored in a removable SD memory card (FARO, 2011). Figure 2.2.B) presents the vertical and horizontal rotation of the laser scan. The laser scan unit used during this study was a FARO® Focus3D, acquired by the Mining and Minerals Engineering Department of Virginia Tech in 2011.

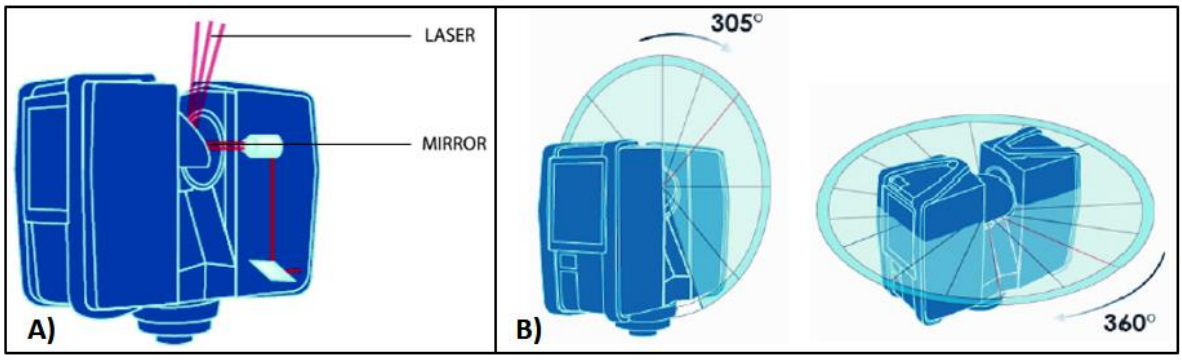


**Figure 2.2. A) Laser deflection and B) Vertical and horizontal laser rotation (FARO, 2011).**

The two main variables to be defined during the scan are the resolution and the quality. These two variables affect the time of the scan and the density of the point cloud (DiCarlo, 2013). The size of the excavation to be scanned, the distance of the scanner from the tunnel face, and the spacing between stations also affect the results. According to Fekete, the optimal

positioning of a laser scan from the face is between 0.5 to 1 times the diameter of the excavation (2010b). In this particular case, the diameter of the excavation is 13 m, and 1 times the diameter was used as the distance between the scanner and the face.

Once the distance from the face to the scanner was defined, the adequate resolution and quality were selected. Since these parameters vary from site to site, a set of scans were performed in order to define which combination of resolution and quality values provided, in a reasonable scan time, a scan with an acceptable point cloud density to perform an adequate structural mapping of the rock mass.

Table 2.1 shows the different operational conditions tested in the mine, the real time that it took to perform each scan, and the point cloud size and the point cloud density. Twelve scans were performed, processed, and converted into point clouds, which were imported to I-Site Studio for analysis. The total point count for each cloud was measured. To measure the average point cloud density, three 5 m x 5 m mapping windows were generated, one on the right wall, another one on the left wall, and the last one on the roof. The amount of points contained within each mapping window was measured and recorded. The point cloud density was calculated by dividing the number of points by the area of each mapping window (25 $m^2$). Then, for each scan, the average point cloud density was calculated by averaging the point cloud density on each mapping window. The scans performed with the resolutions of 710.7 million of points and 177.7 million of points were discarded since the amount of data obtained exceeded the requirements and significantly increased the scan time.

**Table 2.1. Proposed resolutions and qualities evaluated on the field.**

| Scan | Resolution | | Quality | Real Scan time [hh:mm:ss] | Point Count | Average Point Cloud Density [Points/$cm^2$] | Overall Rating |
|---|---|---|---|---|---|---|---|
| | Millions of Points/Scan | | | | | | |
| S-006 | 44.4 | 1/4 | 1x | 0:05:12 | 38,103,388 | 11.42 | 5.04 |
| S-007 | 44.4 | 1/4 | 2x | 0:06:06 | 41,229,797 | 12.48 | 4.31 |
| S-008 | 44.4 | 1/4 | 3x | 0:07:53 | 41,684,133 | 12.64 | 3.36 |
| S-009 | 44.4 | 1/4 | 4x | 0:11:28 | 41,229,797 | 12.66 | 2.34 |
| S-010 | 28.4 | 1/5 | 2x | 0:05:27 | 26,273,301 | 8.06 | 4.79 |
| S-011 | 28.4 | 1/5 | 3x | 0:06:36 | 26,573,225 | 8.13 | 3.96 |
| S-012 | 28.4 | 1/5 | 4x | 0:08:54 | 26,630,099 | 7.97 | 2.95 |

For selecting the best operational conditions, the real scan time and the average point cloud density were taken into account. These values were normalized and averaged. The best operational conditions for this case were a resolution of 1/4 and a quality of 1x, which required a scan time of 5 minutes and 12 seconds and yielded a point cloud density of 11 points/$cm^2$. The obtained point cloud density is considered acceptable for structural mapping, bearing in mind that previous work has performed structural mapping on a LiDAR extracted

point cloud with either a density of 4 points/cm$^2$ (Lato, Diederichs, Hutchinson, and Harrap, 2009) or with a density of 16 points/cm$^2$ (Cacciari and Futai, 2017).

### 3.2. Stations location

Laser scanning has been used for multiple applications in both the tunneling and mining industry, such as support evaluation, scaling assessments, leakage mapping, analysis of structurally controlled overbreak, structural mapping, roughness evaluation, and deformation analysis (Fekete & Diedrichs, 2013). Fekete (2010b) determined that the best practice for the laser scanner distance from the face is from 0.5 to 1 diameter. In addition, Fekete defined the optimal separation between stations is 1 diameter of the excavation to ensure the maximum coverage of the area with minimum overlap between scans and data redundancy (2010b).

Using these recommendations, the stations were positioned 13 m apart. Figure 2.3 shows the estimated locations of the different stations in which the laser scanner was set. The survey was performed around the pillar between crosscuts 15 and 16.

### 3.3. Scans Referencing

The laser scanner used does not have an integrated global positioning system. This means the scans are not georeferenced unless there is a reference point with known coordinates. The laser scanner used does have an internal compass and inclinometer that allows orientation of each scan with respect to magnetic north (FARO, 2011).

Without a georeferencing tool, the only way to integrate different scans into a single model is to identify common reference points, or objects, present between scans. FARO suggests the use of checkboards or spherical references placed in strategic places that can be detected from the two stations that will be referenced together. In this particular case, 21.5 cm diameter inflatable balls were used as spherical targets between scans. Table 2.2 shows the recommended distance from the target to the laser as a function of the target size and laser scan operational conditions. Considering the recommended target distances, spacing between stations, and reference target sizes, four references were used in order to reference the current station with the two other stations (one forward and one behind). As the station moves, the references that were behind it will be leapfrogged forward as the scans advance in order to reference all the scans performed in the area together. This procedure is depicted in Figure 2.4.

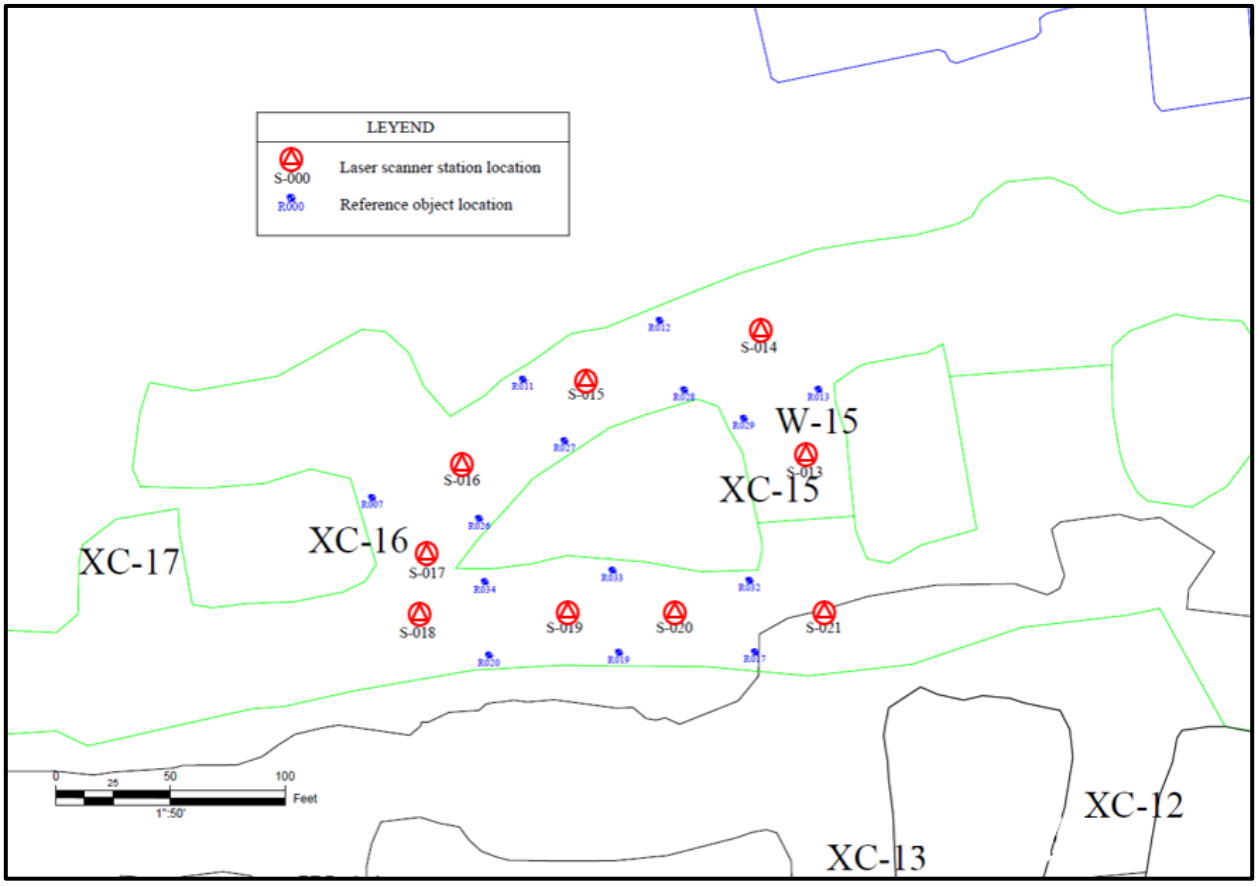


**Figure 2.3. Estimated location of the laser scan stations.**

**Table 2.2. Recommended target spacing from laser scanner (DiCarlo, 2013).**

| Recommended target spacing | | | |
|---|---|---|---|
| Sphere size | 145 mm | Sphere size | 230 mm |
| Resolution Setting | Target Distance (max) in m | Resolution Setting | Target Distance (max) in m |
| 1/16 | 5 | 1/16 | 7 |
| 1/10 | 7 | 1/10 | 11 |
| 1/8 | 9 | 1/8 | 14 |
| 1/5 | 15 | 1/5 | 22 |
| 1/4 | 18 | 1/4 | 27 |
| 1/2 | 37 | 1/2 | 55 |
| 1/1 | 73 | 1/1 | 110 |

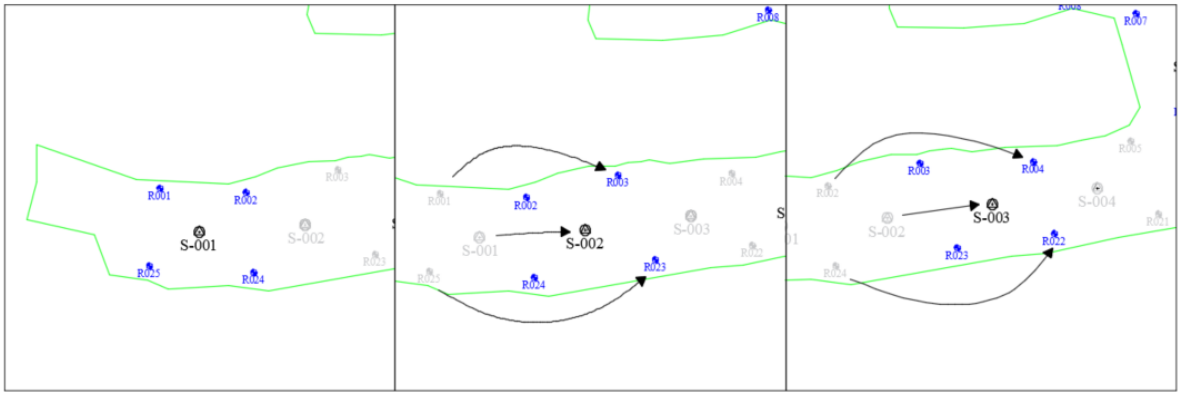


**Figure 2.4. Reference objects placement along different scan stations.**

### 3.4. Data importing and processing

Once the operational conditions and the scanning procedure were defined, the laser scans were performed. Nine laser scanning stations were set around the pillar between crosscuts 15 and 16. In order to download the laser scans and convert them into point clouds, the software SCENE was used. Before generating the final compiled point cloud, the scans were spatially referenced with each other using the reference points. This process is defined as "registration."

When a laser scan is performed, the scanner sets the position of the mirror as the coordinates x=0, y=0 and z=0. If a reference point is observed from two different places, a spatial relation between those stations can be made (FARO, 2018). SCENE allows the user to open two stations at the same time and select the common points between them. Figure 2.5 presents the spatial registration process at Stations 015 and 016. There are two reference spheres on each scan.

After referencing all the scans, SCENE evaluates the distance error between points and the overlap between scan stations. This software suggests that errors with a value of less than 8 mm and overlap values greater than 25% provide acceptable results on the registration process (FARO, 2018). When the errors are greater than 20 mm and the overlap between stations is less than 10%, the results from the laser scan are not acceptable; therefore, the scanning process must be repeated by using more reference objects or by reducing the distance between stations. Values between this ranges may still be accepted, considering a less precision on the laser scan results.

Table 2.3 presents the results obtained from the registration of the nine laser scans, which obtained acceptable values for both the errors (maximum point error 6.7 mm) and the overlap (minimum overlap 25.2 %). According to these results, the recommendations made by Fekete (2010b) regarding the laser scan station locations are acceptable in this particular case. Finally, in order to proceed with the analysis, the point cloud was saved as a laser scan file.

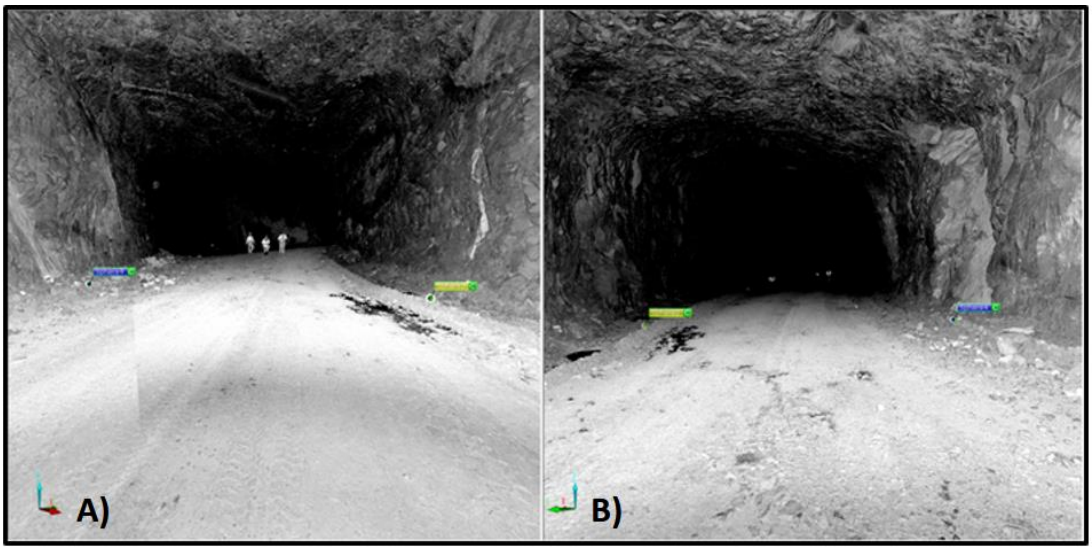


**Figure 2.5. Registration and verification of stations 015 and 016. A) View from the station 015 towards station 016 and the reference spheres. B) View from the station 016 towards station 015 and the reference spheres.**

**Table 2.3. Point cloud registrations statistics (FARO, 2018).**

| Scan Point Statistics | Obtained Values | Acceptable values | Unacceptable values |
|---|---|---|---|
| Maximum Point Error | 6.7 mm | < 8 mm | > 20 mm |
| Mean Point Error | 4.3 mm | | |
| Minimum Overlap | 25.2 % | > 25.0 % | < 10.0 % |

### 3.5. Structural data processing

I-Site Studio is a point cloud processing software that allows users to edit and process laser scans. This software contains a set of geotechnical analysis tools that assist engineers during the structural mapping process. This software allows for greater and more representative data regarding the structural information of the rock mass, which can be used to generate DFNs. The point cloud generated from the laser scans was imported into I-Site Studio to perform a structural mapping along the scanned tunnels. The generated file contained 331,230,871 points, or 14.7 gigabytes, of spatial data. Due to computational limitations, the point cloud was divided into 10 smaller sections, and each section was divided into right wall, left wall, and roof. This allowed researchers to perform the structural mapping with a useful amount of information that prevented the system from crashing.

Figure 2.6 shows the left wall of the third section generated from the overall point cloud, where it is possible to observe the geological structures. Some of these structures exhibit similar orientations and relatively large exposed areas, while others are not easy to observe due to the sight angle. Additionally, the bottom half of the figure shows the mapped discontinuities output from I-Site Studio. For the mapping process, the points that belong to

the same discontinuity plane have to be manually selected. Using the geotechnical tool "query dip and strike," an average plane is generated that accounts for the coordinates of each selected point. This process was repeated along the whole model section by section. Figure 2.7 shows a plan view of the final point cloud with the mapped discontinuities. In total, 874 structures were mapped in the area.

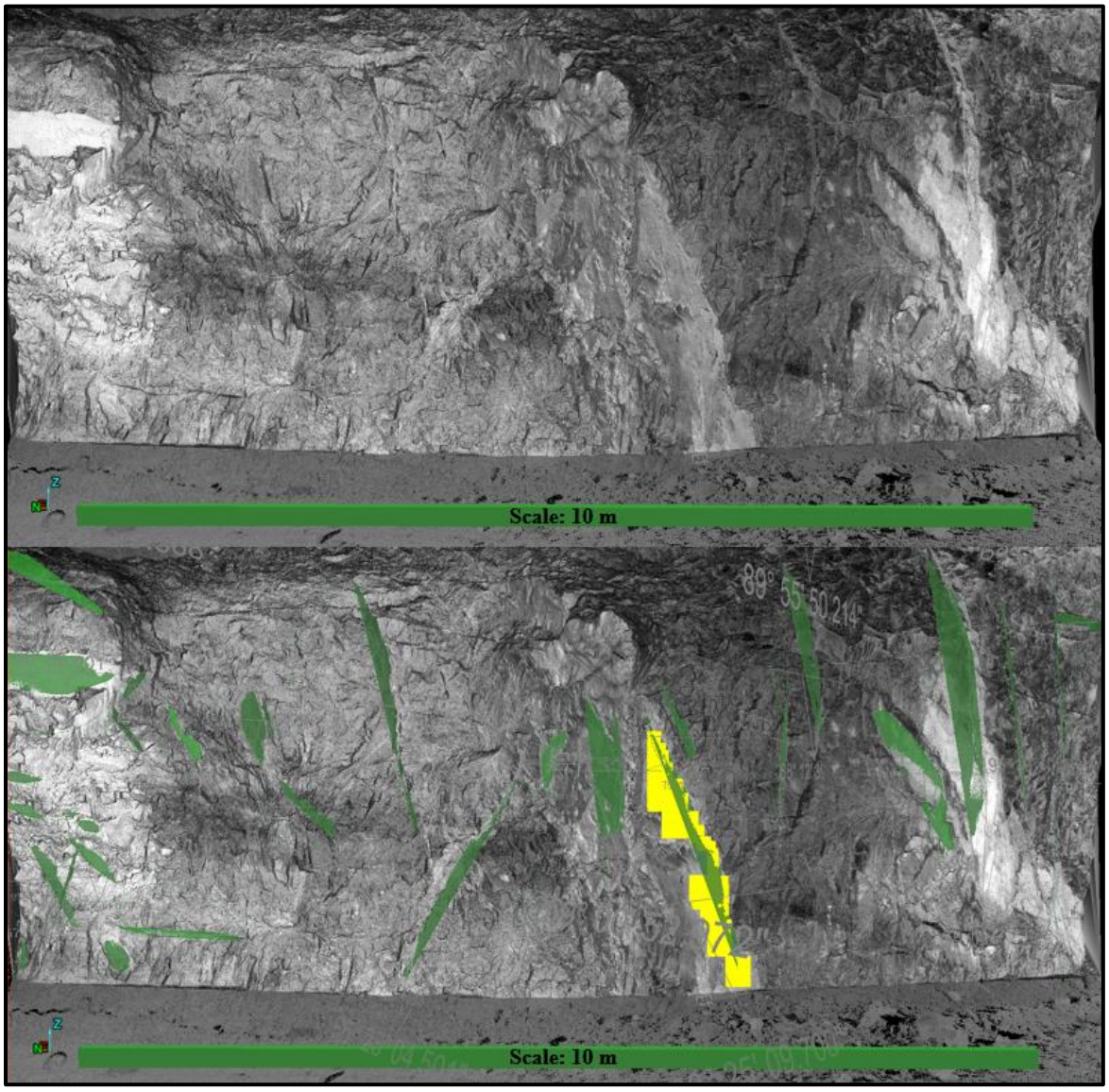


**Figure 2.6. Structural mapping in I-Site.**

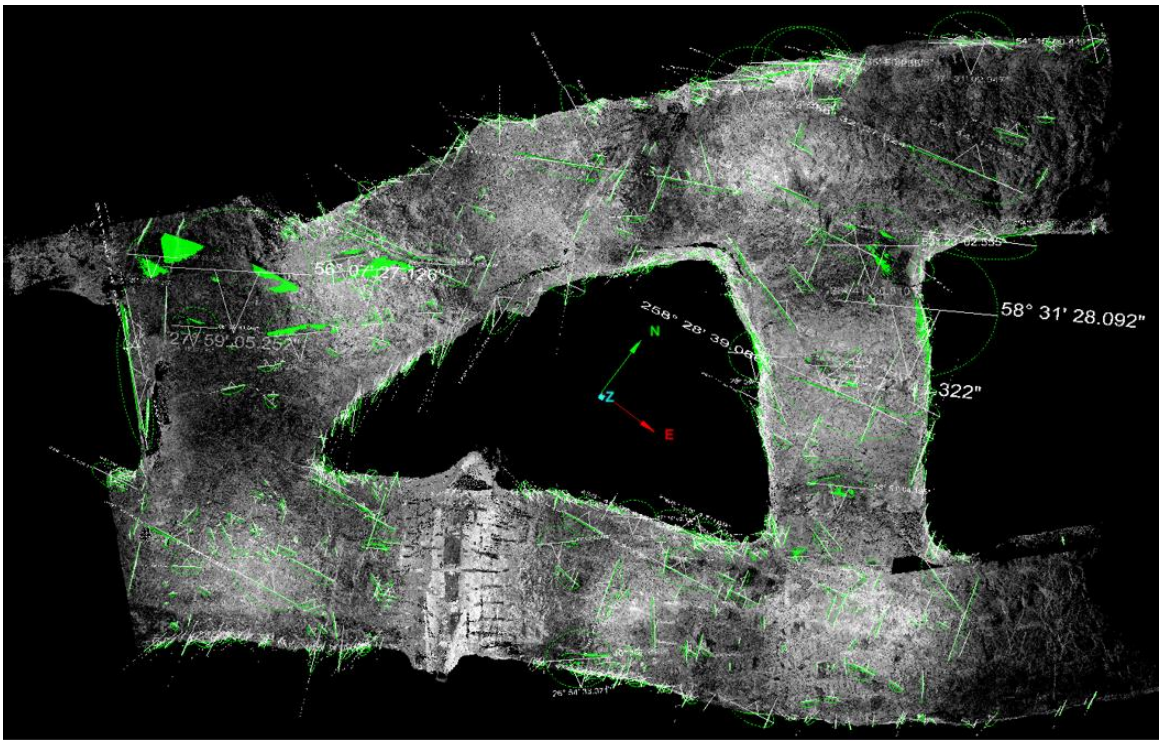


**Figure 2.7. Plan view of the scanned area with structural features mapped.**

### 3.6. DFN generation

Once all the relevant structural features observed in the 3D model were mapped, the structural data was exported into an Excel file. Structural features extracted from a point cloud into I-Site Studio contain x, y, and z coordinates; orientation information (dip, dip direction, and strike); and size information (trace length and area). This information was imported into the software Dips, which was used to analyze and classify the structures into joint sets. The defined joint sets can be filtered and reimported into I-Site Studio as individual joint sets, where geotechnical tools can calculate the spacing between discontinuities from the same family.

3DEC is a DEM software that can use DFNs to generate geological structures in a rock mass. These DFNs are a set of discrete, planar, disk-shaped, and finite size fractures, which are used to cut through the blocks that constitute the model. These sets of disks are defined based on statistical information on the characteristics of the measured fractures in the field, such as orientation, size, and density (Pierce, 2017). All of these characteristics can be obtained from the information mapped from the laser scans.

The orientation is defined by the dip (steepest declination) and dip direction (measured clockwise from true north) of a plane. This defines the spatial position with respect to the true north and a horizontal plane (ISRM, 1978). Orientation parameters are defined as circular data. Due to this, the most adequate distribution to represent this data is the Fisher distribution, which is used to represent 3D orientation vectors (Rocscience, 2018). This

distribution depends on the factor k that can be estimated form datasets greater than 30 poles. The software Dips is able to calculate each k coefficient, mean dip, and dip direction for each joint set.

While the actual size of a structure is difficult to measure, it is regularly estimated as the trace length of the discontinuity, which is the length of the exposed structure. In this case, the trace length was considered the maximum length of the mapped plane. This information provided a statistical distribution for the trace length of each joint set.

Fracture density is a measure of the frequency of discontinuities belonging to the same family. This parameter could be measured as the number of fractures per unit length ($P_{10}$), the length of fractures per unit area ($P_{21}$), or the area of fractures per unit volume ($P_{32}$) (ITASCA, 2018). When a DFN is generated in 3DEC, this parameter serves as a stopping condition (Cacciari, Morikawa, and Futai, 2015). For instance, when $P_{10}$ is used as the density parameter, a sampling line is defined, and 3DEC will randomly create discs based on the predefined size and orientation distributions until the number of fractures intersecting that scan line meet the value set as $P_{10}$. For this work, the $P_{10}$ estimate was based on the spacing of the discontinuities calculated using I-Site Studio, considering the definition of discontinuity frequency on a scan line as the reciprocal of the mean spacing (Hudson and Harrison, 2000). In this case, spacing values less than 50 cm were not considered when calculating the fracture density because their respective fracture densities were not comparable with those observed in the field.

## 4. RESULTS AND DISCUSSION

The methodology described in this work allowed the authors to obtain a 3D virtual structural mapping of the area of interest. This information is important to help visualize and understand the structural setting for an area of interest and to identify possible blocks that may form and generate rock falls. Figure 2.8 summarizes the virtual structural mapping and the statistical analysis for the trace length and the lineal fracture density of each identified structural set. Four discontinuity sets were defined from the mapped discontinuities:

- Set 1 is almost perpendicular to the tunnel orientation and presents a sub-vertical dip.
- Sets 2 and 3 are oblique joints with a steep dip.
- Set 4 corresponds to the bedding planes and contacts between rock units, which are almost parallel to the tunnel orientation and its mean dip of 29°.

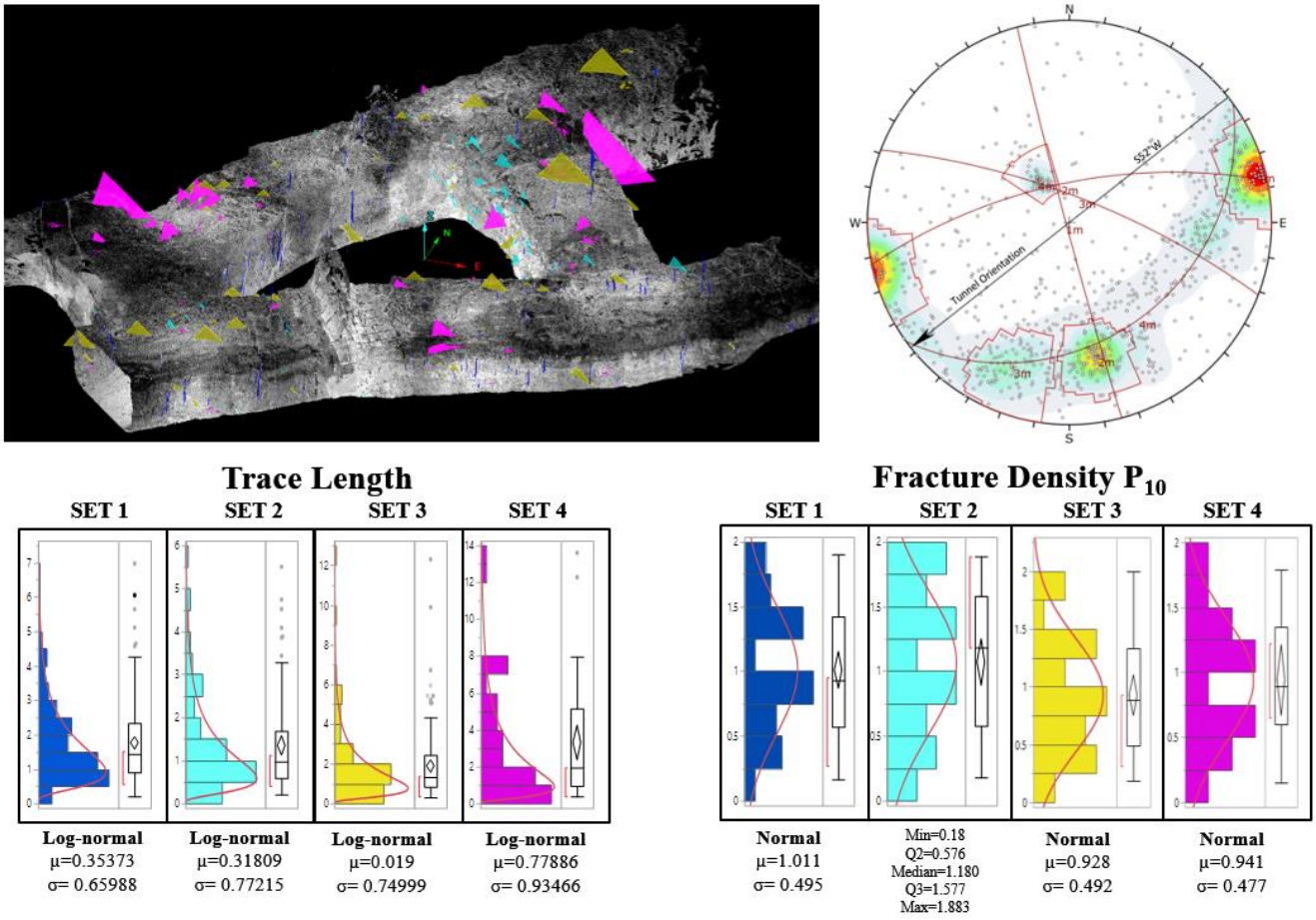


**Figure 2.8. Stereo net Analysis and trace length and fracture density summary statistics.**

Table 2.4 shows the statistical summary for the orientation, size, and density of each individual discontinuity set. This information was used to generate a DFN in 3DEC for each discontinuity set. Figure 2.9 shows each individual DFN and the intersection of all four DFNs. It is also possible to observe a stereographic analysis of the generated disks, which can be compared with the stereographic analysis obtained from the virtual mapping. The major challenge identified during DFN generation was density definition. If the lineal density is considered, the value is only considered along a single sample line. Therefore, if the control volume in which the fracture network is being generated is significantly larger than the sizes of the disks, a large number of disks will be generated before the fracture density condition is met.

**Table 2.4. Statistical Summary of the joint properties for each joint set.**

| SET / PARAMETERS | | S1 N=157 | S2 N=127 | S3 N=97 | S4 (Bedding) N=45 |
|---|---|---|---|---|---|
| Orientation | Dip [°] | 88 | 68 | 75 | 29 |
| | Dip Direction [°] | 255 | 348 | 21 | 144 |
| | K (Fisher) | 103.9 | 102.4 | 69.5 | 197.3 |
| Size | Distribution | Log-normal | Log-normal | Log-normal | Log-normal |
| | Mean | 0.353 | 0.318 | 0.018 | 0.778 |
| | Standard deviation | 0.659 | 0.772 | 0.749 | 0.934 |
| Density | Number of fractures per unit length of scan line (P10) | Normal μ=1.011 σ= 0.495 | Min=0.18 Q2=0.576 Median=1.180 Q3=1.577 Max=1.883 | Normal μ=0.928 σ=0.492 | Normal μ=0.941 σ=0.477 |

It is important to note that the DFNs obtained in this work that resulted from a virtual mapping on a laser-scanned area do not represent the final structural setting of the simulated rock mass. 3DEC uses these discs to cut through the blocks that conform the model, ultimately obtaining a set of blocks with fractures that were generated based on the DFNs. Because of this, it is important to compare the final structural setting of the simulated rock mass with conditions observed in the field. If these differ, the model should be calibrated to obtain the best representation of the actual rock mass. Additionally, it is worth mentioning that the DFN models result from statistical distributions obtained from measured values; therefore, each time the model is run, it generates a different DFN producing different outputs. In order to obtain a significant result for the model, a stochastic analysis must be performed to address significant conclusions from the simulations.

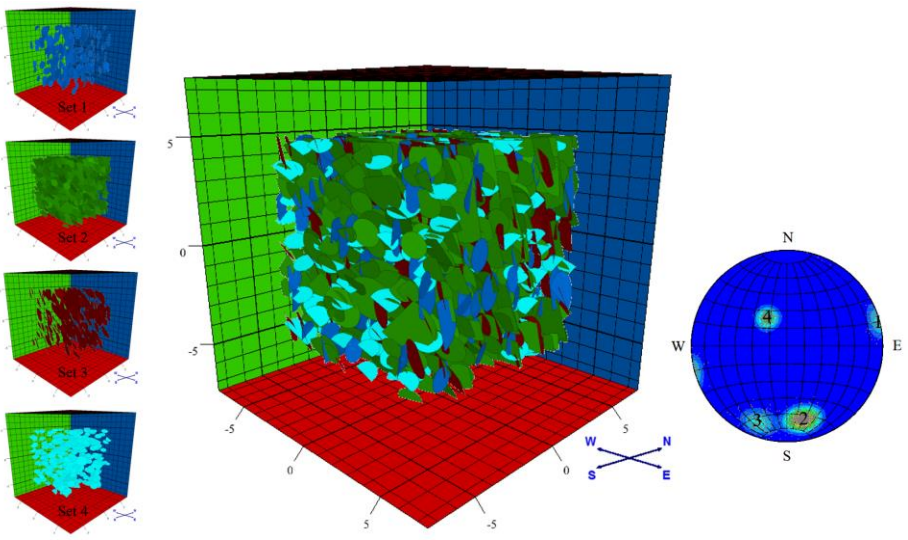


**Figure 2.9. DFN Generated based on the scanned data.**

## 5. FURTHER WORK

Since the methodology presented in the present study was developed to obtain information relevant for generating DFNs only, no mechanical properties of discontinuities on the rock mass have been measured yet. Thus, performing rock mechanics laboratory tests to measure the joint strengths is necessary. In addition, fieldwork aimed at measuring the wall strength and the roughness of each joint set will be performed. In addition, intact rock samples will also be collected to evaluate the mechanical properties of the footwall, orebody, and hanging wall. These parameters will be used as inputs for the numerical models and compared with observed conditions in the mine.

## 6. CONCLUSIONS

This paper describes the methodology used to perform virtual structural mapping in an underground mine from information obtained from a set of laser scans in an area that presents a structurally controlled failure mechanism. The following conclusions are derived from this work:

1. Planning the scanning project is fundamental in order to save time during the scanning process, reduce errors on the resulting point cloud, and obtain the necessary information required for the specific need.

2. While there is no existing guideline for performing an underground laser-scanning project, the experiences from other authors are valuable in defining the conditions of the scanning. For this study, following the recommendations of Fekete and Diedrichs (2013) allowed us to obtain a maximum point error of 6.7 mm and a minimum overlap between scans of 25.2%, both acceptable values according to FARO (2018).

3. It is important that geologists or engineers performing the structural mapping from the project point cloud have spent adequate time in the field in order to avoid any misleading interpretation and to ensure the results concur with those observed in the field.

4. Information extracted from the laser scans provides sufficient information to perform a statistical analysis of the variables required to generate a DFN for each identified structural set. However, further numerical models are required to define the effectiveness of this methodology in accurately representing the rock mass structure.

5. In order to perform this kind of analysis, the integration of four different software packages is required. Therefore, it is important to define an adequate workflow, which identifies the inputs required for each program and the outputs to be obtained. It is also important for the engineer to understand the limitations of each software and how these limitations can affect the results of the models.

6. Finally, the criteria of the engineer, based on their experience in the field and observed ground conditions, are fundamental for deriving a conclusion from the results of the analyses.

## 7. ACKNOWLEDGEMENTS

This work is funded by the NIOSH Mining Program under Contract No. 200-2016-91300. The authors would like to thank ITASCA for their support and guidance during this project. Maptek is acknowledged for providing a license of the software I-Site Studio. Views expressed here are those of the authors and do not necessarily represent those of any funding source.

## REFERENCES

Cacciari, P. and Futai, M. (2017). "Modeling a shallow rock tunnel using terrestrial laser scanning and discrete fracture networks." *Rock Mechanics and Rock Engineering 50*(5): 1217–1242.

Cacciari, P., Morikawa, D., and Futai, M. (2015). "Modelling a railway rock tunnel using terrestrial laser scanning and the distinct element method." In: *Proceedings of the 8th South American Congress on Rock Mechanics*. Lisbon, Portugal: International Society for Rock Mechanics and Rock Engineering, pp. 101–108.

DiCarlo. (2013). *3D Laser Scanning Set Up*. DiCarlo Precision Instrument, Inc.

Esterhuizen, G. S., Dolinar, D. R., Ellenberger, J. L., and Prosser, L. J. (2011). *Pillar and Roof Span Design Guidelines for Underground Stone Mines.* Information Circular 9526. Pittsburgh, PA: National Institute for Occupational Safety and Health (NIOSH). Office of Mine Safety and Health Research.

FARO. (2011). *FARO FOCUS 3D Manual*. FARO Technologies, Inc.

FARO. (2018). *SCENE.* FARO Technologies, Inc.

Fekete, S. (2010a). “Geotechnical and operational applications for 3-dimensional laser scanning in drill and blast tunnels.” *Tunnelling and Underground Space Technology 25*(5): 614–628.

Fekete, S. (2010b). *Geotechnical Applications of LIDAR for Geomechanical Characterization in Drill and Blast Tunnels and Representative 3-Dimensional Discontinuum Modelling*. Thesis. Kingston, Ontario: Queen's University, pp. 296.

Fekete, S. and Diedrichs, M. (2013). “Integration of three-dimensional laser scanning with discontinuum modelling for stability analysis of tunnels in blocky rockmasses.” *International Journal of Rock Mechanics and Mining Sciences 57*: 11–23.

Hudson, J. and Harrison, J. (2000). *Engineering Rock Mechanics: An Introduction to the Principles.* New York, NY: Elsevier, pp. 456.

ISRM. (1978). “Suggested methods for the quantitative description of discontinuities in rock masses.” *International Society for Rock Mechanics*, pp. 49.

ITASCA. (2018). *3DEC™.* Minneapolis, MN: Itasca Consulting Group, Inc.

Lato, M., Diederichs, M., Hutchinson, D., and+ Harrap, R. (2009). “Optimization of LiDAR scanning and processing for automated structural evaluation of discontinuities in rock masses.” *International Journal of Rock Mechanics and Mining Sciences 46*(1): 194–199.

Maptek. (2018). *I-Site Studio.* Golden, CO: Maptek Pty Ltd.

Monsalve, J., Baggett, J., Bishop, R., and Ripepi, N. (2018). “A preliminary investigation for characterization and modeling of structurally controlled underground limestone mines by integrating laser scanning with discrete element modeling.” Forthcoming In: *Proceedings of the North American Tunneling Conference.* Englewood, CO: Society for Mining, Metallurgy & Exploration.

MSHA. (2016). *Accident Injuries Data Set.* U.S. Department of Labor, Mine Safety and Health Administration (MSHA).

Pierce, M. (2017). An Introduction to Random Disk Discrete Fracture Network (DFN) for Civil and Mining Engineering Applications. *ARMA e-Newslatter 20*, 3-8.

Rocscience. (2018). *Dips*. Toronto, Ontario: Rocscience Inc.

Slaker, B. A. (2015). *Monitoring Underground Mine Displacement Using Photogrammetry and Laser Scanning*. PhD Dissertation. Blacksburg, VA: Virginia Polytechnic Institute and State University, pp. 155.

# Chapter 3 Stability Analysis of an Underground Limestone Mine Using Terrestrial Laser Scanning with Stochastic Discrete Element Modeling.[3]

Juan J. Monsalve[1], Jon Baggett[1], Aman Soni[1], Nino Ripepi[1], Jim Hazzard[2]
[1]Mining and Minerals Engineering Department, Virginia Polytechnic Institute & State University
[2]ITASCA Consulting Group

**Abstract.**

The underground limestone mining industry has one of the highest fatality rates compared to all other types of mining in the United States (MSHA, 2016). Ground control issues heavily contribute to these fatalities. According to the National Institute for Occupational Safety and Health (NIOSH, 2011), structurally controlled instability is a predominant failure mechanism in underground limestone mines. Existing analysis methods, such as the limit equilibrium method, do not represent the real structure and behavior of a rock mass in-situ. The Discrete Element Method (DEM) when coupled with representative Discrete Fracture Networks (DFN) has been proven to provide accurate models of the actual response of a rock mass undergoing excavation. However, considering the statistical nature of DFN's, multiple simulations need to be run in order to obtain statistically significant results of the model. The following paper introduces a stochastic approach for analyzing rock block falls in underground excavations. This approach utilizes DEM (Itasca's 3DEC) and DFN's representing virtually mapped discontinuities obtained from terrestrial laser scans. The numerical models were carried out considering rigid blocks. Failed blocks were defined as those blocks that had displaced more than 2 cm and presented velocities indicating that the block was still in movement. This approach allows engineers to define the probability of block failure based on the geometry and weight of failed blocks formed by the intersection of discontinuities in the section of interest, as well as to define kinematics of the blocks. Such information can provide mining operators control measures to evaluate, map and mitigate risks associated with rock falls in underground mines, ultimately improving safety in the underground limestone industry.

## 1. INTRODUCTION

Ground control instability issues are one of the main causes of accidents and fatalities in underground mining in the U.S. (MSHA, 2016). Within these ground control issues, structurally controlled instability is one of the main failure mechanisms in underground limestone mines (NIOSH, 2011). This type of instability takes place when two or more structural sets intersect forming rock blocks that can fall as the excavation advances (Goodman & Shi, 1985) (Hudson & Harrison, 2000). Additionally, in room and pillar mining

[3] Conference Paper under review submitted to the **53rd US Rock Mechanics/Geomechanics ARMA Symposium**, 2019. New York, NY.

operations, a rock fall due to structurally controlled instability may affect the shape of a pillar, subsequently reducing its strength parameters, and ultimately leading to a pillar failure (Brady & Brown, 1985). This failure mechanism depends on several factors, such as the structural condition of the rock mass (including number of discontinuity sets, orientation, spacing and size of discontinuities), the mechanical properties of the discontinuities, and the orientation and size of the excavations. These structural features are generated as a response to the stress changes throughout the geological history of the rock mass, and they can vary from location to location and even within the same mine. In order to evaluate the block fall risk these discontinuities should be adequately identified, measured and mapped.

Previous research has shown that terrestrial laser scanning (TLS) and photogrammetry technologies are able to obtain adequate density point clouds for virtual discontinuity mapping (Lato, Diederichs, Hutchinson, & Harrap, 2009) (Cacciari & Futai, 2017) (Monsalve J. , Baggett, Bishop, & Ripepi, 2019). The information obtained from these mapping processes can be used to perform engineering analyses aimed at identifying the potential blocks that form in the excavation. In an earlier work, Monsalve, et al. (2018) describe and compare the two current analysis methodologies to evaluate structurally controlled instability: the Limit Equilibrium Method (LEM) and the Discrete Element Method (DEM). The authors concluded that the DEM with detailed structural information, such as the one obtained from TLS by virtual discontinuity mapping and Discrete Fracture Network (DFN) generation, provides both deterministic and stochastic results to better understand the rock mass behavior under excavation (Monsalve J. , Baggett, Bishop, & Ripepi, 2018).

The DEM is a numerical analysis tool that can simulate the behavior of a discrete body, such as a rock mass, under either static or dynamic loads. The blocks that constitute the rock mass are formed by intersecting explicit fractures whose locations, orientations and dimensions are necessary to define the model (Jing & Stephansson, 2007). Specifically, 3DEC has the capability to generate Discrete Fracture Networks (DFNs) and use them to cut through a block until a structural condition similar to that of the rock mass is reproduced (ITASCA, 2016). Each DFN is composed by a number disk shaped fractures. When a block is cut with a DFN, each fracture belonging the DFN must completely bisect a block. If a fracture is in between two different blocks, both blocks will be completely bisected, even if this fracture is smaller than this blocks. Due to this, in a final fracture model it is not possible to have isolated circular fractures as the ones belonging to the DFN. Figure 3.1 shows a comparison between the DFNs and the final fractured model. It is observable that even though there are similar patterns between both, they are not identical. Due to this discrepancy, it is important to calibrate this model so the final structural conditions are as closely representative of those observed in the field and mapped from the laser scans.

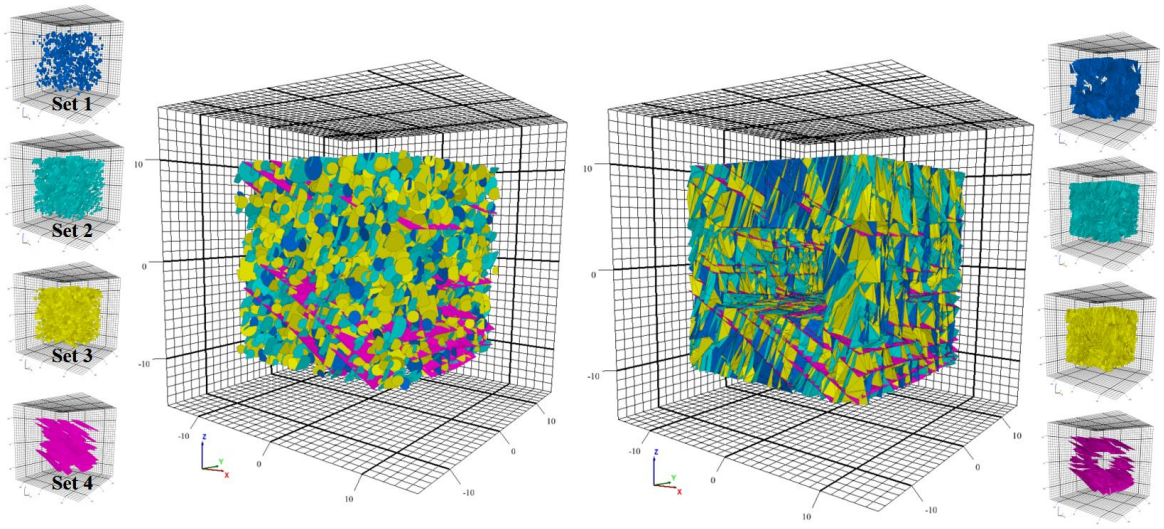


**Figure 3.1. Comparison between DFNs and actual fractures in the model.**

DFNs are a geometrical representation of the structures mapped from the rock mass, based on statistical information of their orientation, size and frequency (Pierce, 2017). Their nature is merely statistical. If further stability analyses are intended, these require a stochastic modeling approach (Monsalve J. , Baggett, Bishop, & Ripepi, 2019). Different authors have performed stochastic stability analyses of failure in fractured rock masses using DFNs; however, they have used LEM analysis. Grenon & Hadjigeorgiou (2003) evaluated the stability of wedges in underground mines at the periphery of mining stopes by integrating a 3D joint network generation model with a 3D limit equilibrium software package. Fu & Ma (2012) presented an algorithm that evaluates progressive failure in rock masses based on the LEM and the key block theory. This method would be extended later to perform a stochastic analysis of progressive failure in rock slopes and underground excavation, obtaining probability density functions indicating the amount of failed blocks (key blocks) and their volumes (Fu, Ma, Qu, & Huang, 2016). Grenon, Landry, Hadjigeorgiou, & Lajoie (2017) compared different fracture network models and evaluated the stability of a drift in an underground mine with stochastic limit equilibrium anlysis based on previous work. Similarily, Rogers, Bewick, Brzovic, & Gaudreau (2017) performed stochastic LEM analysis in an underground excavation, obtaining the DFN's information from photogrammetric surveys. As is shown by these limited number of studies, there is a lack of research in stochastic methods using the DEM.

The following paper presents the stability analysis of a previously defined case study mine based on a stochastic discrete element model approach. This analysis method is performed by running multiple iterations of a discrete element model in 3DEC that simulates a 20-meter long section of the excavation. This method resulted in an estimate of probability for the number of failed blocks and the volume of the unstable mass of rock.

## 2. GEOTECHNICAL CONDITIONS

In previous work, Monsalve et al. described the geotechnical conditions of the CSM. This operation extracts a 30 m thick and 30° dipping limestone body with a room and pillar mining method with eventual stoping. The stopes are conformed along the strike of the body, when the seam is consistent and thick enough. These are conformed by top and bottom drifts, 12.8 m wide and 7.6 m high, which are separated by a 15 m sill which is extracted by vertical long hole drilling (Sill and pillar mining). The stopes are supported by 24 m by 24 m pillars. This rock has a UCS of 159.2 MPa ± 21.25 MPa, a tensile strength of 6.3 MPa ± 1.99 MPa and a Young's modulus of 64.11 GPa ± 2.37 MPa. In addition to this, an average GSI value of 75 was reported throughout the area of interest. The deepest point in the mine is approximately 700 m below ground surface and is exposed to a maximum vertical stress close to 20 MPa.

As described in the above mentioned previous work, according to the risk/Hazard Assessment Chart proposed by Martin, Kaiser, & Christiansson (2003), the main cause of instability in this excavation is due to gravity-induced structurally controlled block movement, which agrees with the observed failure conditions in the mine (Monsalve J. , Baggett, Bishop, & Ripepi, 2018). If the horizontal stress is assumed to be the principal maximum stress and 1.2 times higher than the vertical stress, for the mine to be under stress induced failure the excavations should be deeper than 750 m, as it is presented in Figure 3.2. Considering that the deepest level in the mine is 700 m below ground surface, stress induced failure mechanisms are unlikely to be encountered in this mine.

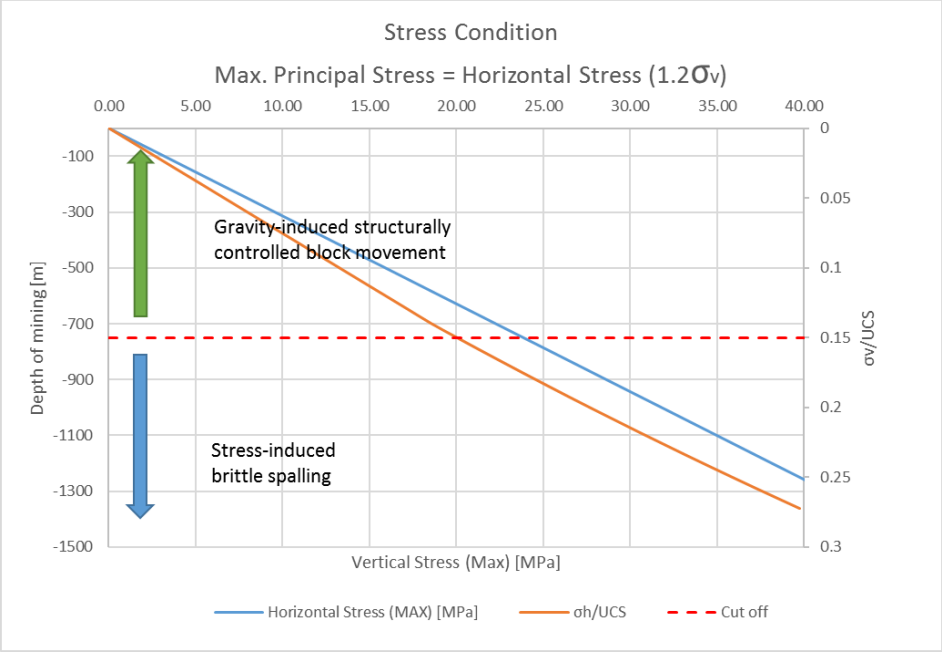


**Figure 3.2. Failure mechanisms depending on the depth of the mine based on the risk/Hazzard Assessment chart proposed by Martin, Kaiser, & Christiansson (2003).**

The ore body is located in the limb of a regional syncline structure. From terrestrial laser scanning and virtual discontinuity mapping, the authors were able to identify four main discontinuity sets. These discontinuity sets were classified as: Set 4, which corresponds to the bedding planes and contacts between rock units, which are almost parallel to the tunnel orientation and has a mean dip of 29°; Set 1, which is almost perpendicular to the tunnel orientation and presents a sub-vertical dip; and Sets 2 and 3, which are oblique joints with a steep dip. These four identified structural sets agree with the model of joints in folded sediments proposed by some authors, where Set 1 corresponds to Dip joints, Set 2 and 3 could be classified as oblique or shear joints, and Set 4 corresponds to bedding planes, as can be observed in Figure 3.3 (Brady & Brown, 1985) (Blyth & de Freitas, 1984).

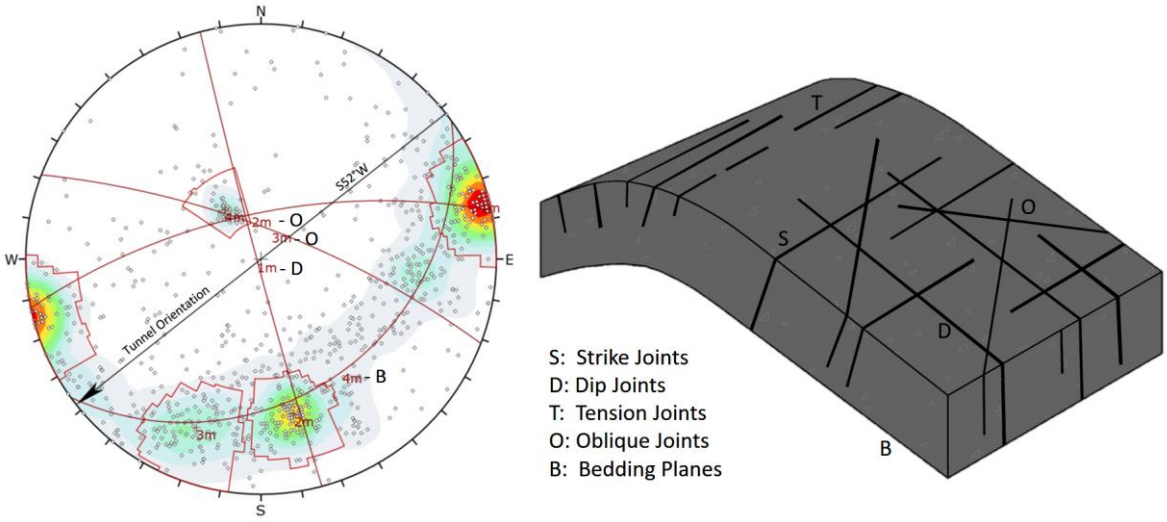


**Figure 3.3. Relation between structural sets defined in the CSM and Jointing model in folded sediments.**

In addition to this, additional field work aimed at measuring the mechanical properties of the discontinuities was carried out. In general, it was determined that all discontinuity sets are mainly very closed. The weathering conditions ranged between decolored and fresh for all the discontinuity sets. The majority of the discontinuities were completely damp, except for some discontinuities located closer to karst features, which were encountered wet and a few of them were dripping. Fifty-four percent of the mapped discontinuities did not present any filling material, while 22% were filled with calcite and the other 24% were filled with mud, mainly coming from the karsts. In addition, 64 % of the fractures from all the families presented a joint roughness coefficient (JRC) between 2 and 4, while the other 38 % of the fractures presented higher JRCs between 6 and 10. The bedding planes were the fractures that presented the highest JRCs. In addition to this, tilt tests were performed which obtained friction angle values ranging from 30° to 35°.

## 3. ANALYSIS METHODOLOGY

Initially, preliminary models were developed considering simple tunnel geometries and simplified DFNs. These initial models were calibrated and improved until the model closely represented the rock mass structure and the excavation section. The final model represents a 20-m long section of the excavation and takes into account the four mapped discontinuity sets. The model was run for 40000 cycles after excavation, with a time step of $3.81 \times 10^{-6}$ seconds, taking 6 hours of processing time. The hardware consisted on a MSI laptop computer with 16 Gb of RAM and a 7$^{th}$ generation Core i7 processor. Once the model was run, a function was written to mark failed blocks (Fekete & Diedrichs, 2013). The failed blocks were defined as those blocks that had displaced more than 2 cm and presented velocities higher than $5 \times 10^{-5}$ mm/s indicating that the blocks were in movement (Curden & Varnes, 1996). Then information about the blocks was stored in a text file. This information included block number, block volume, block mass and velocity.

As mentioned earlier, due to the stochastic nature of the DFNs, the results obtained just from one simulation are not representative of the overall response of the rock mass under excavation. Due to this, the model was run 30 times, reporting the same information for each iteration. This was done by generating a master file which ran the model several times and varying the random seed number to ensure every result was different. The iteration number was stored in the text file along with the block information. This enabled the performance of further analyses on the extracted information. In order to validate the models, the results were compared with the 3 dimensional point clouds obtained from the laser scans. Two dimensional sections from both models were extracted and compared.

The text file was imported into an excel file where information was processed and analyzed. The parameters that were evaluated were total number of failed blocks and total volume of failed blocks. These two parameters give insight into the amount of rock fall that can occur in the excavation given certain structural condition in the rock mass. The statistical analysis software JMP was used to perform a statistical analysis on the results (Proust, 2018). Probability Density Functions were fitted and validated for these two parameters, allowing the probability of block failure in the 20 m long section to be estimated. On the other hand, the x, y and z velocity components were converted to stereographical data. This information allowed the kinematics of the failed blocks to be better interpreted.

## 4. 3DEC MODEL

This section explains how the 3DEC model was programed and describes the conditions and assumptions considered in this study.

Initially, a DFN was generated for each discontinuity set present in the rock mass. These DFNs were defined within a control volume of 20 m x 20 m x 20 m. The input parameters considered for this were obtained from the authors' (Monsalve J. , Baggett, Bishop, & Ripepi, 2019) previous research . The parameters required to generate the DFNs were orientation,

size and density. For orientation, a fisher distribution was considered for all the discontinuity sets. Dip, dip direction and K values are presented for all discontinuity sets in Table 3.1. In order to simplify the model, the y axis was defined parallel to the tunnel orientation (N52°E). Due to this, all discontinuity sets were rotated 52° counterclockwise to maintain their orientations respective to the excavation. For Sets 1, 2 and 3, a log-normal distribution for the size was considered based on the values obtained from the laser scans. A function was written to consider log-normal distributions for joint size, since 3DEC DFN generator does not include these distributions for this parameter. The values measured from the laser scans were not considered for Set 4, since it corresponds to the bedding, which extends consistently along the rock mass. Instead of this, a Gaussian distribution, with a mean of 9 m and a standard deviation of 1 m, was used to generate this DFN, allowing it to better represent this family. The area of fractures per unit volume ($P_{32}$) was considered as the density parameter. The $P_{32}$ value was calibrated until the measured number of fractures per unit length of scan line ($P_{10}$) in the resulting fracture model reached values close to those obtained from the virtual discontinuity mapping.

**Table 3.1. Statistical Summary of the joint properties for each joint set.**

| \|SET / PARAMETERS | | S1 N=157 | S2 N=127 | S3 N=97 | S4 (Bedding) N=45 |
|---|---|---|---|---|---|
| Orientation | Dip [°] | 88 | 68 | 75 | 29 |
| | Dip Direction [°] | 255 | 348 | 21 | 144 |
| | K (Fisher) | 103.9 | 102.4 | 69.5 | 197.3 |
| Size | Distribution | Log-normal | Log-normal | Log-normal | Normal |
| | Mean | 0.353 | 0.318 | 0.018 | 9 |
| | Standard deviation | 0.659 | 0.772 | 0.749 | 1 |
| Density | Input area of fractures per unit volume ($P_{32}$) | 0.1 | 0.4 | 0.4 | 0.5 |

The geometry of the excavation was based on the general mine design. The section is rectangular with a width of 12.8 m and a height of 7.6 m. This geometry was modeled in Rhinoceros and imported into 3DEC using Griddle (ITASCA, 2017). Two sections in the geometry were considered: 1) an inner section, considered as the fractured rock mass which contained the excavation; and 2) an external section, considered as the massive rock mass for the sake of the simplicity for the model. After the geometry was imported, the blocks were cut with the DFNs. The cutting order was a relevant parameter to simulate the rock mass structure, since it altered significantly the fracturing model. For this study, the set bedding planes were used to cut the model first, followed by Set 1 which corresponded to dip joints, followed by Sets 2 and 3 which corresponded to shear joints. Figure 3.4.a) shows the jointing model after the DFNs cut the initial block. Figure 3.4.b) illustrates the inner section, representing the fractured rock mass with the excavation. In addition to this, Figure 3.4.c) displays a two dimensional section of the excavation, where the fractures can be noticed.

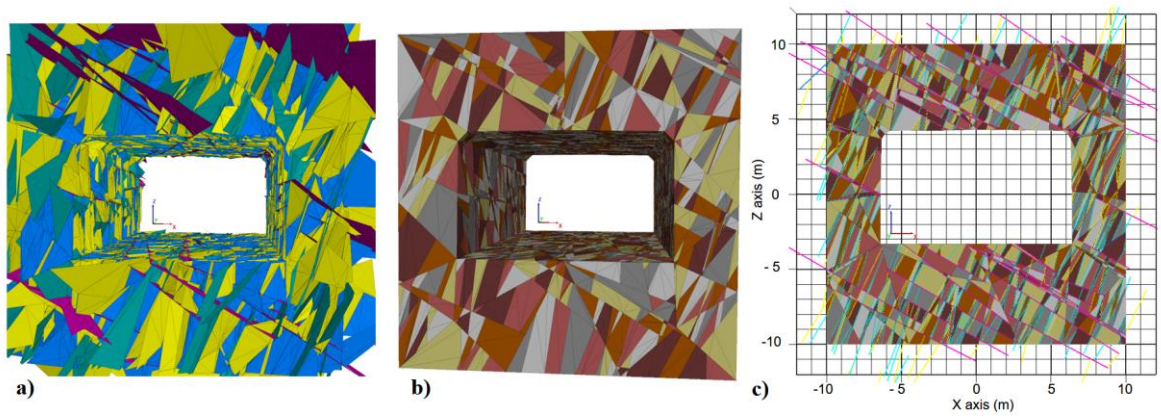


**Figure 3.4. a) Jointed model b) Inner Section of the Geometry indicating the Jointed rock mass. c) XZ 2-Dimensional displaying the excavation the rock blocks and joints.**

Considering that the main failure mechanism defined was gravity-induced, structurally controlled block movement, and that there was no evidence of failure resulting from high stresses, it was decided to use rigid blocks in the model. This means that the only deformation observed in the simulation occurs along discontinuity planes and the blocks do not change their geometries. The gravity was set as 9.81 m/s$^2$. Additionally, the external section of the geometry was fixed, preventing it from displacing. Thus, the only blocks that were displaced were the ones belonging to the fractured rock mass section.

The intact rock properties were obtained from previous laboratory testing performed by the mine operator. Blocks were assigned a density of 2700 kg/m3 and were assumed to be infinitely stiff (rigid). Furthermore, discontinuity properties were assumed to have a friction angle of 30° and no cohesion based on tilt tests and field observations. These values represented the worst discontinuity strength conditions. A joint shear stiffness of 30 MPa/mm and a joint normal stiffness of 300 MPa/mm were used. These values were obtained based on the work performed by Bandis, Lumsden, & Barton (1983).

Once the model was set up, it was cycled 500 times to reach initial equilibrium before excavation. After these initial cycles were run, the material inside the tunnel was excavated and run for an additional 40000 cycles. Once, these cycles were finished, the failed blocks analysis stage proceeded.

## 5. RESULTS AND DISCUSSION

Figure 3.5 shows the results obtained from one of the simulations in 3DEC. In the model, red indicates blocks that defined as failed blocks, while grey indicates those blocks that have not yet failed. Velocity vectors also are marked, indicating blocks that are still displacing. In this particular simulation the maximum displacements obtained are 4.62 cm and the maximum block velocities obtained are 0.6 m/s. Additionally, the figure shows that the majority of failed blocks on the roof presented geometries ranging from oblique triangular pyramids to

irregular prisms, which are shown isolated in Figure 3.6. Not only did working with rigid blocks showed an acceptable rock mass behavior, but this assumption significantly reduced the processing time as well.

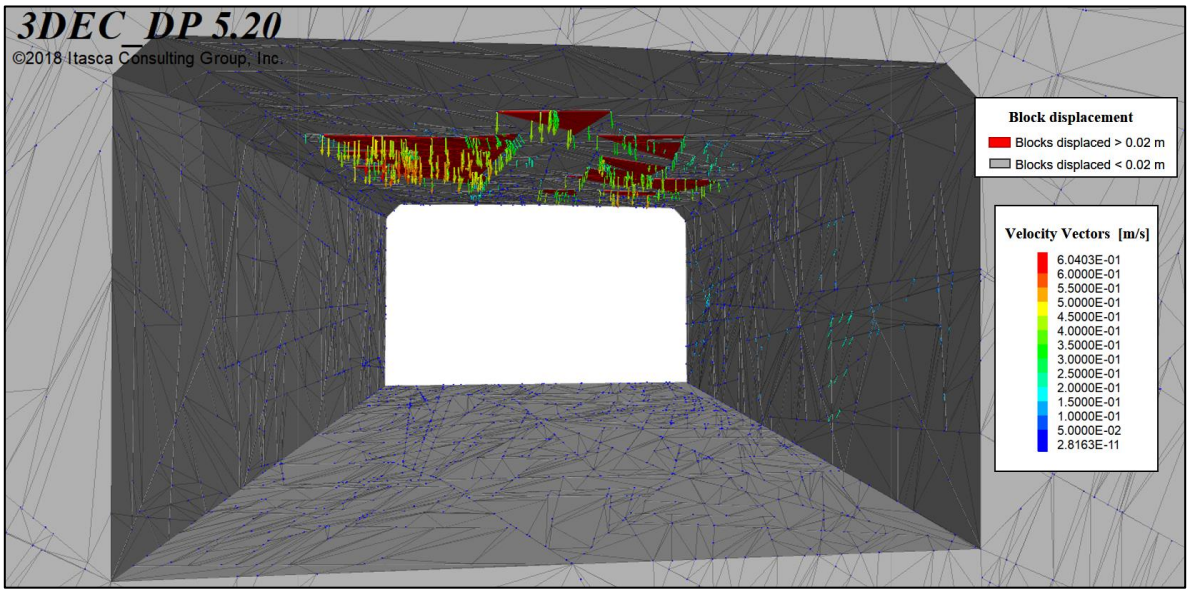


**Figure 3.5. Discrete element model of the study area indicating failed blocks.**

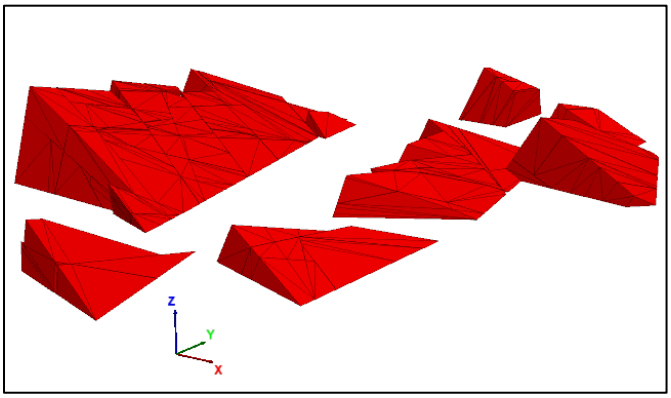


**Figure 3.6. Typical geometries of failed blocks in the discrete element model.**

Results obtained from the simulations were compared with previously Laser-scanned sections. Taking into account that the 3DEC models were stochastic, they were not meant to match exactly the laser scanned sections. However, the blocks formed in the numerical model still shared similar volumes and shapes to those observed in the laser-scanned sections. Figure 3.7 compares two 2-dimensional sections, one extracted from laser scans and the other extracted from numerical models. Results from both show similarities between the locations, sizes and shapes of the blocks. Figure 3.8 shows a failed block from 3DEC matching the gap left from a failed block in a laser scanned section in the study area. These results indicate that the structural model obtained from the virtual discontinuity mapping somehow adequately represents the structure of the rock mass.

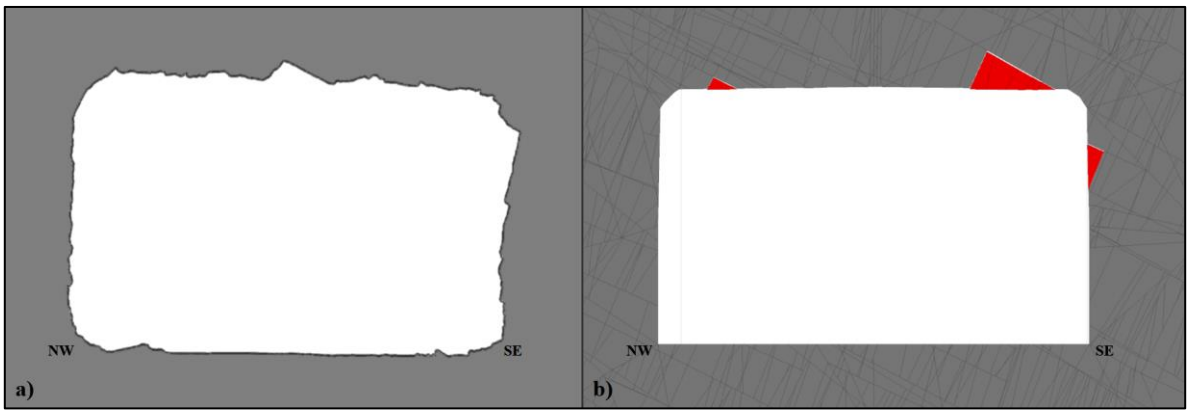


**Figure 3.7. Comparison between 2 dimensional section obtained from a) Laser Scanning Point clouds and b) Discrete Element Model.**

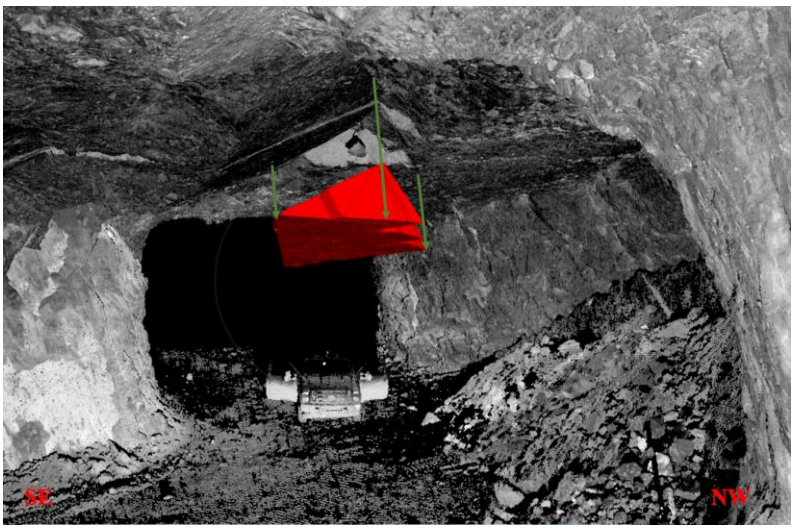


**Figure 3.8. 3DEC failed block matching a gap left from a failed block in a laser scanned section.**

The stochastic modeling stage resulted in 30 discrete element models and took around 180 hours. Figure 3.9 shows some of the models obtained from this analysis. As mentioned earlier, informtion for each of the 3,146 failed blocks was recorded. Two main parameters were evaluated from the models: the number of failed blocks per iteration, and the total volume of failed blocks per iteration. This information was analyzed in the statistical software JMP, where probability density functions were defined for these parameters. The volume of failed blocks was fitted to a log-normal distribution, with a mean of 2.60 $m^3$ and a standard deviation of 0.49 $m^3$. This distribution was validated with the Kolmogorov's D goodness of fit test. On the other hand, the number of failed blocks was distributed normally with a mean value of 104.86 and a standard deviation of 47.58. Similarly, this distribution was validated using the Shapiro-Wilk W goodness of fit test. These results indicate that considering the present structural condition in this section of the mine, there is 35% probability for a total volume of 10 $m^3$ of rock blocks to fall in 20 m of tunneling advance. Results obtained from this methodology offer engineers an accurate tool to estimate the mass of failed blocks in excavations under structurally controlled failure mechanism.

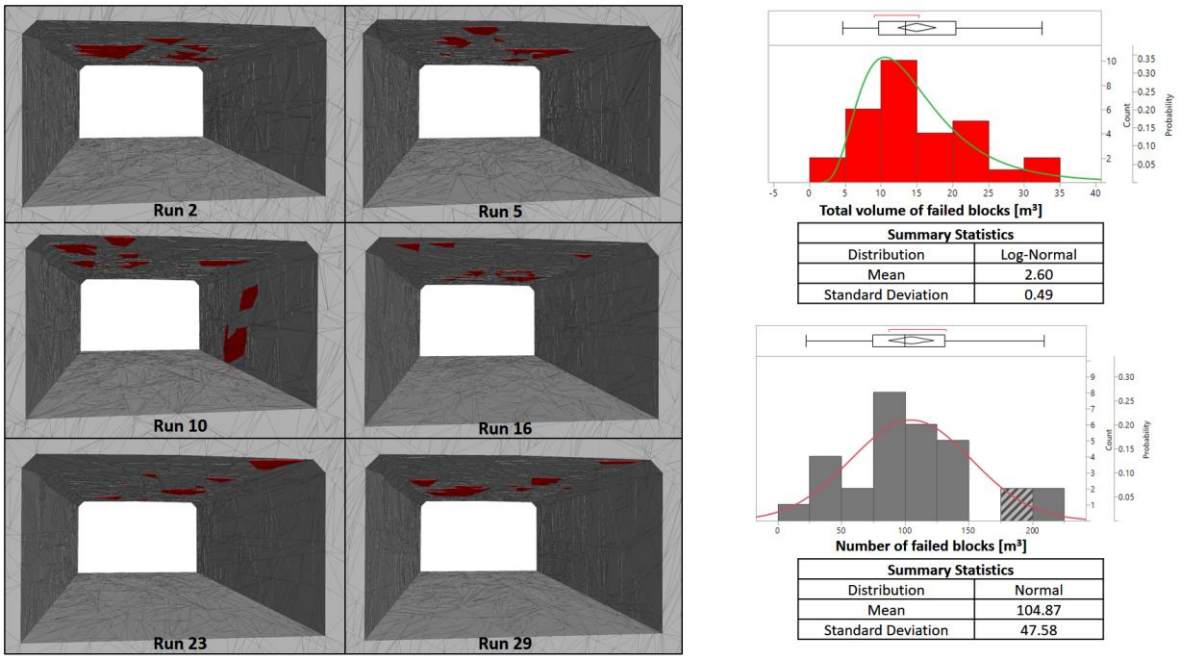


**Figure 3.9. Stochastic approach to block failure analysis.**

Once the failed blocks probability was estimated, as described in previous section, a block kinematics analysis was performed. The velocity vectors from all the models were transformed into spherical coordinates, allowing them to be presented in a stereonet. Figure 3.10 shows a model of failed blocks in the roof and in the south-east wall of the excavation, as well as the velocity vectors for all failed blocks. The figure demonstrates that the majority of the blocks were falling vertically from the roof; however, other vectors were concentrated more towards the NW. These vectors represent blocks falling from the south-east wall torwards the excavation.

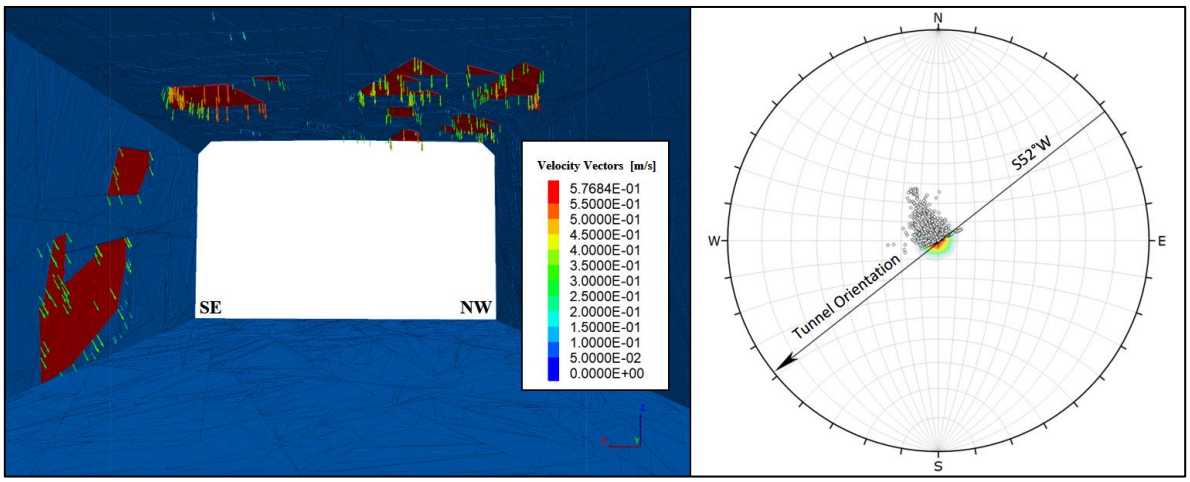


**Figure 3.10. Stereographical analysis of block kinematics.**

Results obtained from this stochastic model can be extended to any sector of the mine sharing similar structural condition as that mapped on the study area. If a different structural condition is reported, these modeles must be repeated considering the new structural setting. The methodology described in this work can be applied in any underground limestone mine presenting a structurally controlled failure mechanism, and the results obtained from these analyses can be used to define probability of block failure. Similarily, the data and information resuling from this work can be integrated into a risk management system to control risks associated with rock fall in a mine, ultimately improving safety in the operation.

## 6. FURTHER WORK

Based on the results of this work, a number of different research opportunities are identified. This methodology can be extended to rock support design under structurally controlled instability. Pillar strength on fractured pillars could also be analyzed by using stochastic discrete element modeling with 3DEC. In underground mines where stresses can be an additional issue, this methodology may also be applied if deformable blocks are considered, even though, the analysis time may significantly increase.

## 7. CONCLUSIONS

This work presented a methodology for analyzing the stability of an underground limestone mine under structurally controlled failure. This methodology integrated results from terrestrial laser scanning with Discrete Fracture Networks and Discrete Element Modeling software. The following conclusions can be drawn from this work:

1. Terrestrial laser scanning was successfully integrated with Discrete Element Modeling by applying discrete fracture networks in the model. The information obtained from virtual discontinuity mapping in the laser scans was used as inputs for generating the DFNs which were then used to build the 3DEC model.

2. It is important to have a general understanding of the geological model of the rock mass. This knowledge dictates how the 3DEC model is built. In this work, the joint set

corresponding to the bedding planes was used to first cut the blocks than the other sets. This enhanced the results of the rock mass model.

3. In this study, working with rigid blocks was an acceptable assumption, which yielded results similar to those observed in the field. Should this methodology be used in an underground excavation presenting both structurally controlled and stress controlled failure mechanisms, it is recommended to work with deformable blocks, which may increase significantly the processing time.

4. The results obtained from the model agreed with the failure mechanisms observed in the field. The results were also comparable with those obtained from laser scans, indicating that the parameters considered in the model were acceptable.

5. Considering the stochastic nature of DFNs, it is necessary to extend the discrete element models to a stochastic approach in order to obtain significant results. A stochastic modeling approach allows engineers to measure the probability of block failure in a section of the excavation. This methodology could also be extended to rock support design and pillar strength determination.

6. The present methodology can be used as a method for rock fall hazard identification in underground limestone mines. It can be easily integrated into a risk management system, allowing engineers and mining operators to have greater control over possible block failures, to reduce ground control related accidents, and to improve the safety of these operations.

## 8. ACKNOWLEGEMENTS

This work is funded by the NIOSH Mining Program under Contract No. 200-2016-91300. The authors would like to thank ITASCA for their support and guidance during this project. Views expressed here are those of the authors and do not necessarily represent those of any funding source.

## REFERENCES

Bandis, S., Lumsden, A., & Barton, N. (1983). Fundamentals of rock Joint Deformation. *International Journal of Rock Mechanics, Mining Sciences & Geomechanics*, 249-268.

Blyth, F., & de Freitas, M. (1984). *A Geology for Engineers.* London: ELSEVIER.

Brady, B., & Brown, E. (1985). *Rock Mechanics for Underground Mining.* UK: Chapman & Hall.

Cacciari, P., & Futai, M. (2017). Modeling a Shallow Rock Tunnel Using Terrestrial Laser Scanning and Discrete Fracture Networks. *Rock Mechanics and Rock Engineering*, 1217-1242.

Curden, D., & Varnes, D. (1996). Landslide types and processes. *Landslides: Investigation and mitigation, transportation research board special report 247*, 36-75.

Fekete, S., & Diedrichs, M. (2013). Integration of Three-dimensional Laser Scanning with Discontinuum Modelling for Stability Analysis of Tunnels in Blocky Rockmasses. *International Journal of Rock Mechanics & Mining Sciences*, 11-23.

Fu, G., & Ma, G. (2012). Progressive failure analysis and support design of blocky rock mass based on extended key block method. *46th US Rock Mechanics / Geomechanics Symposium.* Chicago: ARMA.

Fu, G., Ma, G., Qu, X., & Huang, D. (2016). Stochastic analysis of progressive failure of fractured rock masses containing non-persistent joint sets using key block analysis. *Tunnelling and Underground Space Technology*, 258-269.

Goodman, R., & Shi, G. (1985). *Block Theory and Its Application to Rock Engineering.* London: Prentice-Hall.

Grenon, M., & Hadjigeorgiou, J. (2003). Open Stope Stability Using 3D Joint Networks. *Rock Mechanics and Rock Engineering*, 183-208.

Grenon, M., Landry, A., Hadjigeorgiou, & Lajoie, P. (2017). Discrete Fracture Network Based Drift Stability at the Éléonore Mine. *Mining Technology*, 22-33.

Hudson, J., & Harrison, J. (2000). *Engineering Rock Mechanics.* Oxford: Imperial College of Science, Technology and Medicine, University of London, UK.

ITASCA. (2016). *3 Dimensional Discrete Element Code User's Guide.* Minneapolis: Itasca Consulting Group.

ITASCA. (2017). *Advanced Grid Generation for Engineers and Scientists Griddle and BlockRanger User's Guide.* Minneapolis: Itasca Consulting Group Inc.

Jing, L., & Stephansson, O. (2007). *Fundamentals of Discrete Element Methods for Rock Engineering Theory and Application.* Amsterdam: ELSEVIER.

Lato, M., Diederichs, M., Hutchinson, D., & Harrap, R. (2009). Optimization of LiDAR scanning and processing for automated structural evaluation of discontinuities in rock masses. *International Journal of Rock Mechanics and Mining Siences*, 1217-1242.

Martin, C., Kaiser, P., & Christiansson, R. (2003). Stress, instability and design of underground excavations. *Rock Mechanics and Mining Sciences*, 1-21.

Monsalve, J., Baggett, J., Bishop, R., & Ripepi, N. (2018). A Preliminary Investigation for Characterization and Modeling of Structurally Controlled Underground Limestone Mines by Integrating Laser Scanning with Discrete Element Modeling. *North American Tunneling Conference.* Washington: SME.

Monsalve, J., Baggett, J., Bishop, R., & Ripepi, N. (2019). Application of Laser Scanning for Rock Mass Characterization and Discrete Fracture Network Generation in an Underground Limestone Mine. *International Journal of Mining Science and Technology*, 131-137.

MSHA. (2016). *Metal/Nonmetal Daily Fatality Report.* Mine Safety and Health Administration.

NIOSH. (2011). *Pillar and Roof Span Design Guidelines for Underground Stone Mines.* Pittsburg: National Institute for Occupational Safety and Health.

Pierce, M. (2017). An Introduction to Random Disk Discrete Fracture Network (DFN) for Civil and Mining Engineering Applications. *ARMA e-Newslatter 20*, 3-8.

Proust, M. (2018). *Using JMP*. Cary: SAS Institute Inc.

Rogers, S., Bewick, R., Brzovic, A., & Gaudreau, D. (2017). Integrating Photogrametry and Discrete Fracture Network Modelling for Improved Conditional Simulation of Underground Wedge Stability. *8th International Conference in Deep and High Stress Mining*, 599-610.

# Chapter 4 Conclusions, Recommendations and Future Work

Throughout this work a methodology for analyzing the stability of an underground limestone mine under structurally controlled failure was presented and tested. This methodology integrated results from terrestrial laser scanning (TLS), virtual discontinuity mapping (VDM), Discrete Fracture Network (DFN) generation and Discrete Element Modeling (DEM). This methodology was tested in an underground limestone mine that extracts a 30° dipping limestone body with a room and pillar mining method with eventual stoping. The primary failure mechanism of this mine was structurally controlled block movement. A study area was defined along with mine personal and researchers. In this area 9 laser scans were performed. A point cloud was extracted from this scans, which were used later for VDM. During the VDM process information such as spatial location, orientation, trace length, and spacing was extracted for each discontinuity set. These information was used to generate DFNs for each fracture set. These allowed us to generate fractured rock mass models in 3DEC a DEM software. The DEM allowed us to estimate the probability of rock block failure in a 20 m long tunnel considering the structural parameters obtained from the study area. The following lines present some of the conclusions that arose from this work.

1) Similar to other authors mentioned in this work TLS was proved to be a powerful tool for rock mass characterization. Not only this technology was time efficient, but it also provided detailed information that allowed to generate DFNs which were used later to generate a fractured rock mass model that represented accurately the rock mass behavior under excavation.

2) Planning the scanning project was fundamental in order to save time during the scanning process, reduce errors on the resulting point cloud, and obtain the necessary information required for virtual discontinuity mapping. While there is no existing guideline for performing an underground laser-scanning project, the experiences from other authors were valuable in defining the conditions of the scanning.

3) DEM software such as 3DEC is a powerful tool to interpret and analyze structurally controlled instability in underground excavations. This software with detailed structural information such as the one obtained from TLS and VDM provided not only deterministic but also stochastic analysis, which allowed us to understand better the behavior of the rock mass and provide better estimations of the probability of rock block failure in the case study mine.

4) TLS was successfully integrated with DEM by applying discrete fracture networks in the model. The information obtained from VDM in the laser scans was used as inputs for generating the DFNs which were then used to build the 3DEC model. The integration of both technologies (TLS and DEM) was successfully used in order to estimate the

probability of rock falls in an underground excavations and can be used to enhance worker's safety.

5) A clear understanding of the geological model of the site is important in order to improve the results from virtual discontinuity mapping and the fractured rock mass model. The geologist or the engineer in charge of the structural mapping and the numerical modeling are required to expend adequate time in the field in order to avoid any misleading interpretation and to ensure the results concur with those observed in the field.

6) A rigid block model was utilized based on an empirical risk/hazard assessment and field observations. This assumption yielded results that agreed with the field observations and laser scanning results. Additionally, the computing time was significantly reduced by implementing this assumption. This rigid block model is only applicable if stresses are not a main concern in the excavation. Should stress controlled failure mechanisms start to play a role in the stability of the excavation, a deformable block approach needs to be considered.

7) A stochastic Discrete element modeling approach was selected for the analysis due to the stochastic nature of DFNs. This modeling approach offered broader inference on the rock mass behavior under excavation. The results obtained from this analysis can be applied to any part of the mine where the structural setting is similar to that of the laser scanned area in this study. If a different structural setting is identified or the orientation and dimensions of the excavation changes, it is required to update the stochastic numerical analyses.

8) The present methodology can be used as a method for rock fall hazard identification in underground limestone mines. It can be easily integrated into a risk management system, allowing engineers and mining operators to have greater control over possible block failures, to reduce ground control related accidents, and to improve the safety of these operations.

9) The case study mine offered an ideal environment to apply both technologies (TLS and DEM), and to develop risk analysis methodologies based on these technological advances, ultimately reducing accidents related to rock falls in the underground stone mine industry.

10) The methodology here presented required the integration of different software packages (SCENE, I-Site, DIPS, 3DEC, JMP). Due to this, it was important to define an adequate workflow, identifying the inputs and outputs required and produced for each program. Furthermore, it is also important to understand the limitations of each software and how these limitations can affect the results of the models.

In addition to the conclusions obtained from this work, a series of recommendations that should be followed in order to implement this methodology in any underground limestone mine presenting similar failure mechanism are made. These recommendations are detailed in the following lines.

1) Considering that structurally controlled failure mechanism is governed by the structural setting of the rock mass, it is important for mining operators to keep track of these conditions. An adequate mapping and reporting of this sets of fractures and their properties will allow engineers and miners to be aware of the possible rock block fall that can occur in certain sectors of the mine.

2) If the structural mapping is decided to be done by using TLS, it is not necessary to perform these laser scans after every advance. In order to avoid collecting excessive information, periodical weekly surveys are proposed. These surveys could also be complemented with conventional rock mass characterization. The information obtained from this mapping process should be used mainly to keep track of changes in the structural sets along the mine.

3) Considering that underground limestone mines are generally continuous and regular deposits, and the majority of the excavations are made in the same rock type, the structural geology can be used as main parameter for defining the different geotechnical units throughout the mine. TLS and virtual discontinuity mapping offer a useful methodology to keep track of these changes and mapping these geotechnical units.

4) Not only this methodology can be applied in already on going mining projects, but also it can be implemented from the beginning of a mining project since exploration and prefeasibility studies. Current technologies such as borehole scoping and borehole discontinuity mapping, can be used for generating preliminary structural models and Discrete Fracture Network models for the areas where the tunnels will be projected. This models will allow planning engineers to evaluate rock fall risk in early stages of the project.

This work sets the bases for more detailed research on application of Laser Scanning and Discrete Element Modeling for hazard recognition and failure analysis in underground stone mines. A series of additional research are proposed from this work:

1) A comparison between Stochastic Discrete Element Modeling with Conventional Limit Equilibrium Methods.

2) A comparison between Automated Discontinuity Extraction Software versus Manual Virtual discontinuity Mapping.

3) Application of Stochastic Discrete Element Modeling for support design in underground excavations.

4) Stochastic Discrete Element Modeling extended to structurally and stress controlled underground mines.

5) Stochastic Discrete Element Modeling for pillar strength determination and comparison with empirical pillar strength estimation methods.

# APPENDIX A. Mapped Structural Data

| # Format is <X/E (m)> | <Y/N (m)> | <Z/RL (m)> | <Dip (°)> | <Dip direction (°)> | <Strike (°)> | <Length> | <Area> | SET |
|---|---|---|---|---|---|---|---|---|
| -12.834 | 23.132 | 2.647 | 73.481 | 352.586 | 262.586 | 1.42 | 0.794 | 2 |
| -12.713 | 23.665 | -0.124 | 82.978 | 296.001 | 206.001 | 0.844 | 0.33 | |
| -12.386 | 24.048 | 0.064 | 77.927 | 345.873 | 255.873 | 0.399 | 0.07 | 2 |
| -12.53 | 23.802 | 0.809 | 73.735 | 342.894 | 252.894 | 1.084 | 0.126 | 2 |
| -20.427 | 11.803 | 3.911 | 77.609 | 357.703 | 267.703 | 1.88 | 0.263 | 2 |
| -20.181 | 12.43 | 1.757 | 89.308 | 84.99 | 354.99 | 4.645 | 1.214 | 1 |
| -21.225 | 10.075 | 3.93 | 65.352 | 320.047 | 230.047 | 1.842 | 0.24 | |
| -19.727 | 13.771 | 3.661 | 88.171 | 257.817 | 167.817 | 3.339 | 1.562 | 1 |
| -19.767 | 14.031 | 3.755 | 67.801 | 319.448 | 229.448 | 0.954 | 0.024 | |
| -12.49 | 23.588 | 1.509 | 73.128 | 351.057 | 261.057 | 1.066 | 0.301 | 2 |
| -19.703 | 14.803 | 3.015 | 83.882 | 16.761 | 286.761 | 2.615 | 0.221 | 3 |
| -19.748 | 14.394 | 3.886 | 83.453 | 0.507 | 270.507 | 1.24 | 0.096 | |
| -18.299 | 17.576 | 1.763 | 77.315 | 329.984 | 239.984 | 3.025 | 1.203 | |
| -18.876 | 16.769 | 1.793 | 69.69 | 349.2 | 259.2 | 1.925 | 0.182 | 2 |
| -16.148 | 19.27 | 1.633 | 78.894 | 55.709 | 325.709 | 0.963 | 0.052 | |
| -16.6 | 18.578 | 0.979 | 80.037 | 328.887 | 238.887 | 2.323 | 1.271 | |
| -10.974 | 1.427 | 3.105 | 85.51 | 257.409 | 167.409 | 5.113 | 5.92 | 1 |
| -10.601 | 2.584 | 3.075 | 80.102 | 285.278 | 195.278 | 2.835 | 1.4 | |
| -9.669 | 4.338 | 4.768 | 88.211 | 256.065 | 166.065 | 2.923 | 1.237 | 1 |
| -11.117 | 0.24 | 4.103 | 83.506 | 248.003 | 158.003 | 4.055 | 1.377 | 1 |
| -12.611 | 23.129 | 4.242 | 74.352 | 5.552 | 275.552 | 1.467 | 0.302 | |
| -11.58 | -0.374 | 4.52 | 85.584 | 243.164 | 153.164 | 3.273 | 0.938 | 1 |
| -11.841 | -0.603 | 5.899 | 29.88 | 144.958 | 54.958 | 0.959 | 0.186 | 4 |
| -8.632 | 5.546 | 0.868 | 68.419 | 265.784 | 175.784 | 5.241 | 1.848 | |
| -9.356 | 4.711 | 3.654 | 87.224 | 58.344 | 328.344 | 2.566 | 0.509 | |
| -8.009 | 5.792 | 3.747 | 75.265 | 274.777 | 184.777 | 1.585 | 0.239 | |
| -6.3 | 9.926 | 0.766 | 66.468 | 349.015 | 259.015 | 4.321 | 1.251 | 2 |
| -7.309 | 8.314 | 3.247 | 66.476 | 321.46 | 231.46 | 1.066 | 0.236 | |
| -7.423 | 7.159 | 3.139 | 78.723 | 265.347 | 175.347 | 2.816 | 1.812 | 1 |
| -5.963 | 10.621 | 4.218 | 85.477 | 243.559 | 153.559 | 4.278 | 1.033 | 1 |
| -4.619 | 12.29 | 3.973 | 79.277 | 183.787 | 93.787 | 0.614 | 0.103 | |
| -12.634 | 22.813 | 5.54 | 76.476 | 8.058 | 278.058 | 0.788 | 0.159 | 3 |
| -4.53 | 12.56 | 3.998 | 89.424 | 256.908 | 166.908 | 1.243 | 0.329 | 1 |
| -2.054 | 14.636 | 1.431 | 63.712 | 280.56 | 190.56 | 1.426 | 0.175 | |
| -1.432 | 15.321 | 1.166 | 57.318 | 270.417 | 180.417 | 1.796 | 0.302 | |
| -0.994 | 15.831 | -0.383 | 57.374 | 290.162 | 200.162 | 0.541 | 0.034 | |
| -2.128 | 15.304 | 4.838 | 68.233 | 295.333 | 205.333 | 2.361 | 1.341 | |
| -3.424 | 13.319 | 3.607 | 89.24 | 77.553 | 347.553 | 1.014 | 0.154 | 1 |
| -2.784 | 14.224 | 3.841 | 72.73 | 242.993 | 152.993 | 0.798 | 0.089 | |

| | | | | | | | | |
|---|---|---|---|---|---|---|---|---|
| -1.412 | 15.837 | 3.02 | 54.836 | 308.225 | 218.225 | 0.803 | 0.111 | |
| -1.4 | 15.726 | 2.435 | 61.48 | 300.094 | 210.094 | 1.548 | 0.216 | |
| -2.045 | 14.782 | 2.14 | 55.328 | 311.883 | 221.883 | 0.495 | 0.07 | |
| -13.501 | 22.038 | 4.036 | 68.383 | 24.185 | 294.185 | 5.505 | 1.328 | 3 |
| -3.14 | 13.459 | 0.205 | 58.448 | 131.734 | 41.734 | 2.324 | 0.313 | |
| -2.485 | 14.44 | -0.205 | 70.817 | 271.502 | 181.502 | 0.62 | 0.134 | |
| -1.617 | 15.152 | 1.007 | 72.994 | 27.999 | 297.999 | 1.317 | 0.141 | 3 |
| -3.004 | 14.138 | 4.625 | 66.85 | 342.843 | 252.843 | 0.643 | 0.152 | 2 |
| -3.121 | 15.391 | 6.227 | 84.942 | 79.077 | 349.077 | 2.241 | 0.446 | 1 |
| -2.784 | 16.289 | 6.562 | 50.433 | 319.762 | 229.762 | 0.84 | 0.081 | |
| -12.186 | 22.47 | 6.559 | 69.686 | 353.965 | 263.965 | 0.869 | 0.192 | 2 |
| -12.883 | 22.587 | 5.605 | 83.966 | 112.885 | 22.885 | 0.657 | 0.165 | |
| -12.741 | 23.394 | 1.238 | 87.746 | 288.266 | 198.266 | 0.733 | 0.216 | |
| -16.005 | 19.046 | 5.306 | 76.437 | 1.495 | 271.495 | 1.836 | 0.24 | 2 |
| -4.796 | 11.713 | 2.507 | 67.824 | 279.609 | 189.609 | 1.457 | 0.199 | |
| -16.009 | 5.156 | 7.546 | 31.084 | 147.152 | 57.152 | 3.822 | 2.949 | 4 |
| -14.452 | 4.986 | 7.191 | 64.809 | 347.708 | 257.708 | 2.629 | 0.381 | 2 |
| -15.251 | 8.016 | 7.292 | 76.565 | 75.927 | 345.927 | 0.55 | 0.092 | |
| -15.504 | 8.367 | 7.258 | 56.449 | 10.04 | 280.04 | 0.355 | 0.066 | |
| -12.187 | 7.548 | 7.402 | 89.931 | 256.487 | 166.487 | 3.77 | 1.364 | 1 |
| -13.667 | 1.791 | 7.458 | 25.568 | 143.729 | 53.729 | 1.951 | 0.757 | 4 |
| -13.813 | 2.436 | 7.379 | 41.087 | 23.579 | 293.579 | 0.773 | 0.26 | |
| -14.106 | 2.705 | 7.216 | 37.747 | 20.343 | 290.343 | 0.598 | 0.126 | |
| -14.381 | 2.394 | 7.351 | 41.214 | 322.034 | 232.034 | 0.379 | 0.083 | |
| -13.574 | 3.154 | 7.085 | 58.406 | 34.968 | 304.968 | 0.276 | 0.021 | |
| -8.224 | 15.064 | 7.333 | 82.929 | 258.152 | 168.152 | 2.721 | 0.365 | 1 |
| -13.105 | 7.982 | 7.664 | 74.138 | 308.2 | 218.2 | 0.492 | 0.109 | |
| -12.919 | 8.067 | 7.804 | 73.199 | 28.024 | 298.024 | 0.205 | 0.016 | 3 |
| -13.356 | 7.738 | 7.623 | 65.545 | 299.17 | 209.17 | 0.744 | 0.121 | |
| -14.299 | 7.749 | 7.284 | 38.981 | 324.029 | 234.029 | 0.361 | 0.063 | |
| -14.057 | 7.622 | 7.356 | 54.042 | 52.987 | 322.987 | 0.364 | 0.048 | |
| -13.056 | 6.078 | 7.399 | 88.975 | 77.31 | 347.31 | 1.484 | 0.103 | 1 |
| -16.798 | 9.913 | 7.413 | 87.467 | 257.901 | 167.901 | 1.147 | 0.106 | 1 |
| -16.135 | 12.234 | 7.191 | 44.762 | 75.175 | 345.175 | 0.802 | 0.139 | |
| -15.275 | 11.26 | 7.257 | 64.88 | 342.016 | 252.016 | 1.629 | 0.155 | 2 |
| -14.457 | 11.115 | 7.217 | 62.062 | 341.321 | 251.321 | 0.615 | 0.077 | 2 |
| -18.165 | 10.84 | 7.316 | 65.387 | 327.853 | 237.853 | 0.437 | 0.041 | |
| -18.666 | 10.988 | 7.178 | 50.566 | 230.704 | 140.704 | 0.239 | 0.025 | |
| -10.254 | 19.498 | 8.116 | 50.223 | 260.937 | 170.937 | 2.435 | 1.478 | |
| -8.589 | 20.5 | 8.849 | 59.869 | 280.698 | 190.698 | 1.249 | 0.422 | |
| -10.011 | 20.198 | 8.313 | 8.615 | 84.34 | 354.34 | 0.693 | 0.165 | |
| -10.267 | 20.73 | 7.976 | 63.123 | 334.44 | 244.44 | 0.863 | 0.255 | 2 |
| -15.375 | 15.327 | 7.097 | 43.992 | 24.139 | 294.139 | 0.693 | 0.173 | |

| | | | | | | | | |
|---|---|---|---|---|---|---|---|---|
| -11.516 | 18.894 | 7.974 | 77.1 | 331.167 | 241.167 | 7.815 | 3.731 | |
| -7.765 | 18.975 | 8.577 | 89.951 | 66.119 | 336.119 | 1.428 | 0.703 | 1 |
| -7.942 | 20.061 | 8.669 | 89.473 | 260.062 | 170.062 | 3.996 | 2.619 | 1 |
| -8.102 | 17.767 | 8.091 | 89.537 | 78.318 | 348.318 | 0.635 | 0.106 | 1 |
| -5.122 | 16.778 | 7.033 | 64.397 | 347.612 | 257.612 | 1.284 | 0.173 | 2 |
| -5.094 | 18.334 | 7.491 | 56.899 | 321.439 | 231.439 | 1.944 | 0.695 | |
| 8.871 | 46.253 | 2.991 | 37.517 | 144.25 | 54.25 | 7.055 | 2.78 | 4 |
| 16.837 | 28.633 | 1.183 | 31.138 | 183.354 | 93.354 | 2.371 | 0.564 | |
| 16.98 | 28.448 | 4.995 | 89.472 | 254.424 | 164.424 | 0.804 | 0.167 | 1 |
| 17.304 | 28.194 | 4.651 | 82.46 | 256.703 | 166.703 | 0.589 | 0.148 | 1 |
| 16.645 | 28.944 | 4.861 | 80.28 | 54.837 | 324.837 | 1.555 | 0.97 | |
| 16.742 | 30.036 | 3.487 | 85.18 | 251.228 | 161.228 | 0.817 | 0.268 | 1 |
| 16.65 | 30.042 | 4.433 | 28.171 | 137.6 | 47.6 | 0.713 | 0.133 | 4 |
| 18.817 | 33.648 | 4.565 | 76.17 | 330.579 | 240.579 | 10.114 | 8.699 | |
| 22.976 | 37.371 | 0.509 | 73.311 | 300.653 | 210.653 | 1.867 | 1.301 | |
| 22.742 | 36.93 | 3.005 | 85.2 | 129.803 | 39.803 | 1.489 | 0.276 | |
| 18.485 | 33.158 | 1.933 | 85.71 | 296.275 | 206.275 | 1.862 | 0.701 | |
| 9.891 | 47.074 | 1.58 | 76.365 | 357.569 | 267.569 | 2.449 | 0.793 | 2 |
| 17.821 | 32.406 | 1.316 | 74.751 | 275.482 | 185.482 | 0.324 | 0.036 | |
| 15.965 | 31.454 | 0.237 | 67.389 | 272.444 | 182.444 | 1.441 | 0.318 | |
| 16.154 | 29.997 | 0.937 | 54.909 | 313.45 | 223.45 | 0.485 | 0.05 | |
| 15.906 | 31.166 | 0.249 | 42.475 | 331.91 | 241.91 | 1.272 | 0.115 | |
| 16.355 | 30.842 | 1.285 | 78.396 | 263.533 | 173.533 | 0.85 | 0.178 | 1 |
| 19.382 | 34.222 | 0.759 | 85.378 | 346.035 | 256.035 | 3.817 | 2.802 | |
| 26.194 | 39.909 | 1.315 | 66.606 | 45.559 | 315.559 | 1.069 | 0.105 | |
| 26.218 | 39.968 | 0.764 | 76.304 | 62.489 | 332.489 | 0.969 | 0.116 | |
| 17.1 | 45.503 | 9.598 | 54.302 | 327.291 | 237.291 | 1.348 | 0.24 | |
| 15.755 | 42.868 | 9.955 | 54.677 | 343.676 | 253.676 | 2.569 | 1.21 | 2 |
| 8.413 | 45.934 | 5.099 | 76.752 | 330.828 | 240.828 | 0.904 | 0.114 | |
| 19.953 | 41.198 | 8.927 | 78.774 | 82.828 | 352.828 | 1.919 | 0.455 | 1 |
| 14.557 | 38.222 | 9.716 | 68.737 | 346.541 | 256.541 | 9.882 | 3.189 | 2 |
| 8.146 | 45.739 | 4.813 | 67.347 | 346.999 | 256.999 | 0.727 | 0.052 | 2 |
| 8.075 | 45.763 | 1.262 | 82.495 | 332.626 | 242.626 | 3.373 | 2.522 | |
| 10.978 | 47.835 | 5.617 | 88.919 | 343.234 | 253.234 | 1.87 | 0.839 | |
| 14.313 | 50.126 | 6.171 | 64.999 | 0.633 | 270.633 | 1.499 | 0.294 | 2 |
| 14.251 | 50.476 | 4.843 | 68.499 | 345.698 | 255.698 | 1.435 | 0.44 | 2 |
| 16.826 | 52.453 | 5.331 | 55.505 | 39.802 | 309.802 | 3.194 | 0.365 | |
| -2.802 | 33.938 | 4.787 | 82.229 | 345.07 | 255.07 | 4.866 | 1.897 | |
| -6.421 | 29.036 | 6.735 | 74.737 | 273.038 | 183.038 | 1.109 | 0.171 | |
| 12.931 | 24.159 | 8.08 | 87.366 | 76.697 | 346.697 | 1.394 | 0.211 | 1 |
| 12.914 | 25.68 | 8.272 | 87.261 | 75.172 | 345.172 | 1.589 | 0.442 | 1 |
| -6.491 | 28.979 | 6.617 | 70.732 | 344.288 | 254.288 | 1.27 | 0.105 | 2 |
| -8.605 | 27.47 | 1.498 | 63.703 | 335.615 | 245.615 | 1.58 | 0.46 | 2 |

| | | | | | | | | |
|---|---|---|---|---|---|---|---|---|
| -8.291 | 27.853 | 2.545 | 60.005 | 339.055 | 249.055 | 0.9 | 0.289 | 2 |
| -8.545 | 27.462 | 3.22 | 57.711 | 340.793 | 250.793 | 0.669 | 0.062 | 2 |
| -10.176 | 25.631 | 2.669 | 73.362 | 342.785 | 252.785 | 1.731 | 0.686 | 2 |
| -10.25 | 25.645 | 1.961 | 73.571 | 355.375 | 265.375 | 0.535 | 0.108 | 2 |
| -10.198 | 25.716 | 1.556 | 72.859 | 357.883 | 267.883 | 0.377 | 0.044 | 2 |
| -10.188 | 25.737 | 1.352 | 72.039 | 0.149 | 270.149 | 0.36 | 0.051 | 2 |
| -10.044 | 25.53 | 4.485 | 73.395 | 327.214 | 237.214 | 0.743 | 0.181 | |
| 1.981 | 38.639 | 6.1 | 65.313 | 343.366 | 253.366 | 1.497 | 0.477 | 2 |
| -9.696 | 25.999 | 4.147 | 68.122 | 326.602 | 236.602 | 1.176 | 0.353 | |
| -6.568 | 30.055 | 2.023 | 73.635 | 348.926 | 258.926 | 2.675 | 0.929 | 2 |
| -6.616 | 30.057 | 3.6 | 71.086 | 340.965 | 250.965 | 1.501 | 0.363 | 2 |
| -6.632 | 30.063 | 4.162 | 32.928 | 140.963 | 50.963 | 2.082 | 0.32 | 4 |
| -4.04 | 32.873 | 3.847 | 35.824 | 140.302 | 50.302 | 7.147 | 1.161 | 4 |
| 2.074 | 39.107 | 5.135 | 74.656 | 347.055 | 257.055 | 2.19 | 0.566 | 2 |
| -0.123 | 36.158 | 6.532 | 85.361 | 50.194 | 320.194 | 3.452 | 1.139 | |
| -2.761 | 33.962 | 4.781 | 80.791 | 330.85 | 240.85 | 5.695 | 3.825 | |
| 1 | 38.666 | 0.526 | 78.109 | 334.157 | 244.157 | 3.194 | 1.108 | |
| -1.575 | 36.072 | 1.581 | 30.494 | 144.597 | 54.597 | 7.566 | 2.041 | 4 |
| -0.256 | 36.362 | 6.059 | 87.716 | 257.601 | 167.601 | 2.511 | 0.686 | 1 |
| -0.57 | 36.926 | 2.059 | 32.348 | 140.716 | 50.716 | 1.404 | 0.24 | 4 |
| 1.954 | 38.612 | 6.155 | 65.751 | 345.658 | 255.658 | 1.476 | 0.469 | 2 |
| 2.474 | 39.232 | 6.072 | 85.996 | 258.789 | 168.789 | 2.557 | 0.526 | 1 |
| 1.084 | 37.228 | 7.145 | 86.525 | 160.083 | 70.083 | 0.897 | 0.278 | |
| 3.04 | 18.918 | 1.952 | 82.423 | 31.838 | 301.838 | 1.893 | 0.694 | 3 |
| 2.357 | 19.079 | 3.945 | 79.383 | 29.767 | 299.767 | 1.125 | 0.2 | 3 |
| 1.415 | 19.205 | 5.195 | 88.025 | 188.532 | 98.532 | 1.591 | 0.1 | |
| 1.025 | 18.815 | 4.897 | 77.925 | 23.635 | 293.635 | 1.027 | 0.106 | 3 |
| 1.481 | 18.678 | 3.79 | 83.581 | 203.762 | 113.762 | 0.57 | 0.09 | |
| 1.609 | 18.602 | 3.38 | 86.216 | 202.252 | 112.252 | 0.231 | 0.015 | |
| 2.492 | 39.209 | 6.191 | 86.945 | 256.955 | 166.955 | 2.602 | 0.492 | 1 |
| 3.603 | 18.811 | 1.702 | 78.035 | 27.591 | 297.591 | 0.832 | 0.184 | 3 |
| -0.952 | 17.283 | 5.407 | 62.648 | 330.025 | 240.025 | 1.281 | 0.168 | |
| -1.228 | 16.635 | 4.674 | 71.203 | 341.997 | 251.997 | 0.485 | 0.078 | 2 |
| 0.764 | 18.547 | 4.579 | 51.87 | 346.263 | 256.263 | 0.809 | 0.057 | |
| 0.042 | 18.024 | 5.029 | 63.971 | 323.65 | 233.65 | 0.398 | 0.047 | |
| 2.985 | 20.026 | 5.473 | 56.027 | 352.521 | 262.521 | 1.293 | 0.232 | 2 |
| -0.341 | 16.416 | 1.396 | 61.489 | 306.221 | 216.221 | 1.494 | 0.318 | |
| 5.802 | 17.914 | 0.479 | 72.367 | 32.439 | 302.439 | 2.009 | 0.335 | 3 |
| 5.095 | 18.132 | 1.691 | 63.245 | 333.273 | 243.273 | 0.713 | 0.073 | 2 |
| 4.733 | 18.698 | 0.654 | 66.812 | 332.657 | 242.657 | 0.369 | 0.032 | 2 |
| 0.855 | 38.555 | 0.751 | 79.684 | 332.94 | 242.94 | 2.377 | 1.054 | |
| 4.708 | 18.57 | 0.943 | 62.624 | 335.374 | 245.374 | 0.373 | 0.022 | 2 |
| 4.115 | 18.866 | 0.913 | 72.979 | 347.073 | 257.073 | 1.107 | 0.272 | 2 |

| | | | | | | | | |
|---|---|---|---|---|---|---|---|---|
| 4.657 | 19.027 | -0.051 | 62.632 | 325.066 | 235.066 | 1.015 | 0.098 | |
| 4.427 | 18.983 | 0.016 | 71.478 | 39.493 | 309.493 | 0.387 | 0.013 | |
| 4.308 | 19.123 | -0.246 | 76.43 | 44.932 | 314.932 | 0.335 | 0.009 | |
| 3.614 | 19.806 | 4.839 | 89.581 | 229.9 | 139.9 | 0.643 | 0.08 | |
| 3.371 | 19.915 | 4.917 | 46.598 | 150.611 | 60.611 | 0.573 | 0.052 | |
| 3.068 | 19.892 | 4.9 | 44.761 | 133.266 | 43.266 | 0.723 | 0.105 | |
| 6.668 | 17.655 | 5.381 | 82.004 | 27.709 | 297.709 | 1.263 | 0.225 | 3 |
| 4.83 | 18.815 | 4.605 | 70.818 | 15.879 | 285.879 | 0.708 | 0.068 | 3 |
| -0.855 | 36.718 | 1.645 | 30.499 | 144.577 | 54.577 | 7.428 | 1.721 | 4 |
| 4.977 | 19.075 | 5.188 | 80.386 | 157.082 | 67.082 | 0.639 | 0.11 | |
| 5.253 | 19.114 | 5.422 | 62.808 | 13.766 | 283.766 | 0.625 | 0.112 | 3 |
| 5.654 | 19.518 | 6.344 | 83.96 | 9.525 | 279.525 | 1.238 | 0.456 | 3 |
| 6.265 | 19.271 | 6.17 | 58.538 | 225.159 | 135.159 | 0.881 | 0.345 | |
| 4.652 | 19.6 | 6.109 | 66.352 | 3.044 | 273.044 | 0.313 | 0.031 | 2 |
| 4.224 | 19.568 | 5.618 | 66.206 | 147.021 | 57.021 | 0.265 | 0.016 | |
| 2.404 | 20.087 | 5.691 | 68.6 | 356.413 | 266.413 | 0.466 | 0.069 | 2 |
| 5.758 | 17.752 | 3.812 | 78.818 | 330.948 | 240.948 | 1.66 | 0.116 | |
| 6.089 | 17.29 | 2.279 | 74.444 | 25.442 | 295.442 | 1.636 | 0.547 | 3 |
| 5.273 | 18.101 | 1.412 | 63.246 | 347.663 | 257.663 | 0.432 | 0.027 | 2 |
| -6.245 | 29.675 | 6.042 | 73.812 | 342.623 | 252.623 | 2.431 | 0.773 | 2 |
| 4.16 | 19.035 | 3.613 | 78.992 | 221.764 | 131.764 | 2.339 | 1.789 | |
| 3.104 | 19.125 | 3.434 | 73.941 | 341.86 | 251.86 | 1.429 | 0.317 | 2 |
| 0.385 | 17.915 | 3.673 | 80.024 | 281.388 | 191.388 | 0.561 | 0.073 | |
| 0.929 | 18.933 | 5.327 | 89.321 | 123.716 | 33.716 | 1.027 | 0.177 | |
| 5.276 | 20.715 | 8.095 | 79.606 | 18.628 | 288.628 | 3.27 | 2.978 | 3 |
| 5.173 | 20.748 | 8.086 | 80.555 | 17.777 | 287.777 | 4.084 | 3.894 | 3 |
| 2.328 | 21.572 | 8.033 | 82.425 | 16.527 | 286.527 | 0.801 | 0.108 | 3 |
| -4.813 | 21.527 | 8.725 | 85.949 | 255.343 | 165.343 | 4.123 | 1.615 | 1 |
| -3.605 | 23.864 | 8.637 | 76.861 | 29.55 | 299.55 | 1.053 | 0.188 | 3 |
| 0.104 | 25.152 | 8.92 | 60.933 | 330.696 | 240.696 | 1.395 | 0.363 | |
| -6.295 | 29.341 | 6.624 | 72.144 | 276.109 | 186.109 | 1.287 | 0.309 | |
| -1.744 | 24.13 | 8.693 | 61.553 | 333.19 | 243.19 | 2.376 | 0.445 | 2 |
| -4.27 | 22.943 | 8.92 | 67.226 | 334.254 | 244.254 | 2.829 | 0.706 | 2 |
| -6.088 | 22.234 | 8.905 | 76.364 | 7.969 | 277.969 | 0.592 | 0.024 | 3 |
| -6.277 | 22.543 | 8.864 | 74.589 | 352.503 | 262.503 | 0.559 | 0.097 | 2 |
| -7.893 | 23.444 | 8.84 | 78.355 | 259.983 | 169.983 | 0.722 | 0.096 | 1 |
| -7.352 | 23.774 | 9.041 | 77.654 | 261.208 | 171.208 | 1.171 | 0.428 | 1 |
| 2.894 | 27.661 | 9.084 | 66.456 | 345.851 | 255.851 | 5.42 | 1.729 | 2 |
| 10.437 | 27.315 | 9.158 | 64.878 | 349.391 | 259.391 | 5.062 | 1.529 | 2 |
| 12.05 | 28.289 | 8.819 | 28.692 | 143.384 | 53.384 | 7.943 | 17.577 | 4 |
| 7.693 | 26.27 | 9.291 | 65.881 | 278.567 | 188.567 | 2.277 | 0.562 | |
| -6.347 | 29.159 | 6.64 | 74.698 | 358.442 | 268.442 | 1.045 | 0.11 | 2 |
| 9.186 | 24.249 | 8.945 | 86.584 | 75.266 | 345.266 | 3.066 | 1.195 | 1 |

| | | | | | | | | |
|---|---|---|---|---|---|---|---|---|
| -2.976 | 25.473 | 8.493 | 86.195 | 218.234 | 128.234 | 3.763 | 0.696 | |
| 2.707 | 38.329 | 8.585 | 86.492 | 261.966 | 171.966 | 2.452 | 1.135 | 1 |
| 1.951 | 35.965 | 9.189 | 80.075 | 318.853 | 228.853 | 2.004 | 0.396 | |
| 1.791 | 37.544 | 7.995 | 81.504 | 263.016 | 173.016 | 1.4 | 0.201 | 1 |
| 1.972 | 37.626 | 8.233 | 63.353 | 351.589 | 261.589 | 1.621 | 0.309 | 2 |
| 2.607 | 35.571 | 9.503 | 65.001 | 248.518 | 158.518 | 1.185 | 0.199 | |
| 2.432 | 31.258 | 9.443 | 76.751 | 172.972 | 82.972 | 2.4 | 0.963 | |
| 1.51 | 32.124 | 9.349 | 69.922 | 251.691 | 161.691 | 1.748 | 0.624 | |
| 8.979 | 22.704 | 8.507 | 71.092 | 14.865 | 284.865 | 2.807 | 0.585 | 3 |
| -23.279 | 6.282 | 1.174 | 64.961 | 2.199 | 272.199 | 2.607 | 0.432 | 2 |
| -25.239 | 1.205 | 5.378 | 69.783 | 358.081 | 268.081 | 1.191 | 0.264 | 2 |
| -18.174 | -5.615 | 6.951 | 42.292 | 354.926 | 264.926 | 1.049 | 0.225 | |
| -21.308 | -9.427 | 6.934 | 54.119 | 305.381 | 215.381 | 0.862 | 0.15 | |
| -21.016 | -8.889 | 6.817 | 50.319 | 317.288 | 227.288 | 0.427 | 0.049 | |
| -21.867 | -9.976 | 6.937 | 49.18 | 321.764 | 231.764 | 1.207 | 0.156 | |
| -25.136 | -10.382 | 7.025 | 52.417 | 324.397 | 234.397 | 0.691 | 0.076 | |
| -15.875 | -3.534 | 7.225 | 54.046 | 266.359 | 176.359 | 0.911 | 0.134 | |
| -15.626 | -2.569 | 7.258 | 39.648 | 340.021 | 250.021 | 1.448 | 0.398 | |
| -26.085 | 0.634 | 4.578 | 69.644 | 359.742 | 269.742 | 2.496 | 0.46 | 2 |
| -22.295 | 8.337 | 2.709 | 68.842 | 327.295 | 237.295 | 1.253 | 0.276 | |
| -22.286 | 8.364 | 1.916 | 78.232 | 330.249 | 240.249 | 1.28 | 0.299 | |
| -23.829 | 5.333 | 1.279 | 70.744 | 81.337 | 351.337 | 0.937 | 0.143 | |
| -23.657 | 5.565 | 0.559 | 64.175 | 80.537 | 350.537 | 0.232 | 0.018 | |
| -23.721 | 5.353 | 0.566 | 72.374 | 75.393 | 345.393 | 0.38 | 0.05 | |
| -25.272 | 2.167 | 2.888 | 80.668 | 2.708 | 272.708 | 1.056 | 0.054 | |
| -24.64 | 2.543 | 2.349 | 56.539 | 67.191 | 337.191 | 0.717 | 0.155 | |
| -24.57 | 2.844 | 3.534 | 84.545 | 18.289 | 288.289 | 0.708 | 0.042 | 3 |
| -22.858 | 7.294 | 0.746 | 51.535 | 317.406 | 227.406 | 0.854 | 0.133 | |
| -24.765 | 2.404 | 1.97 | 49.274 | 303.538 | 213.538 | 0.406 | 0.083 | |
| -26.467 | 0.837 | 1.498 | 89.406 | 196.927 | 106.927 | 1.857 | 0.51 | |
| -26.349 | 0.82 | 2.767 | 82.144 | 10.522 | 280.522 | 0.746 | 0.085 | 3 |
| -27.749 | 0.436 | 1.707 | 85.392 | 313.322 | 223.322 | 0.246 | 0.011 | |
| -26.948 | 0.801 | 2.314 | 85.171 | 3.026 | 273.026 | 0.476 | 0.099 | |
| -26.79 | 0.335 | 0.486 | 78.991 | 99.961 | 9.961 | 0.527 | 0.092 | |
| -26.485 | -0.262 | 5.602 | 67.732 | 16.46 | 286.46 | 0.49 | 0.054 | 3 |
| -26.562 | -0.014 | 5.263 | 71.235 | 17.221 | 287.221 | 0.371 | 0.062 | 3 |
| -26.167 | -0.088 | 5.477 | 73.571 | 9.698 | 279.698 | 0.195 | 0.014 | 3 |
| -27.148 | -0.45 | 5.752 | 60.814 | 18.643 | 288.643 | 0.704 | 0.288 | 3 |
| -25.098 | 2.364 | 1.501 | 86.55 | 30.655 | 300.655 | 2.849 | 0.898 | 3 |
| -27.113 | -0.037 | 5.128 | 70.054 | 348.79 | 258.79 | 0.929 | 0.427 | 2 |
| -27.291 | 0.619 | 2.03 | 80.544 | 311.787 | 221.787 | 1.353 | 0.301 | |
| -25.51 | 1.881 | 2.981 | 73.606 | 8.816 | 278.816 | 0.404 | 0.05 | 3 |
| -25.693 | 1.679 | 2.092 | 82.954 | 16.856 | 286.856 | 0.699 | 0.022 | 3 |

| | | | | | | | | |
|---|---|---|---|---|---|---|---|---|
| -25.496 | 1.947 | 1.773 | 70.437 | 348.364 | 258.364 | 0.565 | 0.026 | 2 |
| -25.525 | 1.982 | 2.436 | 67.781 | 275.544 | 185.544 | 0.597 | 0.069 | |
| -25.406 | 1.961 | 2.991 | 71.113 | 267.474 | 177.474 | 0.373 | 0.045 | |
| -23.688 | 4.883 | 3.189 | 76.902 | 335.178 | 245.178 | 0.774 | 0.161 | |
| -24.699 | 1.721 | 5.949 | 89.165 | 39.288 | 309.288 | 0.951 | 0.063 | |
| -24.633 | 1.969 | 6.18 | 87.381 | 39.879 | 309.879 | 0.406 | 0.025 | |
| -23.902 | 4.269 | 5.303 | 55.857 | 137.649 | 47.649 | 0.873 | 0.13 | |
| -24.634 | 1.537 | 6.216 | 84.623 | 29.634 | 299.634 | 0.417 | 0.017 | 3 |
| -24.979 | 1.897 | 5.088 | 77.266 | 21.878 | 291.878 | 0.329 | 0.018 | 3 |
| -24.821 | 2.415 | 4.16 | 76.51 | 350.101 | 260.101 | 0.543 | 0.083 | 2 |
| -13.149 | -5.68 | 2.804 | 82.436 | 261.46 | 171.46 | 3.585 | 2.899 | 1 |
| -12.937 | -4.256 | 4.776 | 84.801 | 259.744 | 169.744 | 2.368 | 1.382 | 1 |
| -12.264 | -2.802 | 3.306 | 77.864 | 261.499 | 171.499 | 2.454 | 1.892 | 1 |
| -12.437 | -2.961 | 2.174 | 74.32 | 266.762 | 176.762 | 1.605 | 0.889 | |
| -12.113 | -1.849 | 2.768 | 85.987 | 255.39 | 165.39 | 1.113 | 0.282 | 1 |
| -12.37 | -2.898 | 4.427 | 80.048 | 270.414 | 180.414 | 1.104 | 0.55 | |
| -12.519 | -3.025 | 5.346 | 73.86 | 280.437 | 190.437 | 1.315 | 0.33 | |
| -23.882 | 4.297 | 4.939 | 47.062 | 147.801 | 57.801 | 0.134 | 0.007 | |
| -12.795 | -3.322 | 6.365 | 82.874 | 252.482 | 162.482 | 1.021 | 0.316 | 1 |
| -12.684 | -2.852 | 6.257 | 87.443 | 305.806 | 215.806 | 0.274 | 0.034 | |
| -13.17 | -5.251 | 5.499 | 89.235 | 258.301 | 168.301 | 1.586 | 0.413 | 1 |
| -13.209 | -6.039 | 3.691 | 78.396 | 279.264 | 189.264 | 1.528 | 0.21 | |
| -13.811 | -8.433 | 2.396 | 81.004 | 241.725 | 151.725 | 4.662 | 3.793 | |
| -13.964 | -9.598 | 1.51 | 63.038 | 246.449 | 156.449 | 1.985 | 0.552 | |
| -14.023 | -9.93 | 2.048 | 73.659 | 262.519 | 172.519 | 1.356 | 0.218 | |
| -14.316 | -10.562 | 2.521 | 84.694 | 248.167 | 158.167 | 2.571 | 0.767 | 1 |
| -13.819 | -7.343 | 0.97 | 81.653 | 51.694 | 321.694 | 0.634 | 0.099 | |
| -13.953 | -7.701 | 1.508 | 86.929 | 57.633 | 327.633 | 0.663 | 0.068 | |
| -24.026 | 4.11 | 4.863 | 50.065 | 146.08 | 56.08 | 0.138 | 0.006 | |
| -14.004 | -7.856 | 1.515 | 67.524 | 345.479 | 255.479 | 0.474 | 0.048 | 2 |
| -13.964 | -7.624 | 1.031 | 67.58 | 348.039 | 258.039 | 0.426 | 0.023 | 2 |
| -14.055 | -8.052 | 1.411 | 84.842 | 257.057 | 167.057 | 0.826 | 0.143 | 1 |
| -13.707 | -9.544 | 2.098 | 84.294 | 244.378 | 154.378 | 0.566 | 0.064 | 1 |
| -13.872 | -9.676 | 2.939 | 51.442 | 62.312 | 332.312 | 0.513 | 0.085 | |
| -13.47 | -6.096 | 0.02 | 78.99 | 259.366 | 169.366 | 1.519 | 0.897 | 1 |
| -14.092 | -7.474 | -0.001 | 82.759 | 244.267 | 154.267 | 1.066 | 0.328 | 1 |
| -12.104 | -2.004 | 1.121 | 81.409 | 250.12 | 160.12 | 1.319 | 0.278 | 1 |
| -12.454 | -2.773 | 0.766 | 78.39 | 263.399 | 173.399 | 0.952 | 0.396 | 1 |
| -13.236 | -5.554 | 0.925 | 81.708 | 249.425 | 159.425 | 1.282 | 0.419 | 1 |
| -23.745 | 4.5 | 5.1 | 47.079 | 140.097 | 50.097 | 0.916 | 0.098 | |
| -14.192 | -8.76 | 5.15 | 80.453 | 256.038 | 166.038 | 2.814 | 1.259 | 1 |
| -14.236 | -9.69 | 5.108 | 80.843 | 254.567 | 164.567 | 0.668 | 0.162 | 1 |
| -12.874 | -4.044 | 1.205 | 77.191 | 79.544 | 349.544 | 0.539 | 0.109 | 1 |

| | | | | | | | | |
|---|---|---|---|---|---|---|---|---|
| -13.172 | -4.766 | 0.128 | 80.428 | 259.147 | 169.147 | 1.315 | 0.472 | 1 |
| -12.482 | -2.423 | 6.019 | 87.055 | 270.348 | 180.348 | 0.893 | 0.479 | 1 |
| -12.579 | -3.066 | 5.637 | 75.066 | 284.708 | 194.708 | 0.785 | 0.189 | |
| -13.237 | -5.57 | 5.625 | 69.828 | 345.824 | 255.824 | 0.835 | 0.102 | 2 |
| -28.605 | -5.114 | 7.391 | 27.985 | 146.124 | 56.124 | 12.274 | 28.811 | 4 |
| -34.604 | -5.002 | 8.203 | 82.623 | 259.062 | 169.062 | 1.503 | 0.346 | 1 |
| -22.236 | 0.913 | 7.071 | 27.997 | 133.593 | 43.593 | 4.283 | 2.536 | 4 |
| -23.232 | 6.131 | 4.554 | 42.633 | 123.804 | 33.804 | 0.442 | 0.065 | |
| -22.631 | 1.415 | 7.235 | 61.139 | 307.465 | 217.465 | 0.437 | 0.105 | |
| -22.258 | -0.459 | 7.069 | 87.16 | 44.14 | 314.14 | 2.192 | 0.657 | |
| -20.946 | 3.539 | 7.285 | 61.568 | 344.774 | 254.774 | 5.223 | 2.099 | 2 |
| -22.531 | 4.099 | 6.929 | 67.907 | 347.943 | 257.943 | 2.796 | 0.981 | 2 |
| -18.992 | 4.551 | 7.561 | 66.075 | 346.807 | 256.807 | 3.426 | 1.324 | 2 |
| -20.149 | 1.308 | 7.283 | 22.333 | 140.075 | 50.075 | 6.865 | 9.118 | 4 |
| -28.621 | -10.961 | 7.116 | 26.301 | 146.612 | 56.612 | 3.822 | 3.589 | 4 |
| -21.398 | -6.343 | 6.751 | 25.071 | 137.96 | 47.96 | 5.369 | 5.887 | 4 |
| -18.922 | -3.764 | 6.997 | 24.055 | 153.144 | 63.144 | 1.917 | 1.366 | 4 |
| -17.042 | -1.954 | 7.39 | 29.263 | 139.597 | 49.597 | 1.652 | 0.799 | 4 |
| -24.211 | 3.781 | 4.79 | 55.876 | 107.644 | 17.644 | 0.369 | 0.031 | |
| -16.279 | -0.278 | 7.311 | 39.247 | 27.514 | 297.514 | 1.269 | 0.363 | |
| -16.279 | -0.278 | 7.311 | 39.247 | 27.514 | 297.514 | 1.269 | 0.363 | |
| -17.172 | -0.864 | 7.243 | 36.325 | 25.436 | 295.436 | 1.21 | 0.508 | |
| -19.395 | -0.196 | 7.143 | 70.753 | 354.049 | 264.049 | 1.92 | 0.472 | 2 |
| -19.316 | 0.346 | 6.975 | 71.249 | 328.831 | 238.831 | 0.511 | 0.074 | |
| -18.83 | 0.919 | 7.068 | 52.651 | 353.413 | 263.413 | 1.129 | 0.144 | |
| -19.014 | 1.313 | 7.095 | 61.736 | 356.958 | 266.958 | 0.941 | 0.211 | 2 |
| -23.119 | -13.124 | 7.069 | 64.792 | 311.602 | 221.602 | 2.045 | 0.524 | |
| -20.025 | -11.566 | 7.045 | 49.096 | 327.76 | 237.76 | 0.875 | 0.258 | |
| -19.819 | -12.158 | 7.208 | 46.931 | 9.221 | 279.221 | 1.095 | 0.258 | |
| -27.133 | -19.41 | 1.997 | 86.652 | 55.145 | 325.145 | 4.038 | 8.218 | |
| -33.321 | -14.107 | 5.125 | 83.267 | 45.91 | 315.91 | 2.225 | 1.822 | |
| -31.951 | -14.743 | 2.52 | 81.998 | 40.612 | 310.612 | 7.734 | 16.477 | |
| -31.662 | -15.386 | 3.917 | 36.255 | 79.651 | 349.651 | 1.824 | 0.191 | |
| -31.837 | -15.437 | 5.141 | 32.839 | 186.071 | 96.071 | 1.373 | 0.273 | |
| -31.419 | -11.201 | 7.271 | 89.007 | 55.702 | 325.702 | 3.939 | 1.272 | |
| -29.61 | -17.823 | 7.471 | 78.398 | 41.848 | 311.848 | 10.764 | 11.111 | |
| -36.757 | -7.036 | 8.147 | 86.326 | 261.676 | 171.676 | 2.485 | 1.711 | 1 |
| -34.935 | -8.283 | 7.748 | 21.666 | 147.615 | 57.615 | 4.175 | 8.603 | 4 |
| -0.846 | -23.535 | 0.105 | 67.714 | 278.686 | 188.686 | 2.472 | 0.561 | |
| -1.545 | -24.418 | 3.424 | 72.075 | 263.093 | 173.093 | 0.679 | 0.078 | |
| -13.255 | -14.966 | -0.263 | 74.258 | 342.398 | 252.398 | 0.983 | 0.303 | 2 |
| -13.337 | -14.326 | 4.933 | 66.944 | 356.768 | 266.768 | 1.193 | 0.261 | 2 |
| -13.741 | -14.314 | 5.268 | 76.578 | 243.838 | 153.838 | 0.326 | 0.032 | |

| | | | | | | | | |
|---|---|---|---|---|---|---|---|---|
| -14.426 | -12.447 | 1.383 | 75.872 | 330.968 | 240.968 | 1.159 | 0.094 | |
| -25.539 | -24.625 | 0.795 | 71.667 | 345.088 | 255.088 | 1.641 | 0.301 | 2 |
| -26.12 | -25.235 | 3.381 | 68.154 | 349.714 | 259.714 | 4.126 | 2.342 | 2 |
| -25.036 | -22.916 | 5.724 | 74.067 | 29.333 | 299.333 | 0.496 | 0.108 | 3 |
| -24.951 | -24.041 | 0.817 | 82.103 | 265.658 | 175.658 | 0.503 | 0.088 | 1 |
| -24.913 | -24.25 | 0.377 | 65.336 | 105.138 | 15.138 | 0.336 | 0.035 | |
| -26.329 | -25.565 | 1.708 | 83.014 | 54.167 | 324.167 | 1.32 | 0.309 | |
| -2.322 | -24.971 | 4.44 | 61.032 | 303.145 | 213.145 | 1.242 | 0.357 | |
| -25.658 | -24.714 | 2.961 | 70.284 | 339.556 | 249.556 | 0.711 | 0.11 | 2 |
| -25.008 | -24.554 | -0.139 | 28.28 | 144.759 | 54.759 | 0.949 | 0.297 | 4 |
| -24.916 | -24.137 | 4.208 | 63.194 | 48.94 | 318.94 | 0.523 | 0.057 | |
| -25.183 | -22.883 | 4.484 | 78.977 | 56.697 | 326.697 | 0.725 | 0.125 | |
| -25.409 | -24.772 | 4.171 | 73.063 | 346.27 | 256.27 | 1.367 | 0.436 | 2 |
| -25.32 | -25.366 | 5.327 | 61.987 | 344.13 | 254.13 | 0.918 | 0.151 | 2 |
| -25.984 | -25.418 | 4.597 | 66.312 | 329.533 | 239.533 | 0.743 | 0.158 | |
| -25.368 | -24.439 | 0.949 | 81.642 | 108.869 | 18.869 | 0.523 | 0.085 | |
| -25.856 | -25.082 | 1.019 | 86.504 | 72.406 | 342.406 | 0.4 | 0.039 | 1 |
| -25.043 | -24 | 3.274 | 70.949 | 70.133 | 340.133 | 0.636 | 0.131 | |
| -0.96 | -23.55 | 4.269 | 69.988 | 271.017 | 181.017 | 0.337 | 0.036 | |
| -11.277 | -14.876 | 6.101 | 64.915 | 349.716 | 259.716 | 4.098 | 1.767 | 2 |
| -8.612 | -21.244 | 6.315 | 68.679 | 350.15 | 260.15 | 4.046 | 1.183 | 2 |
| -11.39 | -21.146 | 6.294 | 57.961 | 346.005 | 256.005 | 1.72 | 0.351 | 2 |
| -11.895 | -21.79 | 6.279 | 86.591 | 63.465 | 333.465 | 0.977 | 0.076 | 1 |
| -12.177 | -22.078 | 6.257 | 71.176 | 355.347 | 265.347 | 0.828 | 0.128 | 2 |
| -13.133 | -19.196 | 6.398 | 85.439 | 72.524 | 342.524 | 0.905 | 0.103 | 1 |
| -10.915 | -24.778 | 6.3 | 64.61 | 351.941 | 261.941 | 5.944 | 1.29 | 2 |
| -7.925 | -18.891 | 6.468 | 88.012 | 37.44 | 307.44 | 0.859 | 0.086 | |
| -9.234 | -18.694 | 6.451 | 72.305 | 95.389 | 5.389 | 1.064 | 0.242 | |
| -9.42 | -17.949 | 6.514 | 86.087 | 40.654 | 310.654 | 0.854 | 0.163 | |
| -1.803 | -24.506 | 4.013 | 65.146 | 276.705 | 186.705 | 0.55 | 0.087 | |
| -9.553 | -19.288 | 6.508 | 81.585 | 87.601 | 357.601 | 0.63 | 0.105 | |
| -8.636 | -19.395 | 6.411 | 87.898 | 63.645 | 333.645 | 0.83 | 0.109 | 1 |
| -11.048 | -20.142 | 6.317 | 86.647 | 246.379 | 156.379 | 0.446 | 0.054 | 1 |
| -11.213 | -20.222 | 6.523 | 24.266 | 235.781 | 145.781 | 0.265 | 0.038 | |
| -11.337 | -20.097 | 6.404 | 51.368 | 301.598 | 211.598 | 0.413 | 0.069 | |
| -11.133 | -20.172 | 6.456 | 82.946 | 69.012 | 339.012 | 0.391 | 0.051 | 1 |
| -17.019 | -23.886 | 6.109 | 50.388 | 35.779 | 305.779 | 1.004 | 0.103 | |
| -15.778 | -23.324 | 6.227 | 80.34 | 25.185 | 295.185 | 2.211 | 0.199 | 3 |
| -16.117 | -24.789 | 6.172 | 53.628 | 9.614 | 279.614 | 1.171 | 0.189 | |
| -5.66 | -23.67 | 6.038 | 48.578 | 303.543 | 213.543 | 0.431 | 0.054 | |
| -1.518 | -24.076 | 4.346 | 54.13 | 283.597 | 193.597 | 0.5 | 0.051 | |
| -6.507 | -23.558 | 6.136 | 49.363 | 306.713 | 216.713 | 1.303 | 0.083 | |
| -7.35 | -23.562 | 6.227 | 54.722 | 305.96 | 215.96 | 1.205 | 0.104 | |

| | | | | | | | | |
|---|---|---|---|---|---|---|---|---|
| -4.402 | -23.786 | 5.914 | 84.545 | 44.364 | 314.364 | 2.155 | 0.354 | |
| -4.043 | -25.805 | 5.752 | 89.151 | 251.293 | 161.293 | 0.894 | 0.267 | 1 |
| -5.562 | -25.346 | 5.987 | 50.446 | 22.391 | 292.391 | 1.169 | 0.268 | |
| -4.999 | -24.604 | 5.864 | 38.081 | 12.783 | 282.783 | 0.978 | 0.196 | |
| -14.501 | -21.321 | 6.427 | 65.532 | 31.654 | 301.654 | 1.104 | 0.135 | 3 |
| -14.525 | -21.655 | 6.386 | 38.427 | 332.927 | 242.927 | 0.447 | 0.058 | |
| -14.073 | -21.144 | 6.334 | 42.784 | 328.948 | 238.948 | 0.494 | 0.087 | |
| -13.969 | -21.605 | 6.318 | 60.942 | 103.89 | 13.89 | 0.767 | 0.061 | |
| -1.451 | -24.142 | 3.887 | 53.249 | 289.472 | 199.472 | 0.822 | 0.116 | |
| -13.392 | -21.35 | 6.26 | 61.794 | 98.699 | 8.699 | 0.393 | 0.025 | |
| -13.101 | -22.883 | 6.199 | 67.167 | 352.352 | 262.352 | 0.626 | 0.062 | 2 |
| -12.306 | -22.945 | 6.359 | 52.404 | 13.98 | 283.98 | 0.419 | 0.104 | |
| -12.117 | -22.842 | 6.28 | 65.221 | 10.252 | 280.252 | 0.453 | 0.058 | 3 |
| -12.519 | -22.614 | 6.217 | 66.134 | 11.353 | 281.353 | 0.595 | 0.049 | 3 |
| -14.017 | -24.027 | 6.149 | 20.687 | 146.378 | 56.378 | 1.43 | 0.332 | 4 |
| -13.856 | -18.167 | 6.437 | 71.729 | 33.84 | 303.84 | 0.776 | 0.102 | 3 |
| -13.572 | -18.576 | 6.417 | 70.229 | 30.468 | 300.468 | 0.961 | 0.161 | 3 |
| -13.71 | -18.655 | 6.488 | 65.041 | 29.987 | 299.987 | 0.97 | 0.126 | 3 |
| -14.994 | -18.014 | 6.556 | 64.978 | 22.793 | 292.793 | 0.299 | 0.02 | 3 |
| -1.324 | -24.185 | 0.876 | 88.157 | 170.516 | 80.516 | 0.646 | 0.112 | |
| -15.106 | -18.496 | 6.592 | 41.375 | 3.75 | 273.75 | 0.381 | 0.033 | |
| -15.748 | -18.815 | 6.626 | 50.868 | 332.559 | 242.559 | 0.545 | 0.038 | |
| -15.992 | -19.232 | 6.581 | 24.624 | 156.49 | 66.49 | 1.066 | 0.18 | 4 |
| -16.006 | -17.714 | 6.786 | 66.949 | 17.418 | 287.418 | 0.674 | 0.079 | 3 |
| -24.777 | -23.208 | 6.231 | 75.235 | 27.247 | 297.247 | 1.15 | 0.34 | 3 |
| -14.782 | -27.945 | 5.976 | 48.375 | 359.028 | 269.028 | 1.208 | 0.199 | |
| -17.114 | -27.337 | 5.923 | 65.692 | 325.885 | 235.885 | 2.558 | 0.415 | |
| -18.708 | -25.977 | 6.225 | 67.105 | 352.796 | 262.796 | 5.06 | 1.95 | 2 |
| -24.001 | -24.124 | 6.163 | 88.36 | 254.464 | 164.464 | 0.924 | 0.212 | 1 |
| -23.258 | -25.212 | 6.287 | 58.683 | 244.693 | 154.693 | 1.369 | 0.139 | |
| -1.542 | -24.328 | 1.037 | 89.424 | 169.803 | 79.803 | 0.303 | 0.041 | |
| -22.468 | -27.123 | 6.445 | 79.638 | 71.227 | 341.227 | 1.491 | 0.184 | 1 |
| -22.463 | -28.076 | 6.302 | 79.717 | 232.025 | 142.025 | 0.747 | 0.119 | |
| -20.616 | -29.797 | 6.263 | 86.77 | 65.963 | 335.963 | 3.977 | 0.821 | 1 |
| -19.75 | -26.692 | 6.132 | 35.126 | 235.506 | 145.506 | 0.817 | 0.136 | |
| -19.566 | -23.77 | 6.317 | 58.736 | 276.15 | 186.15 | 1.905 | 0.22 | |
| -18.632 | -24.735 | 6.251 | 66.804 | 290.059 | 200.059 | 0.527 | 0.054 | |
| -16.547 | -21.921 | 6.423 | 58.193 | 51.269 | 321.269 | 1.144 | 0.061 | |
| -16.085 | -21.637 | 6.495 | 45.88 | 295.509 | 205.509 | 0.27 | 0.018 | |
| -16.098 | -21.459 | 6.51 | 68.234 | 343.652 | 253.652 | 1.146 | 0.08 | 2 |
| -14.228 | -30.785 | 5.663 | 84.878 | 248.464 | 158.464 | 0.976 | 0.097 | 1 |
| -1.724 | -24.544 | 0.658 | 80.277 | 255.403 | 165.403 | 0.561 | 0.048 | 1 |
| -14.918 | -31.826 | 5.73 | 35.984 | 356.712 | 266.712 | 0.813 | 0.235 | |

| | | | | | | | | |
|---|---|---|---|---|---|---|---|---|
| -16.669 | -29.821 | 5.902 | 52.983 | 321.152 | 231.152 | 0.656 | 0.085 | |
| -16.625 | -30.801 | 5.967 | 65.541 | 322.815 | 232.815 | 0.373 | 0.029 | |
| -17.632 | -29.48 | 5.938 | 25.845 | 14.278 | 284.278 | 0.487 | 0.076 | |
| -1.556 | -24.335 | 0.469 | 80.175 | 249.516 | 159.516 | 0.499 | 0.026 | 1 |
| -0.573 | -23.117 | -0.444 | 69.345 | 277.947 | 187.947 | 0.961 | 0.139 | |
| -0.433 | -23.351 | 2.005 | 84.121 | 242.758 | 152.758 | 0.423 | 0.039 | 1 |
| -0.09 | -23.095 | 0.993 | 81.842 | 250.159 | 160.159 | 1.032 | 0.127 | 1 |
| -1.151 | -24.029 | 3.308 | 56.26 | 266.262 | 176.262 | 1.513 | 0.194 | |
| -3.18 | -25.76 | 2.643 | 56.955 | 281.212 | 191.212 | 1.26 | 0.187 | |
| -4.282 | -26.502 | 2.992 | 83.495 | 247.075 | 157.075 | 4.166 | 0.835 | 1 |
| -11.434 | -30.937 | 3.048 | 87.521 | 79.849 | 349.849 | 3.17 | 0.984 | 1 |
| -4.488 | -26.62 | 3.524 | 76.323 | 260.306 | 170.306 | 1.47 | 0.16 | 1 |
| -4.926 | -26.886 | 2.277 | 60.503 | 247.795 | 157.795 | 0.573 | 0.046 | |
| -4.73 | -26.789 | 3.491 | 71.856 | 249.488 | 159.488 | 0.771 | 0.071 | |
| -5.146 | -26.987 | 3.556 | 89.402 | 189.019 | 99.019 | 0.896 | 0.174 | |
| -1.187 | -23.9 | -0.017 | 67.197 | 267.051 | 177.051 | 1.511 | 0.266 | |
| -3.919 | -26.204 | 2.841 | 59.47 | 269.245 | 179.245 | 0.767 | 0.112 | |
| -4.092 | -26.385 | 2.656 | 61.051 | 268.116 | 178.116 | 0.724 | 0.079 | |
| -3.974 | -26.259 | 3.181 | 55.679 | 18.345 | 288.345 | 0.405 | 0.033 | |
| -3.008 | -25.596 | 2.105 | 67.723 | 279.994 | 189.994 | 0.525 | 0.034 | |
| -3.02 | -25.578 | 4.12 | 64.605 | 249.36 | 159.36 | 0.36 | 0.026 | |
| -6.115 | -27.594 | 2.939 | 63.446 | 270.231 | 180.231 | 0.933 | 0.146 | |
| -5.682 | -27.467 | 3.975 | 63.06 | 272.679 | 182.679 | 0.638 | 0.096 | |
| -2.597 | -25.351 | 2.178 | 86.813 | 59.533 | 329.533 | 3.893 | 0.572 | |
| -10.581 | -30.077 | 0.813 | 64.218 | 272.33 | 182.33 | 1.278 | 0.19 | |
| -10.79 | -30.313 | 0.916 | 64.955 | 273.738 | 183.738 | 1.703 | 0.24 | |
| -1.961 | -24.964 | 1.083 | 70.025 | 267.064 | 177.064 | 2.105 | 0.612 | |
| -11.083 | -30.584 | 0.613 | 68.966 | 278.971 | 188.971 | 0.891 | 0.109 | |
| -10.705 | -30.25 | 1.131 | 66.309 | 350.691 | 260.691 | 1.593 | 0.266 | 2 |
| -11.151 | -30.7 | 1.033 | 62.243 | 278.996 | 188.996 | 0.786 | 0.11 | |
| -11.288 | -30.81 | 1.159 | 70.308 | 282.96 | 192.96 | 1.015 | 0.157 | |
| -10.656 | -30.101 | 2.229 | 76.885 | 286.071 | 196.071 | 1.092 | 0.094 | |
| -11.469 | -31.054 | 2.911 | 70.942 | 284.686 | 194.686 | 1.694 | 0.515 | |
| -12.311 | -31.731 | 3.695 | 64.42 | 350.266 | 260.266 | 1.681 | 0.376 | 2 |
| -12.904 | -32.116 | 3.986 | 63.186 | 297.131 | 207.131 | 0.828 | 0.098 | |
| -13.134 | -32.289 | 2.075 | 89.57 | 256.837 | 166.837 | 3.101 | 0.529 | 1 |
| -12.986 | -32.16 | 2.645 | 86.121 | 264.47 | 174.47 | 1.248 | 0.212 | 1 |
| -1.249 | -24.115 | 1.915 | 63.901 | 262.545 | 172.545 | 0.54 | 0.098 | |
| -13.05 | -32.135 | 1.575 | 78.182 | 279.771 | 189.771 | 0.701 | 0.095 | |
| -13.577 | -32.539 | 0.79 | 80.302 | 267.798 | 177.798 | 1.189 | 0.143 | 1 |
| -15.107 | -34.235 | 0.711 | 78.311 | 283.175 | 193.175 | 2.453 | 0.639 | |
| -14.479 | -33.618 | 1.14 | 80.229 | 289.107 | 199.107 | 1.91 | 0.619 | |
| -14.133 | -33.131 | 2.339 | 88.344 | 281.302 | 191.302 | 2.102 | 0.609 | |

| | | | | | | | | |
|---|---|---|---|---|---|---|---|---|
| -12.639 | -31.834 | 1.367 | 88.557 | 277.943 | 187.943 | 0.919 | 0.177 | |
| -12.041 | -31.316 | -0.305 | 66.473 | 282.592 | 192.592 | 0.535 | 0.073 | |
| -12.422 | -31.53 | -0.444 | 65.517 | 291.11 | 201.11 | 1.074 | 0.132 | |
| -11.881 | -31.089 | -0.401 | 75.463 | 268.187 | 178.187 | 1.167 | 0.199 | |
| -9.357 | -29.157 | 1.083 | 88.906 | 249.295 | 159.295 | 1.108 | 0.12 | 1 |
| -0.901 | -23.77 | 1.724 | 77.482 | 235.585 | 145.585 | 0.517 | 0.032 | |
| -9.866 | -29.527 | 1.076 | 69.204 | 284.412 | 194.412 | 1.421 | 0.163 | |
| -9.31 | -29.291 | 2.507 | 79.584 | 279.797 | 189.797 | 0.616 | 0.07 | |
| -9.903 | -29.545 | 1.918 | 64.51 | 259.552 | 169.552 | 0.612 | 0.048 | |
| -9.423 | -29.403 | 2.719 | 64.431 | 298.157 | 208.157 | 1.261 | 0.132 | |
| -9.915 | -29.584 | 2.487 | 66.999 | 266.789 | 176.789 | 0.345 | 0.025 | |
| -8.381 | -28.587 | -0.355 | 25.386 | 151.27 | 61.27 | 0.681 | 0.102 | 4 |
| -9.24 | -29.112 | 0.198 | 39.408 | 148.156 | 58.156 | 0.746 | 0.038 | 4 |
| -11.566 | -30.822 | -0.402 | 66.368 | 284.491 | 194.491 | 0.89 | 0.094 | |
| -6.594 | -27.947 | -0.348 | 79.831 | 31.011 | 301.011 | 0.796 | 0.16 | 3 |
| -6.359 | -28.003 | 0.472 | 76.619 | 16.924 | 286.924 | 0.411 | 0.041 | 3 |
| -1.127 | -24.014 | 1.176 | 69.09 | 355.118 | 265.118 | 1.021 | 0.079 | 2 |
| -6.831 | -27.914 | -0.42 | 65.962 | 269.013 | 179.013 | 0.546 | 0.04 | |
| -6.514 | -28.054 | 0.423 | 71.733 | 275.568 | 185.568 | 0.429 | 0.021 | |
| -6.766 | -28.055 | 0.141 | 71.215 | 218.044 | 128.044 | 0.361 | 0.014 | |
| -6.705 | -28.106 | 0.521 | 72.564 | 202.726 | 112.726 | 0.264 | 0.014 | |
| -6.914 | -28.148 | 0.81 | 58.762 | 274.599 | 184.599 | 0.25 | 0.01 | |
| -7.553 | -28.137 | 0.046 | 71.979 | 235.846 | 145.846 | 0.791 | 0.048 | |
| -7.973 | -28.307 | 0.233 | 78.522 | 13.509 | 283.509 | 0.724 | 0.13 | 3 |
| -7.94 | -28.473 | 1.16 | 67.511 | 328.916 | 238.916 | 1.008 | 0.463 | |
| -7.883 | -28.56 | 2.298 | 69.095 | 256.816 | 166.816 | 1.38 | 0.235 | |
| -6.608 | -27.889 | 1.476 | 66.493 | 257.327 | 167.327 | 0.509 | 0.047 | |
| -2.069 | -24.765 | 4.063 | 74.957 | 17.479 | 287.479 | 0.572 | 0.059 | 3 |
| -7.023 | -28.029 | 2.351 | 69.461 | 255.672 | 165.672 | 0.506 | 0.064 | |
| -8.191 | -28.764 | 4.041 | 66.735 | 294.484 | 204.484 | 0.843 | 0.106 | |
| -8.18 | -28.669 | 4.355 | 64.761 | 282.844 | 192.844 | 0.76 | 0.085 | |
| -7.97 | -28.467 | 4.714 | 60.424 | 301.388 | 211.388 | 0.763 | 0.069 | |
| -14.9 | -34.061 | 2.976 | 63.46 | 295.278 | 205.278 | 1.029 | 0.168 | |
| -14.858 | -33.85 | 3.695 | 71.8 | 292.438 | 202.438 | 0.766 | 0.201 | |
| -12.774 | -14.332 | 3.687 | 49.624 | 241.33 | 151.33 | 2.295 | 0.879 | |
| -13.747 | -14.497 | 1.628 | 62.542 | 247.976 | 157.976 | 1.992 | 1.22 | |
| -14.116 | -12.347 | 3.308 | 88.209 | 65.994 | 335.994 | 2.002 | 0.791 | 1 |
| -10.674 | -13.768 | 3.528 | 65.104 | 345.424 | 255.424 | 1.453 | 0.842 | 2 |
| -1.719 | -24.395 | 3.91 | 71.854 | 178.783 | 88.783 | 0.403 | 0.054 | |
| -11.055 | -13.987 | 3.043 | 81.851 | 25.372 | 295.372 | 1.341 | 0.337 | 3 |
| -14.406 | -12.215 | 4.552 | 87.135 | 40.016 | 310.016 | 1.558 | 0.436 | |
| -13.313 | -14.937 | 0.207 | 67.929 | 332.295 | 242.295 | 2.194 | 0.711 | 2 |
| -12.886 | -15.033 | -0.305 | 85.086 | 236.841 | 146.841 | 0.708 | 0.113 | |

| | | | | | | | | |
|---|---|---|---|---|---|---|---|---|
| -12.697 | -14.835 | 0.595 | 85.889 | 238.01 | 148.01 | 0.974 | 0.141 | |
| -12.4 | -14.784 | 1.63 | 89.522 | 49.444 | 319.444 | 1.24 | 0.225 | |
| -11.606 | -14.449 | 0.381 | 82.399 | 224.75 | 134.75 | 0.736 | 0.121 | |
| -11.811 | -14.545 | 1.242 | 74.933 | 232.516 | 142.516 | 0.681 | 0.086 | |
| -12.775 | -14.51 | 2.813 | 83.25 | 241.816 | 151.816 | 2.8 | 0.724 | 1 |
| -11.896 | -14.567 | 5.251 | 64.655 | 351.056 | 261.056 | 3.76 | 6.025 | 2 |
| 17.241 | -13.409 | 1.584 | 89.066 | 259.469 | 169.469 | 2.337 | 0.385 | 1 |
| 16.056 | -14.304 | -0.633 | 60.21 | 92.597 | 2.597 | 0.497 | 0.042 | |
| -4.747 | -15.524 | 6.504 | 67.956 | 147.057 | 57.057 | 1.397 | 0.177 | |
| -1.812 | -19.981 | 5.808 | 54.87 | 327.883 | 237.883 | 0.592 | 0.071 | |
| -3.43 | -19.338 | 6.291 | 88.353 | 253.709 | 163.709 | 1.621 | 0.427 | 1 |
| -3.441 | -19.073 | 6.326 | 64.929 | 19.781 | 289.781 | 0.788 | 0.189 | 3 |
| -3.999 | -18.753 | 6.528 | 63.781 | 23.445 | 293.445 | 1.118 | 0.299 | 3 |
| -3.233 | -19.479 | 6.08 | 57.806 | 61.535 | 331.535 | 0.524 | 0.127 | |
| -3.111 | -19.867 | 6.043 | 72.636 | 21.875 | 291.875 | 0.926 | 0.15 | 3 |
| -2.409 | -19.274 | 5.886 | 49.376 | 336.489 | 246.489 | 1.639 | 0.265 | |
| -2.564 | -18.719 | 6.054 | 48.958 | 94.284 | 4.284 | 1.587 | 0.305 | |
| 8.618 | -8.976 | 5.792 | 46.916 | 8.08 | 278.08 | 2.425 | 0.383 | |
| 16.948 | -13.708 | 0.793 | 81.724 | 78.736 | 348.736 | 0.368 | 0.044 | 1 |
| 9.283 | -8.869 | 5.697 | 89.611 | 73.45 | 343.45 | 1.413 | 0.156 | 1 |
| 13.127 | -8.613 | 5.415 | 56.082 | 80.038 | 350.038 | 2.022 | 0.324 | |
| 6.974 | -4.632 | 6.051 | 63.107 | 352.029 | 262.029 | 3.795 | 1.213 | 2 |
| 13.57 | -14.002 | 5.045 | 26.909 | 139.422 | 49.422 | 5.561 | 4.266 | 4 |
| 15.67 | -12.783 | 5.049 | 41.708 | 320.928 | 230.928 | 1.226 | 0.369 | |
| 16.764 | -12.377 | 5.183 | 34.388 | 27.433 | 297.433 | 0.512 | 0.046 | |
| 16.39 | -12.401 | 5.143 | 33.549 | 295.215 | 205.215 | 0.399 | 0.084 | |
| 17.201 | -11.939 | 5.115 | 78.78 | 68.931 | 338.931 | 1.471 | 0.188 | 1 |
| 16.62 | -10.898 | 5.139 | 49.847 | 345.597 | 255.597 | 0.313 | 0.034 | |
| 16.242 | -11.187 | 5.146 | 52.649 | 304.113 | 214.113 | 0.439 | 0.034 | |
| 16.957 | -13.786 | 0.568 | 48.467 | 297.869 | 207.869 | 0.614 | 0.049 | |
| 16.171 | -10.66 | 5.073 | 45.552 | 342.906 | 252.906 | 0.367 | 0.057 | |
| 15.71 | -11.378 | 5.1 | 49.898 | 339.164 | 249.164 | 0.302 | 0.023 | |
| 15.944 | -11.325 | 5.124 | 48.313 | 317.9 | 227.9 | 0.182 | 0.019 | |
| 11.906 | -8.036 | 5.556 | 67.325 | 252.946 | 162.946 | 5.15 | 0.94 | |
| 6.185 | -7.335 | 6.098 | 26.686 | 138.15 | 48.15 | 3.235 | 2.287 | 4 |
| 13.223 | -7.424 | 5.559 | 53.377 | 273.007 | 183.007 | 1.097 | 0.134 | |
| 17.68 | -13.247 | 1.071 | 45.146 | 316.34 | 226.34 | 0.536 | 0.034 | |
| 16.268 | -14.158 | -0.215 | 55.057 | 297.874 | 207.874 | 1.016 | 0.097 | |
| 15.527 | -14.616 | -0.409 | 88.658 | 281.246 | 191.246 | 2.128 | 0.392 | |
| 16.243 | -13.81 | 2.123 | 86.546 | 78.685 | 348.685 | 1.336 | 0.167 | 1 |
| 16.336 | -13.577 | 2.997 | 61.902 | 299.848 | 209.848 | 0.668 | 0.113 | |
| 17.192 | -13.027 | 4.361 | 56.639 | 308.654 | 218.654 | 0.59 | 0.137 | |
| 17.458 | -12.818 | 3.979 | 47.512 | 334.205 | 244.205 | 0.353 | 0.032 | |

| | | | | | | | | |
|---|---|---|---|---|---|---|---|---|
| 17.615 | -13.501 | -0.228 | 88.767 | 80.86 | 350.86 | 1.331 | 0.117 | 1 |
| 16.435 | -13.429 | 4.304 | 48.576 | 330.778 | 240.778 | 0.72 | 0.062 | |
| 11.403 | -16.348 | 2.241 | 50.768 | 281.553 | 191.553 | 0.627 | 0.111 | |
| 11.126 | -16.534 | 1.386 | 49.137 | 280.032 | 190.032 | 0.62 | 0.087 | |
| 11.661 | -16.388 | -0.713 | 50.193 | 233.873 | 143.873 | 0.659 | 0.046 | |
| 11.982 | -16.059 | 2.853 | 89.596 | 260.275 | 170.275 | 0.722 | 0.062 | 1 |
| 11.308 | -16.412 | 3.11 | 36.739 | 282.126 | 192.126 | 0.817 | 0.087 | |
| 11.376 | -16.425 | 2.744 | 54.568 | 345.303 | 255.303 | 0.395 | 0.033 | 2 |
| 10.591 | -16.79 | 2.566 | 88.804 | 258.361 | 168.361 | 0.881 | 0.063 | 1 |
| 11.214 | -16.548 | -0.601 | 54.793 | 277.508 | 187.508 | 0.746 | 0.075 | |
| 9.867 | -17.091 | 0.428 | 49.152 | 294.883 | 204.883 | 0.457 | 0.049 | |
| 17.266 | -13.712 | -0.132 | 42.382 | 67.919 | 337.919 | 0.355 | 0.035 | |
| 5.066 | -20.243 | 0.171 | 89.821 | 225.456 | 135.456 | 1.371 | 0.295 | |
| 5.895 | -19.251 | -0.005 | 75.364 | 209.461 | 119.461 | 0.875 | 0.104 | |
| 5.796 | -19.303 | -0.677 | 81.622 | 29.902 | 299.902 | 0.311 | 0.015 | 3 |
| 5.957 | -19.283 | -0.576 | 83.774 | 22.308 | 292.308 | 0.351 | 0.012 | 3 |
| 5.606 | -19.412 | -0.331 | 77.291 | 217.923 | 127.923 | 0.328 | 0.02 | |
| 5.513 | -19.497 | 0.086 | 75.783 | 243.159 | 153.159 | 0.21 | 0.01 | |
| 0.592 | -22.685 | 2.113 | 70.643 | 358.953 | 268.953 | 0.507 | 0.092 | 2 |
| 0.987 | -22.575 | 2.171 | 78.224 | 3.216 | 273.216 | 0.648 | 0.142 | |
| 15.114 | -14.784 | 0.981 | 87.189 | 76.159 | 346.159 | 0.89 | 0.085 | 1 |
| 15.788 | -14.158 | 1.773 | 84.734 | 86.064 | 356.064 | 0.733 | 0.069 | 1 |
| 17.534 | -13.607 | -0.676 | 87.74 | 81.833 | 351.833 | 0.211 | 0.014 | 1 |
| 13.527 | -15.246 | 2.402 | 71.167 | 347.578 | 257.578 | 0.992 | 0.112 | 2 |
| 15.008 | -14.645 | 1.652 | 68.398 | 347.338 | 257.338 | 1.895 | 0.306 | 2 |
| 14.223 | -15.289 | 0.922 | 59.355 | 344.177 | 254.177 | 1.082 | 0.212 | 2 |
| 14.522 | -15.062 | 1.346 | 52.836 | 318.257 | 228.257 | 0.647 | 0.069 | |
| 14.621 | -14.692 | 2.281 | 89.738 | 140.546 | 50.546 | 0.361 | 0.052 | |
| 15.197 | -14.698 | 0.812 | 84.13 | 100.686 | 10.686 | 1.62 | 0.209 | |
| 14.091 | -14.836 | 2.832 | 85.068 | 231.159 | 141.159 | 0.678 | 0.037 | |
| 12.84 | -15.637 | 1.803 | 49.344 | 280.523 | 190.523 | 0.699 | 0.066 | |
| 12.566 | -15.769 | 2.402 | 13.631 | 6.153 | 276.153 | 0.295 | 0.029 | |
| 12.932 | -15.483 | 2.462 | 53.68 | 80.773 | 350.773 | 0.322 | 0.031 | |
| 16.976 | -13.914 | -0.477 | 89.508 | 81.86 | 351.86 | 0.277 | 0.025 | 1 |
| 13.034 | -15.467 | 2.189 | 58.305 | 86.368 | 356.368 | 0.254 | 0.019 | |
| 12.688 | -15.964 | 0.384 | 72.6 | 349.604 | 259.604 | 0.297 | 0.03 | 2 |
| 13.517 | -15.524 | 0.775 | 89.028 | 232.024 | 142.024 | 0.341 | 0.026 | |
| 10.719 | -16.438 | 4.079 | 77.443 | 244.677 | 154.677 | 0.637 | 0.048 | 1 |
| 3.91 | -4.633 | 0.344 | 53.548 | 347.896 | 257.896 | 1.217 | 0.525 | 2 |
| 2.144 | -5.618 | 2.55 | 71.986 | 8.121 | 278.121 | 2.243 | 0.37 | 3 |
| 2.487 | -5.323 | 2.302 | 77.517 | 13.156 | 283.156 | 0.749 | 0.114 | 3 |
| 2.686 | -5.307 | 2.152 | 81.741 | 26.725 | 296.725 | 0.581 | 0.103 | 3 |
| 2.89 | -5.198 | 1.562 | 66.044 | 18.828 | 288.828 | 0.812 | 0.174 | 3 |

| | | | | | | | | |
|---|---|---|---|---|---|---|---|---|
| 2.131 | -5.807 | 3.897 | 68.807 | 6.901 | 276.901 | 1.314 | 0.21 | |
| 17.298 | -13.762 | -0.441 | 43.658 | 99.453 | 9.453 | 0.148 | 0.011 | |
| 2.363 | -5.764 | 4.209 | 75.314 | 8.032 | 278.032 | 0.62 | 0.076 | 3 |
| 2.438 | -5.798 | 4.573 | 47.467 | 188.205 | 98.205 | 0.199 | 0.014 | |
| 2.267 | -5.845 | 4.386 | 77.083 | 35.662 | 305.662 | 0.578 | 0.042 | 3 |
| -7.965 | -12.082 | 1.867 | 82.01 | 34.217 | 304.217 | 0.424 | 0.066 | 3 |
| -9.237 | -12.775 | 1.955 | 65.352 | 278.519 | 188.519 | 1.877 | 0.414 | |
| -8.143 | -12.506 | 4.908 | 74.339 | 258.681 | 168.681 | 0.952 | 0.149 | 1 |
| -7.445 | -11.829 | 3.614 | 82.71 | 255.442 | 165.442 | 2.303 | 0.279 | 1 |
| -7.718 | -12.319 | 5.16 | 52.035 | 353.019 | 263.019 | 0.511 | 0.13 | |
| -9.254 | -12.859 | 2.968 | 82.954 | 26.62 | 296.62 | 0.529 | 0.094 | 3 |
| -10.022 | -13.235 | 2.739 | 64.857 | 349.659 | 259.659 | 1.48 | 0.466 | 2 |
| 17.103 | -13.828 | -0.329 | 57.115 | 78.405 | 348.405 | 0.177 | 0.014 | |
| -9.494 | -13.179 | 4.314 | 66.974 | 233.266 | 143.266 | 0.863 | 0.106 | |
| -6.996 | -11.514 | 3.179 | 88.292 | 37.704 | 307.704 | 1.684 | 0.336 | |
| -8.694 | -12.57 | 3.772 | 39.053 | 155.559 | 65.559 | 0.4 | 0.07 | 4 |
| -8.525 | -12.678 | 4.952 | 70.539 | 11.036 | 281.036 | 0.842 | 0.212 | 3 |
| 6.565 | -3.495 | 2.882 | 64.822 | 351.297 | 261.297 | 1.97 | 0.564 | 2 |
| 7.178 | -3.208 | 2.562 | 70.75 | 348.642 | 258.642 | 1.167 | 0.281 | 2 |
| 8.886 | -2.586 | 2.136 | 67.063 | 350.319 | 260.319 | 1.256 | 0.699 | 2 |
| 10.292 | -2.122 | 1.606 | 33.147 | 147.331 | 57.331 | 3.649 | 0.459 | 4 |
| 8.175 | -2.825 | 1.017 | 89.955 | 84.006 | 354.006 | 2.407 | 0.228 | 1 |
| 8.451 | -2.764 | 0.976 | 42.295 | 135.745 | 45.745 | 0.94 | 0.112 | 4 |
| 16.656 | -13.952 | -0.048 | 42.617 | 101.095 | 11.095 | 0.254 | 0.013 | |
| 5.039 | -4.127 | 4.91 | 73.499 | 24.571 | 294.571 | 1.032 | 0.221 | 3 |
| 5.457 | -4.009 | 3.992 | 69.12 | 349.651 | 259.651 | 1.778 | 0.361 | 2 |
| 4.146 | -4.744 | 5.358 | 84.715 | 247.654 | 157.654 | 1.442 | 0.383 | 1 |
| 4.789 | -4.138 | 0.982 | 67.884 | 14.514 | 284.514 | 1.274 | 0.226 | 3 |
| 4.393 | -4.452 | 2.094 | 77.962 | 19.615 | 289.615 | 0.602 | 0.101 | 3 |
| 3.96 | -4.522 | 1.854 | 57.446 | 352.398 | 262.398 | 0.822 | 0.219 | 2 |
| 1.919 | -5.861 | 1.31 | 68.051 | 221.177 | 131.177 | 1.893 | 0.246 | |
| 1.226 | -6.455 | 0.672 | 28.949 | 126.969 | 36.969 | 0.579 | 0.105 | 4 |
| 1.364 | -6.356 | 0.725 | 77.823 | 229.632 | 139.632 | 0.601 | 0.059 | |
| 1.036 | -6.57 | 0.638 | 67.069 | 222.901 | 132.901 | 0.437 | 0.041 | |
| 16.901 | -13.883 | -0.166 | 36.277 | 111.1 | 21.1 | 0.1 | 0.003 | |
| 4.875 | -4.45 | 2.591 | 64.74 | 275.426 | 185.426 | 0.633 | 0.081 | |
| -5.59 | -16.738 | 6.465 | 33.964 | 148.566 | 58.566 | 2.149 | 1.697 | 4 |
| -6.879 | -14.773 | 6.365 | 83.281 | 252.193 | 162.193 | 4.576 | 2.068 | 1 |
| -6.424 | -14.644 | 6.575 | 70.38 | 350.345 | 260.345 | 2.56 | 0.564 | 2 |
| -7.786 | -15.081 | 6.605 | 61.64 | 287.83 | 197.83 | 0.454 | 0.048 | |
| -7.351 | -14.588 | 6.536 | 58.262 | 27.756 | 297.756 | 0.526 | 0.073 | |
| -7.677 | -14.555 | 6.613 | 55.127 | 25.599 | 295.599 | 0.504 | 0.071 | |
| -8.457 | -14.504 | 6.552 | 63.653 | 350.926 | 260.926 | 0.933 | 0.117 | 2 |

| | | | | | | | | |
|---|---|---|---|---|---|---|---|---|
| -8.582 | -14.586 | 6.566 | 63.637 | 352.023 | 262.023 | 1.315 | 0.25 | 2 |
| -8.121 | -13.097 | 5.747 | 66.287 | 20.904 | 290.904 | 1.202 | 0.276 | 3 |
| 20.573 | -11.946 | 1.293 | 87.809 | 262.453 | 172.453 | 0.974 | 0.066 | 1 |
| 32.016 | -6.347 | 3.075 | 70.087 | 277.193 | 187.193 | 1.597 | 0.449 | |
| 34.591 | -5.116 | 1.936 | 63.174 | 305.77 | 215.77 | 0.847 | 0.172 | |
| 33.79 | -5.534 | 2.619 | 87.17 | 235.892 | 145.892 | 1.234 | 0.208 | |
| 34.809 | -5.013 | 2.458 | 86.707 | 40.766 | 310.766 | 1.082 | 0.084 | |
| 29.197 | -8.455 | 0.167 | 89.884 | 256.702 | 166.702 | 2.725 | 0.565 | 1 |
| 22.845 | -11.401 | 0.319 | 89.536 | 260.8 | 170.8 | 2.107 | 0.117 | 1 |
| 23.258 | -11.232 | 0.962 | 43.947 | 299.292 | 209.292 | 1.087 | 0.173 | |
| 21.466 | -11.724 | 0.958 | 89.229 | 261.191 | 171.191 | 0.76 | 0.079 | 1 |
| 22.272 | -11.375 | 1.938 | 89.262 | 31.246 | 301.246 | 1.223 | 0.17 | |
| 22.056 | -11.198 | 3.158 | 89.718 | 225.679 | 135.679 | 1.245 | 0.154 | |
| 22.933 | -11.094 | 2.588 | 34.879 | 342.287 | 252.287 | 0.61 | 0.125 | |
| 22.842 | -11.137 | 2.907 | 81.823 | 196.841 | 106.841 | 0.878 | 0.144 | |
| 20.573 | -11.937 | 1.327 | 87.861 | 262.817 | 172.817 | 0.98 | 0.07 | 1 |
| 20.968 | -11.702 | 1.689 | 59.123 | 310.669 | 220.669 | 0.979 | 0.102 | |
| 19.04 | -12.754 | -0.237 | 25.69 | 141.815 | 51.815 | 0.931 | 0.204 | 4 |
| 20.376 | -12.197 | -0.266 | 58.027 | 159.126 | 69.126 | 0.803 | 0.216 | |
| 20.534 | -11.642 | 3.718 | 30.985 | 145.401 | 55.401 | 1.228 | 0.208 | 4 |
| 27.883 | -9.277 | 0.022 | 67.227 | 349.84 | 259.84 | 4.03 | 1.735 | 2 |
| 24.508 | -10.598 | 1.696 | 87.513 | 89.236 | 359.236 | 1.759 | 0.187 | 1 |
| 18.291 | -12.737 | 1.903 | 50.732 | 309.038 | 219.038 | 1.386 | 0.156 | |
| 18.752 | -12.583 | 1.687 | 59.571 | 312.431 | 222.431 | 1.97 | 0.456 | |
| 18.968 | -12.538 | 1.394 | 67.22 | 298.122 | 208.122 | 0.562 | 0.073 | |
| 31.87 | -6.967 | -0.871 | 83.329 | 260.824 | 170.824 | 0.9 | 0.156 | 1 |
| 30.886 | -7.264 | 0.91 | 19.139 | 153.03 | 63.03 | 0.745 | 0.101 | 4 |
| 30.596 | -7.666 | 0.475 | 29.919 | 161.791 | 71.791 | 0.708 | 0.084 | 4 |
| 29.632 | -8.115 | 0.335 | 82.926 | 176.273 | 86.273 | 0.334 | 0.044 | |
| 30.052 | -7.909 | 0.311 | 77.212 | 184.748 | 94.748 | 0.774 | 0.175 | |
| 14.972 | -0.49 | 0.061 | 66.645 | 345.752 | 255.752 | 6.719 | 4.205 | 2 |
| 16.79 | 0.319 | 1.606 | 61.638 | 4.328 | 274.328 | 4.032 | 1.318 | |
| 19.8 | 4.635 | 4.188 | 84.197 | 34.582 | 304.582 | 1.823 | 0.772 | |
| 20.073 | 4.204 | 3.752 | 79.782 | 39.354 | 309.354 | 1.04 | 0.301 | |
| 19.898 | 3.096 | 2.787 | 88.883 | 24.263 | 294.263 | 1.299 | 0.159 | 3 |
| 19.482 | 4.342 | 1.281 | 57.722 | 236.554 | 146.554 | 1.315 | 0.661 | |
| 17.737 | 0.727 | 2.784 | 69.296 | 0.625 | 270.625 | 2.959 | 1.023 | 2 |
| 16.927 | 0.267 | 3.475 | 67.07 | 7.797 | 277.797 | 1.281 | 0.235 | |
| 16.722 | 0.127 | 4.062 | 74.482 | 4.43 | 274.43 | 2.446 | 0.726 | |
| 15.968 | -0.409 | 5.138 | 64.678 | 8.759 | 278.759 | 1.384 | 0.796 | 3 |
| 15.466 | -0.683 | 5.387 | 26.041 | 50.69 | 320.69 | 0.83 | 0.223 | |
| 15.801 | -0.754 | 5.541 | 81.103 | 350.591 | 260.591 | 0.55 | 0.124 | 2 |
| 18.353 | 0.453 | 5.275 | 65.291 | 26.847 | 296.847 | 1.601 | 0.575 | 3 |

| | | | | | | | | |
|---|---|---|---|---|---|---|---|---|
| 18.611 | 0.882 | 4.921 | 69.627 | 354.267 | 264.267 | 1.33 | 0.545 | 2 |
| 19.236 | 1.379 | 4.719 | 84.78 | 253.692 | 163.692 | 1.238 | 0.271 | 1 |
| 19.002 | 1.605 | 1.113 | 80.062 | 251.214 | 161.214 | 1.464 | 0.15 | 1 |
| 18.808 | 1.532 | 1.524 | 86.971 | 256.898 | 166.898 | 1.198 | 0.175 | 1 |
| 14.546 | -0.762 | 5.004 | 87.979 | 2.755 | 272.755 | 0.77 | 0.175 | |
| 19.809 | 3.411 | 2.261 | 81.397 | 321.982 | 231.982 | 1.804 | 0.204 | |
| 20.547 | 2.372 | 5.202 | 55.812 | 11.108 | 281.108 | 0.816 | 0.129 | |
| 20.151 | 3.632 | 3.558 | 50.74 | 3.497 | 273.497 | 0.543 | 0.072 | |
| 20.029 | 1.756 | 5.141 | 55.96 | 4.758 | 274.758 | 0.911 | 0.204 | |
| 16.668 | -7.766 | 5.545 | 82.415 | 51.153 | 321.153 | 4.174 | 1.156 | |
| 17.905 | -9.616 | 5.703 | 23.543 | 105.493 | 15.493 | 0.922 | 0.21 | |
| 17.166 | -10.768 | 5.15 | 60.748 | 343.993 | 253.993 | 1.018 | 0.133 | 2 |
| 17.004 | -10.389 | 5.212 | 42.457 | 327.324 | 237.324 | 0.621 | 0.051 | |
| 17.307 | -10.499 | 5.217 | 24.675 | 139.353 | 49.353 | 0.432 | 0.102 | 4 |
| 17.962 | -11.107 | 5.199 | 25.985 | 356.625 | 266.625 | 0.306 | 0.019 | |
| 17.973 | -11.236 | 5.195 | 13.829 | 169.921 | 79.921 | 0.288 | 0.04 | |
| 17.839 | -11.218 | 5.163 | 67.616 | 276.981 | 186.981 | 0.214 | 0.01 | |
| 18.351 | -11.364 | 5.112 | 65.408 | 252.74 | 162.74 | 0.625 | 0.043 | |
| 15.728 | -3.235 | 5.836 | 72.761 | 350.606 | 260.606 | 5.423 | 1.152 | 2 |
| 14.266 | -3.045 | 5.852 | 84.312 | 244.957 | 154.957 | 2.362 | 0.356 | 1 |
| 15.296 | -2.054 | 5.819 | 23.363 | 150.356 | 60.356 | 1.855 | 0.51 | 4 |
| 15.831 | -0.41 | 5.177 | 65.056 | 10.281 | 280.281 | 0.985 | 0.428 | 3 |
| 15.76 | -0.76 | 5.532 | 81.115 | 349.947 | 259.947 | 0.573 | 0.136 | 2 |
| 15.516 | -0.626 | 5.348 | 23.106 | 49.636 | 319.636 | 0.593 | 0.129 | |
| 16.373 | -0.224 | 5.234 | 63.085 | 275.136 | 185.136 | 0.608 | 0.052 | |
| 13.776 | -2.662 | 5.88 | 16.981 | 310.242 | 220.242 | 0.76 | 0.193 | |
| 13.091 | -2.055 | 5.868 | 28.384 | 143.719 | 53.719 | 0.848 | 0.089 | 4 |
| 16.8 | -4.827 | 5.681 | 89.033 | 257.658 | 167.658 | 1.419 | 0.237 | 1 |
| 16.578 | -5.112 | 5.698 | 67.898 | 169.534 | 79.534 | 0.548 | 0.105 | |
| 16.196 | -5.075 | 5.709 | 77.063 | 240.025 | 150.025 | 0.14 | 0.008 | |
| 19.108 | -1.146 | 5.712 | 61.276 | 349.673 | 259.673 | 1.561 | 0.224 | 2 |
| 21.115 | -1.65 | 5.613 | 67.781 | 349.546 | 259.546 | 2.599 | 0.658 | 2 |
| 21.692 | -2.013 | 5.651 | 87.866 | 74.334 | 344.334 | 0.858 | 0.111 | 1 |
| 20.087 | -2.098 | 5.747 | 79.073 | 259.822 | 169.822 | 1.42 | 0.191 | 1 |
| 20.484 | -0.497 | 5.741 | 69.91 | 253.791 | 163.791 | 1.702 | 0.272 | |
| 20.054 | 1.708 | 5.191 | 50.631 | 0.081 | 270.081 | 1.169 | 0.307 | |
| 20.571 | 2.348 | 5.229 | 53.166 | 7.642 | 277.642 | 0.847 | 0.148 | |
| 22.958 | 3.794 | 5.589 | 28.071 | 141.749 | 51.749 | 1.873 | 1.809 | 4 |
| 22.503 | -0.907 | 5.597 | 87.922 | 254.132 | 164.132 | 0.768 | 0.114 | 1 |
| 22.774 | -0.549 | 5.521 | 46.806 | 247.349 | 157.349 | 0.343 | 0.039 | |
| 21.059 | 4.549 | 5.656 | 85.322 | 252.985 | 162.985 | 1.656 | 0.309 | 1 |
| 20.842 | 3.764 | 5.449 | 80.209 | 32.774 | 302.774 | 1.121 | 0.114 | 3 |
| 20.588 | 3.87 | 5.158 | 79.994 | 26.828 | 296.828 | 0.483 | 0.062 | 3 |

| | | | | | | | | |
|---|---|---|---|---|---|---|---|---|
| 20.793 | 3.302 | 5.005 | 73.956 | 31.524 | 301.524 | 0.58 | 0.08 | 3 |
| 20.648 | 3.627 | 4.976 | 83.355 | 53.795 | 323.795 | 0.582 | 0.096 | |
| 20.745 | 3.707 | 5.212 | 78.09 | 30.534 | 300.534 | 0.315 | 0.023 | 3 |
| 20.591 | 4.484 | 5.473 | 25.174 | 75.545 | 345.545 | 0.797 | 0.088 | |
| 24.012 | 5.751 | 5.701 | 70.288 | 18.953 | 288.953 | 2.686 | 0.461 | 3 |
| 23.933 | 6.772 | 5.613 | 57.012 | 13.593 | 283.593 | 3.004 | 0.478 | |
| 28.233 | 6.841 | 5.288 | 29.444 | 147.274 | 57.274 | 1.1 | 0.674 | 4 |
| 28.138 | 3.545 | 5.121 | 67.414 | 349.163 | 259.163 | 3.881 | 0.63 | 2 |
| 27.676 | 2.064 | 5.312 | 80.863 | 74.163 | 344.163 | 2.29 | 0.387 | 1 |
| 28.364 | 2.274 | 5.211 | 80.238 | 76.276 | 346.276 | 2.954 | 0.644 | 1 |
| 29.344 | 5.951 | 5.206 | 87.634 | 254.665 | 164.665 | 1.649 | 0.299 | 1 |
| 28.54 | 4.799 | 5.085 | 47.916 | 106.418 | 16.418 | 1.635 | 0.127 | |
| 26.792 | 5.303 | 5.351 | 44.871 | 143.322 | 53.322 | 1.099 | 0.073 | |
| 27.846 | 5.657 | 5.233 | 54.688 | 158.385 | 68.385 | 0.643 | 0.026 | |
| 28.096 | 5.151 | 5.23 | 86.803 | 284.52 | 194.52 | 1.003 | 0.124 | |
| 31.326 | 2.706 | 4.981 | 88.573 | 74.869 | 344.869 | 2.338 | 0.234 | 1 |
| 31.326 | 2.706 | 4.981 | 88.573 | 74.869 | 344.869 | 2.338 | 0.234 | 1 |
| 29.533 | 2.958 | 4.995 | 84.495 | 80.375 | 350.375 | 1.13 | 0.157 | 1 |
| 32.178 | -3.942 | 4.991 | 30.043 | 334.179 | 244.179 | 1.079 | 0.181 | |
| 30.811 | -5.33 | 5.153 | 38.376 | 312.99 | 222.99 | 1.37 | 0.229 | |
| 31.88 | 2.868 | 4.92 | 83.626 | 75.209 | 345.209 | 1.743 | 0.142 | 1 |
| 32.908 | -0.51 | 4.835 | 20.793 | 351.039 | 261.039 | 1.988 | 0.626 | |
| 23.946 | -2.282 | 5.49 | 80.35 | 52.753 | 322.753 | 1.219 | 0.151 | |
| 29.631 | -2.607 | 5.272 | 82.707 | 48.898 | 318.898 | 0.659 | 0.062 | |
| 30.374 | -2.055 | 5.149 | 72.465 | 54.389 | 324.389 | 0.519 | 0.053 | |
| 30.803 | 0.727 | 5.141 | 68.437 | 268.842 | 178.842 | 1.135 | 0.123 | |
| 30.756 | -1.707 | 5.08 | 79.307 | 270.362 | 180.362 | 0.848 | 0.058 | |
| 31.488 | -1.165 | 5 | 74.587 | 227.426 | 137.426 | 1.518 | 0.141 | |
| 20.911 | -7.183 | 5.352 | 82.511 | 67.898 | 337.898 | 2.353 | 0.453 | 1 |
| 19.39 | -2.376 | 5.806 | 87.961 | 75.79 | 345.79 | 1.483 | 0.254 | 1 |
| 20.083 | -3.895 | 5.709 | 67.123 | 49.061 | 319.061 | 1.01 | 0.123 | |
| 20.295 | -7.914 | 5.387 | 52.468 | 352.957 | 262.957 | 1.411 | 0.326 | |
| 20.211 | -7.992 | 5.4 | 78.871 | 55.557 | 325.557 | 1.714 | 0.223 | |
| 26.645 | -3.031 | 5.215 | 57.284 | 85.276 | 355.276 | 0.867 | 0.105 | |
| 21.631 | -7.033 | 5.375 | 44.068 | 349.845 | 259.845 | 1 | 0.173 | |
| 23.891 | -6.975 | 5.317 | 84.612 | 52.106 | 322.106 | 0.692 | 0.094 | |
| 23.203 | -4.731 | 5.561 | 86.194 | 247.469 | 157.469 | 0.632 | 0.091 | 1 |
| 13.908 | 11.08 | 4.395 | 64.951 | 351.845 | 261.845 | 1.211 | 0.134 | 2 |
| 12.874 | 11.886 | 2.2 | 65.026 | 351.186 | 261.186 | 3.765 | 1.191 | 2 |
| 12.277 | 12.935 | -0.056 | 65.595 | 350.547 | 260.547 | 1.534 | 0.238 | 2 |
| 13.978 | 10.495 | 0.722 | 74.699 | 25.198 | 295.198 | 2.939 | 1.186 | 3 |
| 15.79 | 9.038 | 3.832 | 80.388 | 36.438 | 306.438 | 3.038 | 2.339 | 3 |
| 14.983 | 9.798 | 3.429 | 88.883 | 255.45 | 165.45 | 1.547 | 0.42 | 1 |

| | | | | | | | | |
|---|---|---|---|---|---|---|---|---|
| 13.6 | 10.931 | 2.788 | 83.009 | 29.629 | 299.629 | 1.744 | 0.65 | 3 |
| 10.185 | 15.303 | 3.361 | 79.668 | 26.744 | 296.744 | 3.855 | 3.069 | 3 |
| 10.693 | 15.238 | 4.228 | 35.789 | 232.472 | 142.472 | 0.863 | 0.45 | |
| 7.12 | 17.088 | 1.072 | 73.929 | 23.804 | 293.804 | 3.881 | 4.836 | 3 |
| 10.3 | 14.996 | 3.498 | 28.621 | 148.239 | 58.239 | 4.924 | 2.44 | 4 |
| 9.043 | 16.364 | 5.282 | 76.791 | 20.499 | 290.499 | 2.545 | 1.569 | 3 |
| 10.584 | 15.816 | 5.919 | 81.134 | 20.91 | 290.91 | 2.838 | 1.54 | 3 |
| 7.255 | 17.31 | 5.722 | 77.595 | 23.909 | 293.909 | 2.621 | 1.231 | 3 |
| 11.392 | 13.876 | 2.265 | 76.658 | 35.021 | 305.021 | 0.734 | 0.291 | 3 |
| 12.624 | 13.355 | 5.583 | 70.637 | 26.048 | 296.048 | 1.529 | 0.281 | 3 |
| 12.558 | 13.592 | 5.663 | 61.185 | 319.656 | 229.656 | 0.744 | 0.144 | |
| 11.455 | 14.896 | 4.744 | 56.29 | 22.095 | 292.095 | 1.34 | 0.213 | |
| 26.159 | 16.617 | 1.932 | 89.924 | 73.659 | 343.659 | 5.645 | 10.035 | 1 |
| 27.037 | 15.232 | 4.551 | 67.227 | 231.146 | 141.146 | 1.618 | 1.304 | |
| 26.303 | 15.669 | 5.061 | 71.788 | 70.933 | 340.933 | 3.235 | 1.046 | |
| 28.059 | 14.208 | 0.226 | 88.174 | 61.736 | 331.736 | 3.022 | 2.513 | 1 |
| 23.835 | 19.778 | 5.044 | 68.01 | 349.619 | 259.619 | 2.955 | 1.051 | 2 |
| 23.696 | 20.469 | 3.425 | 56.527 | 62.011 | 332.011 | 1.343 | 0.417 | |
| 23.42 | 20.894 | 3.713 | 70.372 | 313.375 | 223.375 | 1.514 | 0.257 | |
| 23.232 | 21.053 | 2.567 | 72.523 | 247.956 | 157.956 | 1.648 | 0.627 | |
| 19.728 | 25.485 | 2.34 | 68.333 | 38.144 | 308.144 | 2.633 | 1.286 | |
| 20.492 | 24.808 | 2.983 | 80.495 | 257.308 | 167.308 | 0.873 | 0.227 | 1 |
| 19.93 | 25.146 | 1.942 | 62.358 | 281.144 | 191.144 | 1.061 | 0.207 | |
| 20.049 | 24.662 | 1.17 | 63.285 | 292.995 | 202.995 | 0.632 | 0.1 | |
| 20.161 | 24.297 | 5.513 | 68.309 | 90.046 | 0.046 | 1.591 | 0.248 | |
| 20.075 | 25.005 | 4.47 | 71.081 | 8.911 | 278.911 | 1.146 | 0.294 | 3 |
| 18.222 | 26.134 | 5.973 | 27.378 | 148.524 | 58.524 | 13.596 | 9.832 | 4 |
| 18.074 | 26.944 | 3.538 | 65.334 | 22.328 | 292.328 | 0.913 | 0.136 | 3 |
| 21.762 | 23.37 | 4.526 | 86.361 | 62.168 | 332.168 | 1.594 | 0.714 | 1 |
| 25.664 | 17.945 | 1.811 | 49.176 | 356.724 | 266.724 | 1.01 | 0.17 | |
| 21.992 | 23.053 | 3.382 | 75.416 | 21.356 | 291.356 | 0.256 | 0.023 | 3 |
| 22.222 | 22.784 | 4.237 | 73.269 | 4.282 | 274.282 | 0.82 | 0.117 | |
| 22.388 | 22.449 | 4.48 | 66.816 | 272.559 | 182.559 | 0.389 | 0.052 | |
| 24.204 | 19.41 | 0.065 | 74.139 | 22.941 | 292.941 | 0.737 | 0.079 | 3 |
| 24.851 | 18.405 | -0.321 | 34.717 | 26.269 | 296.269 | 0.457 | 0.042 | |
| 17.819 | 26.902 | 0.535 | 88.116 | 77.519 | 347.519 | 0.862 | 0.231 | 1 |
| 17.266 | 16.924 | 8.389 | 65.254 | 348.478 | 258.478 | 12.299 | 11.849 | 2 |
| 16.468 | 20.026 | 9.082 | 44.722 | 106.19 | 16.19 | 1.57 | 0.949 | |
| 19.493 | 20.419 | 8.388 | 87.803 | 80.654 | 350.654 | 6.054 | 4.563 | 1 |
| 20.679 | 16.67 | 7.862 | 87.202 | 256.361 | 166.361 | 4.051 | 1.687 | 1 |
| 13.973 | 12.935 | 7.258 | 80.961 | 31.667 | 301.667 | 3.434 | 3.783 | 3 |
| 17.38 | 13.459 | 7.656 | 81.376 | 256.932 | 166.932 | 2.097 | 0.201 | 1 |
| 17.776 | 11.636 | 6.424 | 86.007 | 255.971 | 165.971 | 0.991 | 0.131 | 1 |

| | | | | | | | | |
|---|---|---|---|---|---|---|---|---|
| 22.118 | 10.538 | 6.036 | 27.628 | 148.851 | 58.851 | 5.375 | 8.217 | 4 |
| 15.972 | 10.833 | 5.86 | 48.137 | 349.438 | 259.438 | 1.678 | 0.243 | |
| 18.708 | 11.126 | 6.352 | 32.134 | 326.046 | 236.046 | 1.26 | 0.179 | |
| 22.405 | 20.352 | 7.174 | 78.694 | 231.365 | 141.365 | 1.24 | 0.542 | |
| 22.073 | 20.85 | 6.731 | 80.11 | 234.207 | 144.207 | 0.793 | 0.204 | |
| 22.496 | 20.382 | 6.24 | 79.074 | 241.027 | 151.027 | 1.587 | 0.732 | |
| 14.692 | 17.819 | 9.081 | 28.273 | 145.879 | 55.879 | 2.785 | 2.211 | 4 |
| 16.591 | 17.659 | 8.564 | 26.183 | 154.26 | 64.26 | 2.654 | 1.505 | 4 |
| 18.023 | 12.339 | 7.014 | 65.983 | 353.804 | 263.804 | 0.861 | 0.374 | 2 |
| 17.102 | 12.148 | 6.851 | 55.769 | 4.916 | 274.916 | 0.468 | 0.097 | |
| 16.698 | 11.925 | 6.702 | 76.21 | 269.989 | 179.989 | 0.513 | 0.133 | |
| 5.35 | 20.69 | 8.076 | 79.997 | 18.305 | 288.305 | 2.181 | 2.037 | 3 |
| 9.265 | 19.574 | 7.239 | 74.9 | 15.267 | 285.267 | 4.52 | 1.748 | 3 |
| 9.333 | 21.813 | 7.878 | 78.741 | 198.631 | 108.631 | 1.24 | 0.069 | |
| 12.954 | 24.062 | 8.042 | 87.761 | 76.71 | 346.71 | 1.805 | 0.235 | 1 |
| 12.686 | 23.868 | 8.128 | 78.682 | 356.261 | 266.261 | 0.569 | 0.065 | 2 |
| 14.931 | 24.639 | 7.603 | 65.25 | 17.828 | 287.828 | 1.035 | 0.259 | 3 |
| 34.024 | 11.552 | 2.445 | 61.399 | 351.637 | 261.637 | 1.372 | 0.542 | 2 |
| 32.79 | 10.987 | 0.761 | 69.291 | 22.108 | 292.108 | 1.52 | 0.473 | 3 |
| 31.007 | 11.142 | 1.081 | 77.105 | 25.32 | 295.32 | 1.202 | 0.371 | 3 |
| 30.177 | 11.893 | 1.515 | 59.555 | 225.119 | 135.119 | 0.401 | 0.041 | |
| 39.697 | 17.904 | 4.04 | 77.364 | 38.115 | 308.115 | 0.72 | 0.107 | |
| 38.112 | -2.468 | -0.225 | 89.784 | 255.532 | 165.532 | 1.538 | 0.317 | 1 |
| 37.932 | -2.47 | 0.974 | 87.836 | 76.379 | 346.379 | 0.876 | 0.192 | 1 |
| 38.226 | -1.957 | 1.379 | 76.222 | 258.47 | 168.47 | 1.169 | 0.164 | 1 |
| 36.332 | -3.743 | 1.337 | 84.155 | 244.097 | 154.097 | 1.006 | 0.237 | 1 |
| 39.615 | -1.015 | 1.726 | 84.472 | 57.664 | 327.664 | 0.826 | 0.196 | |
| 39.918 | -0.994 | 1.001 | 89.094 | 74.766 | 344.766 | 0.601 | 0.128 | 1 |
| 31.835 | 10.59 | 3.064 | 70.328 | 16.575 | 286.575 | 1.813 | 1.198 | 3 |
| 40.261 | -0.773 | 1.07 | 80.158 | 7.123 | 277.123 | 0.848 | 0.243 | |
| 42.676 | 0.803 | 1.285 | 72.625 | 352.886 | 262.886 | 1.206 | 0.224 | 2 |
| 43.212 | 1.218 | 0.829 | 85.049 | 252.344 | 162.344 | 0.666 | 0.078 | 1 |
| 43.13 | 1.254 | 1.767 | 85.557 | 89.617 | 359.617 | 0.524 | 0.071 | |
| 44.129 | 2.23 | 0.306 | 57.074 | 277.373 | 187.373 | 1.347 | 0.218 | |
| 49.728 | 8.582 | 1.978 | 87.109 | 260.36 | 170.36 | 1.637 | 0.298 | 1 |
| 49.379 | 8.177 | 1.635 | 86.318 | 252.545 | 162.545 | 0.624 | 0.086 | 1 |
| 48.196 | 6.588 | 1.529 | 88.476 | 258.795 | 168.795 | 1.492 | 0.318 | 1 |
| 48.003 | 6.223 | 2.134 | 89.49 | 83.757 | 353.757 | 1.099 | 0.211 | 1 |
| 38.091 | -2.028 | 2.609 | 75.552 | 254.039 | 164.039 | 0.942 | 0.213 | 1 |
| 31.131 | 10.918 | 2.644 | 87.471 | 256.414 | 166.414 | 2.317 | 1.245 | 1 |
| 39.132 | -1.089 | 2.905 | 52.853 | 281.287 | 191.287 | 0.758 | 0.154 | |
| 39.077 | -0.948 | 3.507 | 45.814 | 292.969 | 202.969 | 0.591 | 0.123 | |
| 33.893 | 7.026 | 4.962 | 87.81 | 76.974 | 346.974 | 2.192 | 0.326 | 1 |

| | | | | | | | | |
|---|---|---|---|---|---|---|---|---|
| 34.23 | 6.18 | 4.798 | 79.673 | 76.096 | 346.096 | 0.592 | 0.034 | 1 |
| 33.617 | 9.122 | 4.739 | 68.059 | 16.877 | 286.877 | 4.74 | 2.32 | 3 |
| 37.058 | 7.548 | 4.692 | 88.5 | 253.173 | 163.173 | 6.973 | 1.724 | 1 |
| 38.322 | 6.188 | 4.629 | 87.744 | 75.322 | 345.322 | 2.328 | 0.346 | 1 |
| 35.861 | 0.092 | 4.698 | 39.433 | 0.306 | 270.306 | 1.34 | 0.419 | |
| 37.593 | 1.409 | 4.619 | 86.219 | 55.218 | 325.218 | 2.237 | 0.399 | |
| 33.947 | 5.17 | 4.88 | 71.195 | 359.969 | 269.969 | 1.001 | 0.142 | 2 |
| 30.481 | 11.33 | -0.635 | 89.782 | 74.498 | 344.498 | 1.782 | 0.616 | 1 |
| 34.604 | 5.839 | 4.762 | 53.656 | 62.92 | 332.92 | 0.684 | 0.101 | |
| 35.24 | 5.531 | 4.808 | 63.659 | 348.82 | 258.82 | 0.608 | 0.051 | 2 |
| 35.969 | 6.424 | 4.685 | 57.531 | 352.108 | 262.108 | 0.957 | 0.093 | 2 |
| 31.344 | 4.873 | 5.059 | 88.755 | 74.669 | 344.669 | 2.051 | 0.456 | 1 |
| 29.397 | 12.418 | -0.472 | 86.967 | 75.682 | 345.682 | 1.927 | 0.439 | 1 |
| 29.79 | 12.022 | 3.026 | 89.345 | 77.427 | 347.427 | 0.601 | 0.171 | 1 |
| 29.432 | 12.487 | 3.442 | 71.346 | 54.876 | 324.876 | 0.593 | 0.148 | |
| 30.012 | 11.811 | 2.748 | 66.386 | 43.373 | 313.373 | 0.972 | 0.356 | |
| 32.064 | 10.793 | -0.056 | 89.873 | 75.471 | 345.471 | 1.616 | 0.332 | 1 |

# APPENDIX B. MAIN VARIABLES DEFINITION CODE

```
def MainVariables
 ; Domain Extents
  x1=-10
  x2=10
  y1=-10
  y2=10
  z1=-10
  z2=10
  ; Number of Joint sets
  JSN=4
  ; Joint Set 1 Properties
  JS1dip= 88
  JS1dd= 250-65
  JS1Kfisher= 104
  JS1P10= 0.000000009 ;1.011
  JS1P32= 0.1
  ; Joint Set 2 Properties
  JS2dip= 68
  JS2dd= 348-65
  JS2Kfisher= 102
  JS2P10= 0.0000000001 ;1.18
  JS2P32= 0.4
  ; Joint Set 3 Properties
  JS3dip=75
  JS3dd=21-65+360
  JS3Kfisher=70
  JS3P10= 0.0000003;0.928
  JS3P32= 0.4
  ; Joint Set 4 Properties
  JS4dip= 29
  JS4dd= 144 - 65
  JS4Kfisher= 197
  JS4P10= 0.00000002
  JS4P32= 0.5
end
def make_NormalScanlineToAVGPlaneJSET1
  Mdip= (JS1dip)*pi/180
  Mstrike= (JS1dd)*pi/180
  s1x1=x1*sin(Mdip)*sin(Mstrike)
  S1x2=x2*sin(Mdip)*sin(Mstrike)
  S1y1=y1*sin(Mdip)*cos(Mstrike)
  S1y2=y2*sin(Mdip)*cos(Mstrike)
  S1z1=z1*cos(Mdip)
  S1z2=z2*cos(Mdip)
  command
    geom edge (@S1x1,@S1y1,@S1z1) (@S1x2,@S1y2,@S1z2)
  endcommand
end
```

```
def make_NormalScanlineToAVGPlaneJSET2
  Mdip= (JS2dip)*pi/180
  Mstrike= (JS2dd)*pi/180
  s2x1=x1*sin(Mdip)*sin(Mstrike)
  S2x2=x2*sin(Mdip)*sin(Mstrike)
  S2y1=y1*sin(Mdip)*cos(Mstrike)
  S2y2=y2*sin(Mdip)*cos(Mstrike)
  S2z1=z1*cos(Mdip)
  S2z2=z2*cos(Mdip)
  command
    geom edge (@S2x1,@S2y1,@S2z1) (@S2x2,@S2y2,@S2z2)
  endcommand
end
def make_NormalScanlineToAVGPlaneJSET3
  Mdip= (JS3dip)*pi/180
  Mstrike= (JS3dd)*pi/180
  s3x1=x1*sin(Mdip)*sin(Mstrike)
  S3x2=x2*sin(Mdip)*sin(Mstrike)
  S3y1=y1*sin(Mdip)*cos(Mstrike)
  S3y2=y2*sin(Mdip)*cos(Mstrike)
  S3z1=z1*cos(Mdip)
  S3z2=z2*cos(Mdip)
  command
    geom edge (@S3x1,@S3y1,@S3z1) (@S3x2,@S3y2,@S3z2)
  endcommand
end
def make_NormalScanlineToAVGPlaneJSET4
  Mdip= (JS4dip)*pi/180
  Mstrike= (JS4dd)*pi/180
  s4x1=x1*sin(Mdip)*sin(Mstrike)
  S4x2=x2*sin(Mdip)*sin(Mstrike)
  S4y1=y1*sin(Mdip)*cos(Mstrike)
  S4y2=y2*sin(Mdip)*cos(Mstrike)
  S4z1=z1*cos(Mdip)
  S4z2=z2*cos(Mdip)
  command
    geom edge (@S4x1,@S4y1,@S4z1) (@S4x2,@S4y2,@S4z2)
  endcommand
end
@MainVariables
@make_NormalScanlineToAVGPlaneJSET1
@make_NormalScanlineToAVGPlaneJSET2
@make_NormalScanlineToAVGPlaneJSET3
@make_NormalScanlineToAVGPlaneJSET4
```

# APPENDIX C. DFN GENERATION CODE

```
call MainVariablesDefinition.3ddat
def DFN_DomainExtent
   command
          domain extent (@x1,@x2 @y1,@y2 @z1,@z2)
  endcommand
end

@DFN_DomainExtent

call LND_TraceLength.txt

; DFN SET 1
; Generating a 3d line perpendicular to the AVG plane generated from the Joint SET 1
; Average plane: dip 88 dd 255 - Reoriented dip 88 dd 190

@LogNorm_TraceLength1

dfn template create name 'SET_1_Template' ...
   size fish @LogNorm_TraceLength1 ...
   orientation fisher @JS1dip @JS1dd @JS1Kfisher ...
   position uniform

dfn generate name 'SET_1' id 1001 template name 'SET_1_Template' ...
          genbox @x1,@x2 @y1,@y2 @z1,@z2 density @JS1P32
   ;P10 @JS1P10 (@x1,@y1,@z1) (@x2,@y2,@z2)

; DFN SET 2
; Generating a 3d line perpendicular to the AVG plane generated from the Joint SET 2
; Average plane: dip 68 dd 348 - Reoriented dip 68 dd 283

@LogNorm_TraceLength2

dfn template create name 'SET_2_Template' ...
   size fish @LogNorm_TraceLength2 ...
   orientation fisher @JS2dip @JS2dd @JS2Kfisher ...
   position uniform

dfn generate name 'SET_2' id 1002 template name 'SET_2_Template' ...
          genbox @x1,@x2 @y1,@y2 @z1,@z2 density @JS2P32
   ;P10 @JS2P10 (@x1,@y1,@z1) (@x2,@y2,@z2)

; DFN SET 3
; Generating a 3d line perpendicular to the AVG plane generated from the Joint SET 3
; Average plane: dip 75 dd 21 - Reoriented dip 75 dd 316

@LogNorm_TraceLength3

dfn template create name 'SET_3_Template' ...
   size fish @LogNorm_TraceLength3 ...
   orientation fisher @JS3dip @JS3dd @JS3Kfisher ...
   position uniform

dfn generate name 'SET_3' id 1003 template name 'SET_3_Template' ...
```

```
   genbox @x1,@x2 @y1,@y2 @z1,@z2 density @JS3P32
   ;P10 @JS3P10 (@x1,@y1,@z1) (@x2,@y2,@z2)

; DFN SET 4 - Bedding
; Generating a 3d line perpendicular to the AVG plane generated from the Joint SET 4
; Average plane: dip 29 dd 144 - Reoriented dip 29 dd 79

dfn template create name 'SET_4_Template' ...
   size gauss (9,1) slimit 1.5 30.0 ...
   orientation fisher @JS4dip @JS4dd @JS4Kfisher ...
   position uniform

dfn generate name 'SET_4' id 1004 template name 'SET_4_Template' ...
   genbox @x1,@x2 @y1,@y2 @z1,@z2 density @JS4P32
   ;P10 @JS4P10 (@x1,@y1,@z1) (@x2,@y2,@z2)

dfn cluster
```

# APPENDIX D. 3DEC ANALYSIS CODE

```
call DFNs_Generation.3ddat
set atol 0.0001
call GVol.3ddat
jset dfn 1004
change dfn 1004 jmat 2 2
jset dfn 1001
change dfn 1001 jmat 2 2
jset dfn 1002
change dfn 1002 jmat 2 2
jset dfn 1003
change dfn 1003 jmat 2 2
;_____________________________________________________________
;
;call p10_DFN1.3dfis
;call p10_DFN2.3dfis
;call p10_DFN3.3dfis
;call p10_DFN4.3dfis
;_____________________________________________________________
;
grav 0 0 -9.81
fix range z -20 -30
;_____________________________________________________________
;
; --- MAT 1: Rock ---
; density = 2.7 Ton/m3
; E=50000 MPa, Poisson's Ratio= 0.3
prop mat 1 dens 0.0027 k 41667 g 19231 ;ymod 50e3 pratio 0.3
; --- JMAT: Discontinuities ---
; Joint Shear Stiffness jks [MPa/m] = 30000; According to Bandis 1983
; Joint Normal Stiffnes jkn [MPa/m] = 300000
prop jmat 1 jks 50e5 jkn 50e5 jcoh 1e20 jfric 89 jten 50e5
prop jmat 2 jks 30000  jkn 300000  jfric 30 jcoh 0.0
change dfn 1002 jmat 2 2
change dfn 1003 jmat 2 2
change dfn 1004 jmat 2 2
change dfn 1001 jmat 2 2
;_____________________________________________________________
;
; --- histories to monitor convergence ---
hist nc=1 unbal
; top of model
hist xdis 0 0 10  ydis 0 0 10  zdis 0 0 10
;
plot create plot Hist
plot hist 2 3 4 yaxis label 'Displacement'
;
cycle 500
;_____________________________________________________________
reset disp
```

```
delete range group "10005"
delete range group "10002"
delete range group "10003"
damp local
cyc 40000
;_____________________________________________________________
;
;identify blocks which have a displacement > 0.02 m
;
mark region 4 range displacement 0.02 10.0  velocity 0.001 5.0  ;mark it re 4 for failed
def block_vol
bb = get_array(500,6)
cc = get_array(500,3)
cc(1,1) = string(cycle) + ' steps'
r=0
bi = block_head
loop while bi # 0
                    if b_region(bi) = 4
                                        if b_vol(bi) # 0 then ; and volume not zero
                                                            r= r + 1
                                                            bb(r,1) = r
                                                            bb( r,2) = bi
                                                            bb( r,3) = b_vol(bi)
                                                             bb( r,4) = b_mass(bi)
                                                             bb( r,5) = b_vel(bi)
                                                             bb(r,6) = runname
                                                            cc( r+1,1) = string(b_vol(bi))
                                        endif
                    endif
                    bi = b_next(bi)
endloop
end
@block_vol
def textsummary
dd = get_array(r+1)
loop n (1,r+1)
   dd(n)=       string(bb(n,1))+","+       string(bb(n,2))+","+       string(bb(n,3))+","+       string(bb(n,4))+","+
string(bb(n,5))+","+ string(bb(n,6))
endloop
end
@textsummary
def volcalc
volc= 0.0
ton= 0.0
loop mm (1,r)
   Tvolc= volc + bb(mm, 3)
   Tton= ton + bb(mm, 4)
endloop
end
@volcalc
list @Tvolc
list @Tton
```

```
def setup
            a_size = 20
  to_read = 0
  to_write = 2 ;appended
  to_fish = 0
  to_ascii = 1
filename = 'FailedBlockSummary.dat'
end
@setup

def fileme
  status=open(filename,to_write,to_ascii)
  status=write(dd,r+1)
  status=close
end
@fileme
save @runname
```

# APPENDIX E. 3DEC STOCHASTIC ANALYSIS CODE

```
new
set random 10001
[runname='run1']
call FullModel
call PauseFunction
@PFunc
;
new
set random 10002
[runname='run2']
call FullModel
call PauseFunction
@PFunc
;
new
set random 10003
[runname='run3']
call FullModel
call PauseFunction
@PFunc
;
new
set random 10004
[runname='run4']
call FullModel
call PauseFunction
@PFunc
;
new
set random 10005
[runname='run5']
call FullModel
call PauseFunction
@PFunc
;
new
set random 10006
[runname='run6']
call FullModel
call PauseFunction
@PFunc
;
```

This code is repeated as many times as iterations are wanted in the stochastic model. The random number needs to be changed and also the run name, so each model is different and is stored with a unique name.